ISSN 0021-9673

VOL. 712 NO. 2 13 OCTOBER 1995

THIS ISSUE COMPLETES VOL. 712

# JOURNAL OF CHROMATOGRAPHY A

## INCLUDING ELECTROPHORESIS AND OTHER SEPARATION METHODS



ELSEVIER

# JOURNAL OF CHROMATOGRAPHY A

## INCLUDING ELECTROPHORESIS AND OTHER SEPARATION METHODS

**Scope.** The *Journal of Chromatography A* publishes papers on all aspects of **chromatography, electrophoresis** and related methods. Contributions consist mainly of research papers dealing with chromatographic theory, instrumental developments and their applications. In the *Symposium volumes*, which are under separate editorship, proceedings of symposia on chromatography, electrophoresis and related methods are published. *Journal of Chromatography B: Biomedical Applications* —This journal, which is under separate editorship, deals with the following aspects: developments in and applications of chromatographic and electrophoretic techniques related to clinical diagnosis or alterations during medical treatment; screening and profiling of body fluids or tissues related to the analysis of active substances and to metabolic disorders; drug level monitoring and pharmacokinetic studies; clinical toxicology; forensic medicine; veterinary medicine; occupational medicine; results from basic medical research with direct consequences in clinical practice.

**Submission of Papers.** The preferred medium of submission is on disk with accompanying manuscript (see *Electronic manuscripts* in the Instructions to Authors, which can be obtained from the publisher, Elsevier Science B.V., P.O. Box 330, 1000 AH Amsterdam, Netherlands). Manuscripts (in English; *four* copies are required) should be submitted to: Editorial Office of *Journal of Chromatography A*, P.O. Box 681, 1000 AR Amsterdam, Netherlands, Telefax (+31-20) 485 2304, or to: The Editor of *Journal of Chromatography B: Biomedical Applications*, P.O. Box 681, 1000 AR Amsterdam, Netherlands. Review articles are invited or proposed in writing to the Editors who welcome suggestions for subjects. An outline of the proposed review should first be forwarded to the Editors for preliminary discussion prior to preparation. Submission of an article is understood to imply that the article is original and unpublished and is not being considered for publication elsewhere. For copyright regulations, see below.

**Publication information.** *Journal of Chromatography A* (ISSN 0021-9673): for 1995 Vols. 683–714 are scheduled for publication. *Journal of Chromatography B: Biomedical Applications* (ISSN 0378-4347): for 1995 Vols. 663–674 are scheduled for publication. Subscription prices for *Journal of Chromatography A*, *Journal of Chromatography B: Biomedical Applications* or a combined subscription are available upon request from the publisher. Subscriptions are accepted on a prepaid basis only and are entered on a calendar year basis. Issues are sent by surface mail except to the following countries where air delivery via SAL is ensured: Argentina, Australia, Brazil, Canada, China, Hong Kong, India, Israel, Japan, Malaysia, Mexico, New Zealand, Pakistan, Singapore, South Africa, South Korea, Taiwan, Thailand, USA. For all other countries airmail rates are available upon request. Claims for missing issues must be made within six months of our publication (mailing) date. Please address all your requests regarding orders and subscription queries to: Elsevier Science B.V., Journal Department, P.O. Box 211, 1000 AE Amsterdam, Netherlands. Tel.: (+31-20) 485 3642; Fax: (+31-20) 485 3598. Customers in the USA and Canada wishing information on this and other Elsevier journals, please contact Journal Information Center, Elsevier Science Inc., 655 Avenue of the Americas, New York, NY 10010, USA, Tel. (+1-212) 633 3750, Telefax (+1-212) 633 3764.

**Abstracts/Contents Lists** published in Analytical Abstracts, Biochemical Abstracts, Biological Abstracts, Chemical Abstracts, Chemical Titles, Chromatography Abstracts, Current Awareness in Biological Sciences (CABS), Current Contents/Life Sciences, Current Contents/Physical, Chemical & Earth Sciences, Deep-Sea Research/Part B: Oceanographic Literature Review, Excerpta Medica, Index Medicus, Mass Spectrometry Bulletin, PASCAL-CNRS, Referativnyi Zhurnal, Research Alert and Science Citation Index.

**US Mailing Notice.** *Journal of Chromatography A* (ISSN 0021-9673) is published weekly (total 52 issues) by Elsevier Science B.V., (Sara Burgerhartstraat 25, P.O. Box 211, 1000 AE Amsterdam, Netherlands). Annual subscription price in the USA US$ 5389.00 (US$ price valid in North, Central and South America only) including air speed delivery. Second class postage paid at Jamaica, NY 11431. **USA POSTMASTERS**: Send address changes to *Journal of Chromatography A*, Publications Expediting, Inc., 200 Meacham Avenue, Elmont, NY 11003. Airfreight and mailing in the USA by Publications Expediting.

**See inside back cover** for Publication Schedule, Information for Authors and information on Advertisements.



0021-9673/95/$09.50



Printed in the Netherlands

VOL. 712, NO. 2 JOURNAL OF CHROMATOGRAPHY A 13 OCTOBER 1995

# CONTENTS

*(Abstracts/Contents Lists published in Analytical Abstracts, Biochemical Abstracts, Biological Abstracts, Chemical Abstracts, Chemical Titles, Chromatography Abstracts, Current Awareness in Biological Sciences (CABS), Current Contents/Life Sciences, Current Contents/Physical, Chemical & Earth Sciences, Deep-Sea Research/Part B: Oceanographic Literature Review, Excerpta Medica, Index Medicus, Mass Spectrometry Bulletin, PASCAL-CNRS, Referativnyi Zhurnal, Research Alert and Science Citation Index)*

## REGULAR PAPERS

*Column Liquid Chromatography*



*Gas Chromatography*



*Electrophoresis*



## SHORT COMMUNICATIONS

*Column Liquid Chromatography*



*Planar Chromatography*

ELSEVIER

Journal of Chromatography A, 712 (1995) 287–301

JOURNAL OF CHROMATOGRAPHY A

# Retention behaviour of polar compounds using porous graphitic carbon with water-rich mobile phases

Marie-Claire Hennion*, Véronique Coquart, Sophie Guenu, Catherine Sella

*Ecole Supérieure de Physique et de Chimie Industrielles de Paris, Laboratoire de Chimie Analytique (URA CNRS 437), 10 rue Vauquelin, 75231 Paris cedex 05, France*

First received 21 February 1995; revised manuscript received 9 May 1995; accepted 11 May 1995

**Abstract**

The retention factors of polar compounds (mono-, di- and trisubstituted aromatic derivatives) were measured on porous graphitic carbon (PGC), alkyl-modified silicas and an apolar copolymer (PRP-1) with water–methanol mobile phases. It was first shown that the mobile phase effects were similar with the three sorbents and that the comparison of retention factors extrapolated to aqueous mobile phases ($k'_w$) could give information on stationary phase–solute interactions. The functional group contribution was examined. For aromatic derivatives containing hydrophobic substituents (alkyl and chloro groups), correlations with octanol–water partition coefficients were obtained for the three sorbents. For aromatic derivatives containing polar substituents, these correlations were obtained only for alkylsilicas and PRP-1. On PGC, the retention factor increased with increase in the number of polar substituents and was shown to depend on both the field and the mutual resonance effects of the different substituents on the aromatic ring. The results indicate that electronic interactions are more important than hydrophobic interactions in the retention mechanism of polar compounds. The parametrization of the polarity of the solutes, taking into account field and resonance effects, was carried out using local dipolar moments and the overall electron-excess charge density. The analyte retention factors could be predicted through correlation between log $k'_w$ and the electron-excess charge density.

## 1. Introduction

One of the objectives in making graphite-based sorbents for use in liquid chromatography (LC) was to provide a reversed-phase stationary phase that would not suffer from the disadvantages of silica-based sorbents, i.e., solubility in the eluent or hydrolysis of the bonded chains at low or high pH and the effects of the unavoidable underivatized silanol groups. After several attempts [1–7], it was only recently that porous graphitic carbons (PGC) were made available, the most common one under the tradename Hypercarb [8]. The PGC sorbent has effectively proved to be unique, showing properties of both reversed-phase (RP) and normal-phase (NP) sorbents, owing to its highly ordered crystalline structure composed of large layers of hexagonally arranged carbon atoms [9–11].

PGC was first described as a stronger reversed-phase sorbent than most $C_{18}$ silicas and provided similar retentions of analytes with a much greater content of organic solvent in the mobile phase. The retention increase caused by the

* Corresponding author.

0021-9673/95/$09.50 
*SSDI* 0021-9673(95)00562-5

addition of a methylene group in a series, considered as a measure of the hydrophobic properties of a RP sorbent, was found to be larger on PGC than on alkyl-bonded silicas [12–14]. Further, the flat rigid surface of PGC allowed unique stereoselectivity of solutes, as illustrated by the separation of geometric isomers and some diastereoisomers, especially under NP conditions [15–18]. Its high stability over the full pH range allowed separations with strongly acidic and basic mobile phases [19,20].

It has also been shown that the retention mechanism was different from that observed on RP silicas [1–5, 21–29]. The delocalization of the $\pi$-electrons in the large graphitic bands and the high polarizability of the carbon are responsible for strong dispersion interactions in addition to solvophobic interactions. Tanaka et al. [12] observed that the presence of hydrophilic groups in the molecule did not cause as great a retention decrease on carbon as on $C_{18}$ silica. Postulating a retention mechanism including dispersion forces, they stated that any molecular mass increase in the solute, be it in hydrophobic or dipolar moieties, tends to cause a retention increase. The term "hydrophobic adsorption" was introduced to characterize the positive interaction between the PGC and the solute, as opposed to the "hydrophobic partitioning" observed with $C_{18}$ silicas [14]. Bassler et al. [22] have shown that PGC acted as an electron-pair acceptor of solutes under non-polar conditions. The capacity factors of a set of non-congeneric aromatic solutes with hexane as eluent were related to structural information extracted from nineteen molecular descriptors of solutes by multivariate analysis [21]. The most important for retention were structural features reflecting the abilities of the solutes to participate in intermolecular interactions of electron-pair donor–acceptor and dipole–dipole induced types, whereas structural factors related to molecular size appeared to have little effect on retention.

The compounds considered up to now in most of the studies in the RP mode were non-polar or moderately polar, so that their retention was governed more by hydrophobic interactions than by electronic interactions. In previous studies, we have shown the high affinity of PGC towards very polar and water-soluble compounds in water-rich mobile phases [27–29]. For example, the capacity factor of 1,3,5-trihydroxybenzene was about 1000 in water as mobile phase whereas this compound was not retained at all by $C_{18}$ silica and was even proposed as an experimental probe to measure the void volume of $C_{18}$ columns. This high retention of polar compounds added a new future to PGC, i.e., a potential for extracting very polar or water-soluble contaminants that could not be extracted by any method up to now from environmental waters and that are consequently very difficult to determine at trace levels.

The objective of the work presented here was to acquire a better knowledge of the retention behaviour of polar analytes with PGC in order to collect more information about the retention mechanism and to be able to predict which compounds possess high retention factors in water. Data were collected for aromatic derivatives containing one or more polar groups. The capacity factors were also measured using two other reversed-phase sorbents, i.e., $C_{18}$ silica and the apolar styrene–divinylbenzene copolymer PRP-1, for which the retention mechanism was known. Comparison of data obtained with the three sorbents allowed a better understanding of the respective effects of the polar and the electronic character of the interactions involved in the retention mechanism with PGC.

## 2. Experimental

### 2.1. Apparatus

Retention measurements were carried out with a Model 5060 liquid chromatograph equipped with a UV 200 variable-wavelength spectrophotometer (Varian, Palo Alto, CA, USA) or an electrochemical detector (Coulochem Model 5100; ESA, Bedford, MA, USA.).

### 2.2. Stationary phases and columns

Commercially available columns ($100 \times 4.6$ mm I.D.) packed with Hypercarb porous graphitic carbon of 7-$\mu$m particle size (Shandon,

Runcorn, UK), a laboratory-packed column (100 × 4.6 mm I.D.) containing PRP-1 copolymer of 10-μm particle size (Hamilton, Reno, NV, USA), laboratory-packed columns (100 × 4.6 mm I.D.) containing LiChrosorb RP-8 or RP-18 of 5-μm particle size (Merck, Darmstadt, Germany) or a 250 × 4.6 mm I.D. column prepacked with the spherical 5-μm octylsilica Zorbax (Interchim, Paris, France) were used for retention measurements. Laboratory-made stainless-steel precolumns (22 mm × 4.6 mm I.D. or 27 mm × 4.6 mm I.D.) were used for some retention measurements in water-rich mobile phases. They were laboratory-packed using a thick slurry and a microspatula. The void volume was determined for each mobile phase by injection of 2 *M* sodium nitrate solution.

### 2.3. Chemicals

HPLC-grade acetonitrile was obtained from Rathburn (Walkerburn, UK) and methanol from Prolabo (Paris, France). LC-grade water was prepared by purifying demineralized water in a Milli-Q filtration system (Millipore, Bedford, MA, USA). Other chemicals were obtained from Prolabo, Merck or Fluka (Buchs, Switzerland). Solutions of selected solutes were prepared by weighing and dissolving them in methanol.

### 2.4. Calculations of electron-excess charge density

The charge distribution was calculated using the SYBYL molecular modelling package (version 6.0) running on a Vax 3200/VMS (version 5.42). The molecular mechanics force field implemented in the SYBYL program produced molecular geometries close to crystal structures. A model was calculated for each molecule. The different conformations were systematically examined and the lowest energy conformation was selected by taking into account its atomic charge distribution. The charge distribution was calculated by the semi-empirical molecular orbital method MNDO provided in the MOPAC5 package.

## 3. Results and discussion

Retention factors were measured for the set of mono-, di- and trisubstituted aromatic derivatives reported in Table 1. In order to compare data obtained with the three reversed-phase sorbents, the role of the mobile phase was first investigated.

### 3.1. Comparison of mobile phase effects

In chromatography, the retention factor can be generally defined as the ratio of the sum of the interactions between the solute and the mobile phase and the sum of the interactions between the solute and the stationary phase. Therefore, comparison of retention factors can give information on interactions with the sorbents provided that the sum of interactions between the solutes and the mobile phase is expected to be similar with the three sorbents and provided that the phase ratios are similar. We do not intend to compare the absolute retention values for one sorbent with another, but some relationships with solute structures or their retention order or the effect of some groups, so that a knowledge of the phase ratio is not required. However, comparison at a given composition of the mobile phase was impossible, owing to the polarity range of the compounds of interest, because some of them were not retained and others were too retained for measurements. Therefore, it was decided to measure the retention factors in mobile phases made of water and methanol over the largest range possible and to extrapolate the data to pure water conditions. In water-rich mobile phases, short analytical columns were laboratory packed to obtain shorter retention volumes.

Fig. 1 shows the variations of the experimental retention factors of three analytes, benzene, phenol and acetophenone, with the methanol volume fraction of the mobile phase for $C_{18}$ silica, PRP-1 and PGC. These three analytes were selected because the shapes of the curves were different. The variations were linear in a certain range of methanol concentrations and deviation from linearity was observed for benzene and for acetophenone with mobile phases

Table 1
Extrapolated retention factor values ($\log k'_w$) from the linear variations $\log k'$ versus volume fraction of methanol in the mobile phase for each benzene derivative for the three stationary phases, $C_{18}$ silica, PRP-1 and PGC. The range of methanol used for the measurements is indicated in square brackets. Compounds are characterized by their water–octanol partition coefficient ($\log P_{oct.}$). The positions of the substituents in the benzene ring are indicated by the number in brackets.

| Solute: functional group | | | Log $P_{oct.}$ | Extrapolated $\log k'_w$ | | | | |
|---|---|---|---|---|---|---|---|---|
| | | | | $C_{18}$ | PRP-1 | | PGC | |
| *Monosubstituted* | | | | | | | | |
| $CH(CH_3)_2$ | | | 3.68 | – | 5.55 | [80, 100] | 3.5 | [50, 80] |
| $C_3H_7$ | | | 3.55 | – | 5.35 | [80, 100] | 3.4 | [50, 80] |
| $C_2H_5$ | | | 3.15 | 3.2 | 4.85 | [70, 90] | 2.85 | [30, 60] |
| $CH_3$ | | | 2.74 | 2.75 | 4.2 | [60, 80] | 2.3 | [20, 70] |
| H | | | 2.14 | 2.25 | 3.5 | [0, 60] | 1.5 | [0, 70] |
| Cl | | | 2.84 | 2.8 | nd | – | 2.65 | [20, 90] |
| $OCH_3$ | | | 2.08 | 2.15 | nd | – | 2.2 | [20, 80] |
| COOH | | | 1.86 | 1.9 | 3.3 | [40, 80] | 2.45 | [30, 90] |
| $NO_2$ | | | 1.84 | 2.05 | 3.6 | [60, 90] | 2.45 | [50, 100] |
| $COCH_3$ | | | 1.70 | 2.0 | 2.9 | [0, 80] | 2.5 | [20, 90] |
| CN | | | 1.67 | 1.8 | nd | – | 2.1 | [30, 80] |
| OH | | | 1.50 | 1.55 | 2.4 | [0,90] | 1.8 | [0, 100] |
| CHO | | | 1.5 | 1.55 | 2.9 | [50, 80] | 1.8 | [20, 50] |
| $CH_2OH$ | | | 1.10 | 1.5 | 2.45 | [0, 60] | 2.2 | [30, 50] |
| $NH_2$ | | | 0.9 | 1.10 | 2.5 | [20, 80] | 1.35 | [0, 60] |
| *Disubstituted* | | | | | | | | |
| (1) OH | (2) OH | | 1.0 | nd[a] | 1.6 | [0, 90] | 2.0 | [0, 100] |
| (1) OH | (3) OH | | 0.8 | 0.5 | 1.25 | [0, 70] | 2.3 | [0, 100] |
| (1) OH | (4) OH | | 0.6 | nd | 0.85 | [0, 70] | 2.20 | [0, 100] |
| (1) COOH | (2) OH | | | nd | 3.05 | [30, 70] | 2.8 | [50, 90] |
| (1) COOH | (3) OH | | 2.4 | nd | 2.4 | [30, 70] | 2.6 | [50, 70] |
| (1) COOH | (4) OH | | 2.3 | nd | 2.3 | [30, 70] | 2.65 | [50, 90] |
| (1) $NH_2$ | (2) $NH_2$ | | 0.15 | nd | 1.7 | [10, 60] | 1.4 | 0, 60] |
| (1) $NH_2$ | (3) $NH_2$ | | | nd | 1.35 | [0, 60] | 1.6 | [0, 60] |
| (1) $NH_2$ | (4) $NH_2$ | | | nd | 1.2 | [0,50] | 2.3 | [0, 60] |
| (1) OH | (2) $NH_2$ | | 0.52 | nd | 1.7 | [30, 60] | 1.7 | [20, 90] |
| (1) OH | (3) $NH_2$ | | 0.17 | nd | 1.3 | [30, 60] | 1.6 | [20, 90] |
| (1) OH | (4) $NH_2$ | | 0.04 | nd | 1.1 | [30, 60] | 2.05 | [20, 90] |
| (1) COOH | (2) $NH_2$ | | 1.21 | nd | 2.85 | [30, 60] | 2.9 | [30, 60] |
| (1) COOH | (3) $NH_2$ | | | nd | 1.6 | [30, 60] | 2.8 | [30, 60] |
| (1) COOH | (4) $NH_2$ | | 0.68 | nd | 2.0 | [30, 60] | 2.85 | [30, 60] |
| (1) $NO_2$ | (2) $NO_2$ | | 1.58 | 1.9 | 3.95 | [70, 90] | 2.7 | [70, 100] |
| (1) $NO_2$ | (3) $NO_2$ | | 1.49 | 1.8 | 4.0 | [70, 90] | 3.6 | [80, 100] |
| (1) $NO_2$ | (4) $NO_2$ | | 1.46 | 1.7 | 4.05 | [70, 90] | 3.1 | [80, 100] |
| (1) COOH | (2) COOH | | 0.79 | nd | 2.2 | [30, 50] | 2.75 | [40, 80] |
| (1) COOH | (3) COOH | | 1.67 | nd | 3.1 | [30, 60] | 3.5 | [40, 80] |
| (1) $NH_2$ | (4) $NO_2$ | | 1.39 | 1.5 | 2.85 | [30, 60] | 3.0 | [60, 90] |
| (1) OH | (4) $NO_2$ | | 1.91 | 2.0 | 2.7 | [30, 60] | 3.1 | [70, 100] |
| *Trisubstituted* | | | | | | | | |
| (1) OH | (2) OH | (3) OH | | nd | 0.8 | [0, 70] | 2.2 | [0, 100] |
| (1) OH | (3) OH | (5) OH | | nd | 0.5 | [0, 70] | 2.7 | [0, 100] |
| (1) COOH | (2) OH | (3) OH | | nd | 2.4 | [30, 70] | 2.9 | [50, 90] |
| (1) COOH | (2) OH | (6) OH | | nd | 2.85 | [30, 70] | 2.65 | [50, 90] |
| (1) COOH | (3) OH | (4) OH | | nd | 1.5 | [30, 70] | 2.95 | [50, 90] |
| (1) COOH | (3) OH | (5) OH | | nd | 1.35 | [30, 60] | 3.0 | [50, 90] |
| (1) COOH | (2) COOH | (3) COOH | | nd | 1.95 | [30, 50] | 3.95 | [50, 80] |
| (1) COOH | (3) COOH | (5) COOH | 1.15 | nd | 2.6 | [30, 50] | 4.5 | [70, 90] |
| (1) OH | (2) Cl | (4) $NH_2$ | | nd | 2.85 | [30, 60] | 2.45 | [30, 90] |

[a] nd = Not determined.

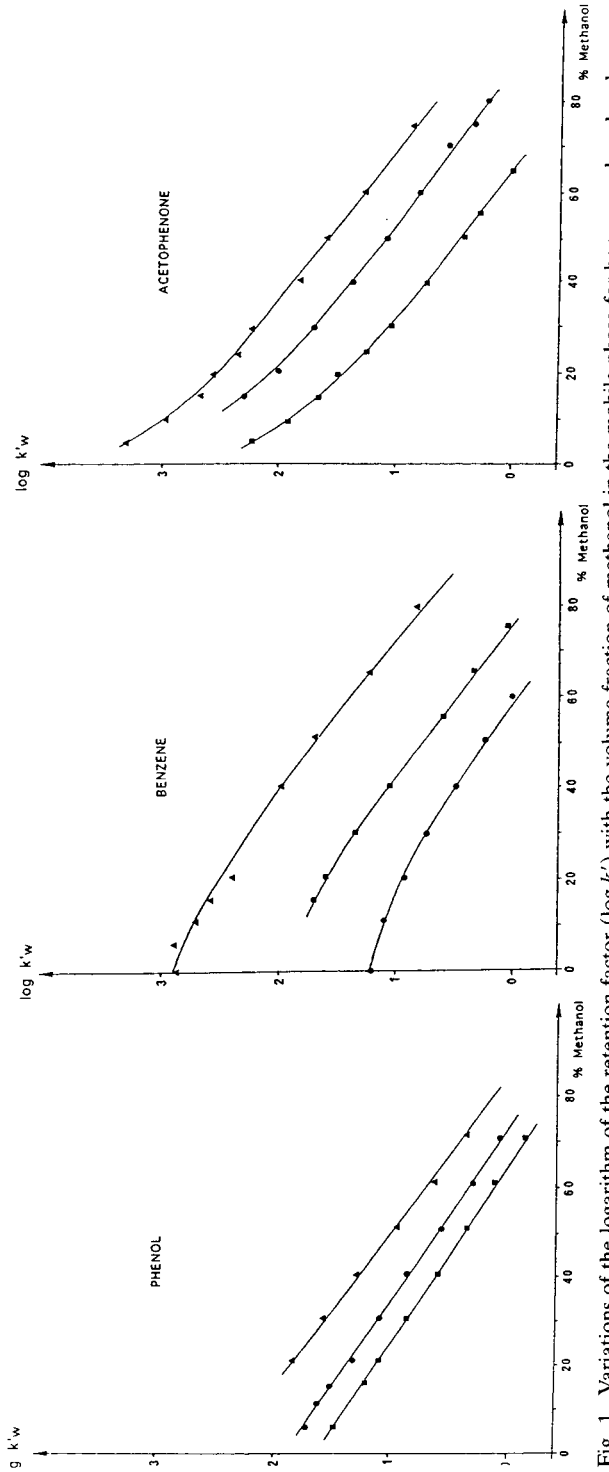


Fig. 1. Variations of the logarithm of the retention factor ($\log k'$) with the volume fraction of methanol in the mobile phase for benzene, phenol and acetophenone. ■ = RP-18 silica; ▲ = PRP-1; ● = PGC.

containing more than 75% water. These variations are well known for alkylsilicas and have been the subject of many studies. As pointed out by Schoenmakers et al. [30], for some analytes, the linear variation turned out to be quadratic when the whole range of methanol content was investigated. The retention factor in water, $k'_w$, was extrapolated from the linear log $k'$–methanol volume fraction relationship and the difference between the extrapolated and the real values can be positive or negative depending on the solutes. In a previous study, we had shown that the more polar the analyte, the less retained it was by $C_{18}$ silicas and the closer the extrapolated and experimental values were [31].

However, the most important point to be considered in the comparison of experimental variations obtained for each stationary phase is the parallelism of the curves. The same deviations from the linear range are observed for the three sorbents, which are striking results. With $C_{18}$ silicas, the retention process has received much attention but the fundamental aspects are still unclear as to whether the retention is described by a partition or an adsorption process, or a combination of the two. However, it is well established that there is preferential wetting of the alkyl chains by the mobile phase organic solvent which causes an imprecise demarkation of the mobile and stationary phases, that the conformation of the chains can change with variations in the experimental conditions and finally that the retention of some molecules can occur by an NP process on surface silanol groups as well as by an RP process. To a first approximation, at low water concentrations, it was shown that water is adsorbed to a slight extent and at higher water concentrations starting at ca. 10–30% (v/v), the organic component is adsorbed [32]. We have demonstrated that in a limited range of composition from around 20% to 70% of water, the change in retention was mainly due to the change in the solubility of the solute in the mobile phase [33]. In this range, when only the methanol content of the mobile phase varies in the chromatographic system, the variation of the retention factor results only from the variation of the interactions between the mobile phase and the solute, the interactions between the stationary phase and the solute being constant in this range. This classical view of the passive role of the bonded ligand was recently challenged and some experiments have shown that the free energy of retention can arise also from net attractive processes in the stationary phase [34].

It is therefore difficult to explain the parallelism of the curves observed in Fig. 1, except that the same preferential wetting is observed with change in composition of methanol. To a first approximation, the results indicate that since the same interactions between the solutes and the mobile phase are observed with the three sorbents, the interactions between the stationary phase and the solute are of course different from one sorbent to another, but for each sorbent they are constant in the limited range of mobile phase composition where the relationship is linear. Therefore, for a given composition of the mobile phase in the linear range, the difference in retention factor from one sorbent to the other is related to the difference in interactions with the stationary phases and can be measured by the nearly constant difference in log $k'$ between the curves. Comparison of data extrapolated to pure water from the linear range can be a first approach for comparison of sorbent–solute interactions.

The extrapolated values of log $k'_w$ are reported in Table 1, together with the water–octanol partition coefficients. The experimental range of mobile phase composition giving a linear relationship is also reported. The retention factors of di- and trisubstituted derivatives were not determined on $C_{18}$ silicas because, in general, they are not retained by this sorbent. As some compounds are ionizable, the pH of the mobile phase was adjusted in order that the analyte should be in its molecular form.

### 3.2. Comparison of log $k'_w$ data

In the literature, PGC is often compared with $C_{18}$ silicas and is described as a stronger hydrophobic sorbent. The results reported in Table 1 for monosubstituted derivatives indicate that the log $k'_w$ values are higher on $C_{18}$ than on PGC for ethylbenzene, toluene, chlorobenzene and ben-

zene and that the reverse order is observed for a polar functional group on substituted aromatic rings. This comparison does not allow one to compare hydrophobic properties and the methylene increment, $\alpha(CH_2)$, that can be roughly estimated from our data for the alkyl derivatives is higher for PGC (average $\log \alpha = 0.55$) than for $C_{18}$ silica (average $\log \alpha = 0.45$). These results are consistent with more accurate values of $\alpha(CH_2)$ calculated from measurements of the retention times of alkanols and reported to be 4.50 and 3.84, respectively [14]. No comparison was made with apolar copolymers, but PRP-1 shows higher values for each monosubstituted compound. The differences are fairly high, the retention of benzene being 100 times higher on PRP-1 than on PGC. The methylene increment is found to be slightly higher for PRP-1 (average $\log \alpha = 0.60$) than for PGC.

The results are very different for di- and trisubstituted analytes. Most of the analytes contain polar functional substituents and are characterized by log $P_{oct.}$ values below 1.5. All these compounds were weakly retained by $C_{18}$ silica and their $\log k'_w$ values were not evaluated. For PRP-1, a close examination of the data indicates that the retention factor of a compound having two polar aromatic substituents is always lower than that measured for each corresponding monosubstituted benzene, whereas the opposite is observed with PGC. Except for dinitro derivatives, the $\log k'_w$ values are higher on PGC than on PRP-1. The difference is especially large for very polar compounds such as some dihydroxy-, diamino- or hydroxyamino-substituted and other trisubstituted derivatives.

As the hydrophilic properties of analytes decreases with increasing number of substituted polar groups, these results indicate first a different behaviour of PGC from that of $C_{18}$ silica or PRP-1 copolymer.

### 3.3. Correlation with octanol–water partition coefficients ($P_{oct.}$)

The relationship between the hydrophobic parameter log $P_{oct.}$ and the extrapolated $\log k'_w$ from methanol–water measurements obtained with $C_{18}$ silicas is well known, although it can only be an approximation, as pointed out by Kaliszan [35] in a recent review of quantitative structure–retention relationships (QSRR) applied to reversed-phase chromatography. Even if extrapolated $\log k'_w$ values have no physical meaning, it is an easy means of normalizing retention, provided that appropriate $C_{18}$ silicas are used and that extrapolated data are derived from water–methanol measurements [36]. Braumann [36] gathered many extrapolated $\log k'_w$ data obtained with these conditions and good relationships between $\log k'_w$ values and log $P_{oct.}$ were observed for a large number of compounds differing in polarity and chemical properties. These correlations suggest that retention with $C_{18}$ silicas is primarily governed by hydrophobic effects, which closely reflect the water–octanol partition coefficients [35,36]. These correlations were examined with our experimental data on the three sorbents (see below).

*Octadecylsilicas*

The relationship between the $\log k'_w$ data in Table 1 and log $P_{oct.}$ is shown in Fig. 2a. The slope of $0.92 \pm 0.03$ is in agreement with other published work. The more hydrophilic the analyte is, the lower its retention is and the correlation in Fig. 2a leads to an approximate value of $\log k'_w$ with no measurement.

*Apolar copolymer PRP-1*

The same correlation is also represented in Fig. 2a for the styrene–divinylbenzene porous copolymer PRP-1. Values of $\log k'_w$ were determined for a large number of compounds with this sorbent, although trisubstituted derivatives were not represented here because their log $P_{oct.}$ values were not found. A perfect linear relationship is observed for the series of alkylbenzenes. For other compounds, the correlation is not really linear but a general trend is visible and indicates that $\log k'_w$ decreases with increase in log $P_{oct.}$, showing that the retention is also mainly governed by hydrophobic interactions. Strong electron–donor interactions can be involved, especially $\pi$–$\pi$ interactions with the aromatic ring of the solutes due to aromatic rings in the network of the polymer matrix, in addition to

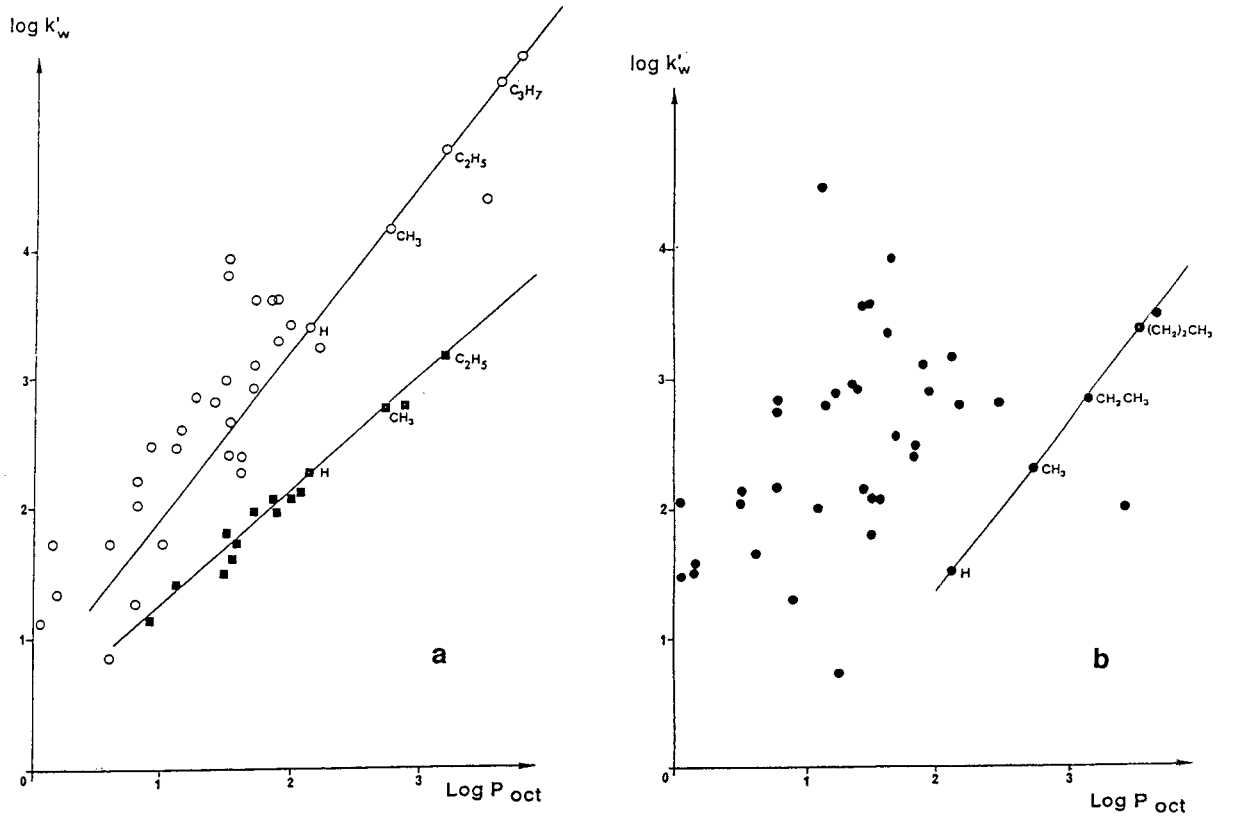


Fig. 2. Relationship between $\log k'_w$ and $\log P_{oct.}$ (a) $\log k'_w$ values obtained on (□) $C_{18}$ silica and (○) PRP-1 copolymer; (b) $\log k'_w$ values on PGC. See Table 1 for solutes.

hydrophobic interactions. Therefore, the interaction is sensitive to changes in the electron density of the solute caused by the electron-withdrawing or -donating ability of the substituent. The correlation between $\log k'_w$ and $\log P_{oct.}$ cannot be similar to that obtained with $C_{18}$ silicas, because some substituents can have both a hydrophobic and an electronic effect. As PRP-1 can only be a $\pi$-donor, the effect of strong electron-withdrawing substituents such as nitro groups is responsible for a higher retention, and the $\log k'_w$ values of these compounds are effectively above those corresponding to alkylbenzenes. On the other hand, the $\log k'_w$ values of compounds having strong electron-donating substituents such as amino or hydroxy groups are lower. We previously compared the retention data of moderately polar compounds characterized with $\log P_{oct.}$ values above 1.5 and found that the $k'_w$ data for PRP-1 were about 25–50 times higher than those for $C_{18}$ silicas [28]. Obviously, the lower $\log P_{oct.}$ is, the smaller is the difference in $\log k'_w$ and very polar analytes are only slightly more retained by PRP-1 than they were by $C_{18}$ silicas. The limitation of using PRP-1 for extracting polar degradation products of atrazine from water has already been pointed out for compounds with $\log P_{oct.}$ values below 1 [37].

*Porous graphitic carbon*

As can be seen in Fig. 2b, there is no trend between solute hydrophobicity and retention for the set of compounds examined in this study. Hydrophobic interactions are not the most important interactions that govern the retention

mechanism. If more compounds containing only hydrophobic moieties were to be studied, the trend should be obtained. This is illustrated by the linear relationship observed for the series of alkylbenzenes, which includes chlorobenzene.

### 3.4. Functional group contribution

*Monosubstituted*

The functional group contribution is usually determined by the difference ($\tau_X$) in the logarithm of retention factors of the two analytes which differ by the presence and absence of the functional group X of interest. The functional group contribution to RP liquid chromatography was recently reviewed by Smith [38]. In Table 2, the $\tau_X$ values calculated from extrapolated $\log k'_w$ values in pure water are reported for the three sorbents. The groups have been classified in order of decreasing $\tau_X$ values on $C_{18}$ silica and the same order is observed for the characterization of the groups by their Hansch $\pi$ constants. Since this parameter takes mainly into account both the size and the polarity of the functional group, the relationship (not presented here) between $\tau_X$ and the Hansch constant is similar to that obtained between $\log k'_w$ and $\log P_{oct.}$ and in agreement with the hydrophobic retention mechanism. The Hansch $\pi$ value is useful for characterizing the "polarity" of groups. Polar groups are often characterized by negative Hansch values, whereas groups with positive values are often named "hydrophobic groups".

Little work has been devoted to the retention behaviour of analytes with polystyrene–divinylbenzene copolymers. The capacity factors of some mono- and disubstituted aromatic compounds were compared with those of $C_{18}$ silicas and it was found that the contributions for the hydrophobic groups were more positive and for the more polar groups more negative [39,40]. In Table 2, the $\tau_X$ values on PRP-1 shows about the same decreasing order as the Hansch $\pi$ constant, except for nitro and hydroxy groups. As stated, these results can be explained by the electronic effects of the group on the benzene ring. The Hammett equation allows one to characterize the different functional groups by a $\sigma$ value that sums the resonance and field effects of a group X when attached to a benzene ring. This value correlated many reaction data, especially for groups in *meta* and *para* positions [41]. The $\sigma$ values are reported in Table 2, a positive value indicating an electron-withdrawing group and a negative value an electron-donating group. The high $\sigma$ value for the nitro group explains the difference in retention on PRP-1. However, the close values of $\tau_X$ for hydroxy and amino groups are more difficult to explain.

The results for PGC are different and no

Table 2
Functional group contribution for various aromatic compounds

| Substituent X | $\tau_X$ values on sorbent | | | Hansch constant | Hammett parameter |
|---|---|---|---|---|---|
| | RP-18 | PRP-1 | PGC | | |
| Cl | 0.5 | – | 1.11 | 0.71 | 0.23 |
| $CH_3$ | 0.46 | 0.74 | 0.80 | 0.56 | – |
| $COOCH_3$ | −0.08 | – | 1.66 | −0.01 | 0.44 |
| $OCH_3$ | −0.15 | – | 0.68 | −0.02 | −0.28 |
| COOH | −0.30 | −0.1 | 0.92 | – | 0.44 |
| $NO_2$ | −0.25 | 0.22 | 0.78 | −0.28 | 0.80 |
| $COCH_3$ | −0.30 | −0.30 | 1.03 | −0.55 | 0.47 |
| CN | −0.57 | – | 0.54 | −0.57 | 0.70 |
| OH | −0.80 | −1.0 | 0.28 | −0.67 | −0.38 |
| $NH_2$ | −1.20 | −0.92 | −0.20 | −1.23 | −0.57 |

The values of $\tau_X$ are defined as $\log k'_{RX} - \log k'_{RH}$, R being the aromatic ring and X the substituent. Values of $k'$ extrapolated to pure water according to Table 1.

correlation can be found with the $\sigma$ constant, even for the nitro group.

*Polysubstituted*

The information given for polysubstituted derivatives is more interesting. For $C_{18}$ silica and PRP-1, generally, we can predict if the retention will increase or decrease on adding a second group to the benzene ring, depending on its Hansch $\pi$ constant value: whatever the first group attached on the aromatic ring, any addition of a hydrophobic group will cause an increase in retention, whereas any addition of a polar group will cause a decrease.

On PGC, an increase in retention is always observed when a second group is added, as shown from the comparison of values in Table 1. Fig. 3 shows the increase in $\log k'_w$ data with the number of OH, or COOH groups in the aromatic molecules. A linear relationship is obtained for monosubstituted, disubstituted in positions 1 and 3 and trisubstituted in positions 1, 3 and 5. This increase in retention with the increasing number of $NO_2$ groups in similar positions has been already pointed out by Colin et al. [42], working with experimental pyrocarbon-modified silicas. However, when considering the different positions and when adding a second nitro group in position 2 or 4, the retention increases, but not as much as for position 3. This will be explained below by the different magnitudes of the resonance effects in the different positions on the ring.

These results indicate that the interactions between PGC and solutes are mainly dispersive (London) interactions. Because of the high polarizability of the $\pi$-electrons, especially strong dispersion interactions can occur with molecules possessing conjugated $\pi$-electrons. This explains why the highest retention is obtained for substituents in a position where the resonance effect between the polar functional groups and the benzene ring is at a maximum.

A specific feature of London interactions is their additivity. Therefore, the energy of interaction is approximately the sum of the individual energies between each group. Golkiewicz et al. [7] have shown that the increment of $\log k'$ on

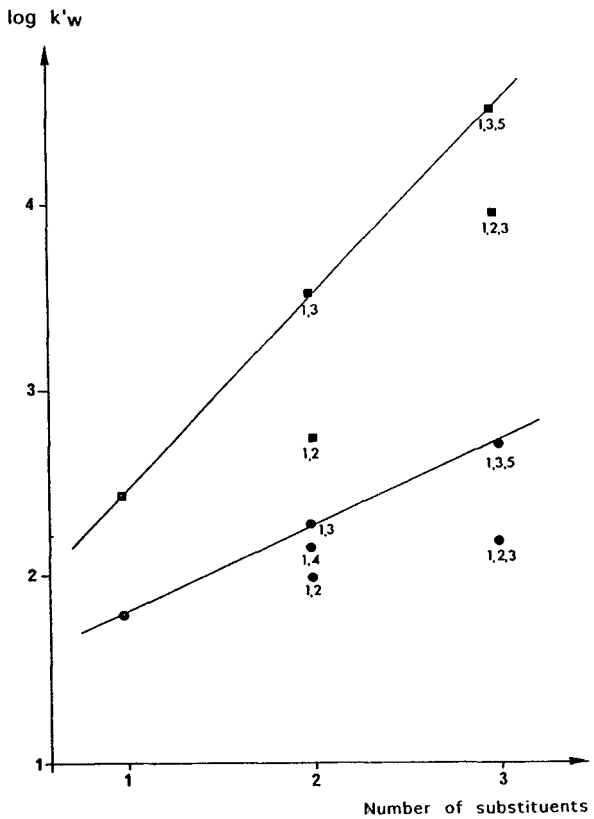


Fig. 3. Variation of $\log k'_w$ with the number $N$ of (O) hydroxy or (□) carboxylic groups on the aromatic ring. The numbers indicate the positions of the substituents on the ring.

adding a $CH_3$ or a Cl group in an aromatic molecule was constant and did not depend on the nature of the first substituent or on the position of the added group. However, $CH_3$ and Cl groups are hydrophobic and do not induce resonance effects. Table 3 shows the increment in $\log k'_w$ observed on adding an OH group in position 2, 3 or 4 to a benzene ring already substituted by a Y group. Low increments were observed when the first group was hydrophobic, Cl or $CH_3$, whereas increments between 0.16 and 0.72 were obtained with polar Y groups. It can be seen that the increment depends on the position of the added OH group. Again, the resonance effect induced by the OH group depends on that induced by the first substituent and on the respective positions of the two

Table 3
Increment in $\log k'_w$ for polar monosubstituted aromatic derivatives (Y being the substituent) when a hydroxy group is added to the ring at position 2, 3 or 4

| Substituent Y | OH in position 2 | OH in position 3 | OH in position 4 |
|---|---|---|---|
| $NO_2$ | – | – | 0.72 |
| COOH | 0.36 | 0.16 | 0.20 |
| $NH_2$ | −0.24 | 0.24 | 0.63 |
| OH | 0.22 | 0.40 | 0.25 |
| $CH_3$ | −0.06 | −0.06 | – |
| Cl | 0.02 | 0.12 | 0.07 |
| $OCH_3$ | – | – | 0.40 |
| $COCH_3$ | – | 0.24 | – |
| $COOCH_3$ | – | – | 0.18 |

substituents. Our results indicate that both the polarity of the functional groups and the "induced" polarity on the ring by the different substituents have to be taken into account for predicting retention on PGC. More investigation is required, taking into account also steric or intramolecular effects of substituents and mobile phase interactions.

### 3.5. Polarity parametrization of solutes

Dispersive interactions are of the instantaneous dipole-induced dipole type and can occur between electrically neutral molecules that do not possess any permanent dipole. Kaliszan [35] classified the structural descriptors of solutes used in QSRR analysis into physico-chemical parameters and others related to bulkiness, to geometry or shape, to polarity and to topology. Dipole moments, atomic excess charges, orbital energies, superdelocalizabilities and partially charged surfaces can describe polarity-related or electronic parameters. In QSSRs describing RP-LC retention on $C_{18}$ silicas, various descriptors more or less directly linked to molecular size were not able to account at the same time for structurally specific polar differences, so a polarity parameter was added [43]. It was shown that the overall dipole performed poorly, but it is well known that some symmetrical molecules (e.g., a benzene ring with two identical polar groups in positions 1 and 4) can have an overall dipolar moment near zero and behave as polar solutes. Kaliszan [44] therefore introduced a submolecular measure of the polarity reflecting the largest molecular local dipole in the molecule. A solute in specific contact with a stationary phase has at least one of its fragments close to the interacting surface and, therefore, the polar interaction of a solute would logically be better described by local molecular dipoles. This quantum chemical polarity parameter, $\Delta$, was calculated by the largest difference in the individual atomic electronic excess charges in the molecule. This calculation required first the determination of the electron densities on all the atoms and then locating the atom with the highest electron excess and the atom with the highest electron deficiency.

### 3.6. Interactions with PGC

Tables 4 and 5 report the local dipolar moments corresponding to the various substituents for nitro- and dinitrobenzenes and for phenol and some di- and trihydroxybenzenes. The overall positive electron-excess charge density of the benzene ring in the molecule and the overall negative electron-excess charge density of the whole molecule, including the polar substituents, have also been reported. Nitro- and dinitrobenzene are known to be strong $\pi$-acceptors, since both the electron-withdrawing (or resonance) and the electronic field effects are negative. The benzene ring bears a positive charge [$\Sigma q_+$(ring)] and the nitro group a negative charge. The

Table 4
Values of $\log k'_w$ on RP-18, PRP-1 and PGC for nitro- and dinitrobenzenes, submolecular polarity parameter Δ, overall positive electronic charge of the benzene ring, $\Sigma q_+$(ring), and overall negative excess-electron charge, $\Sigma q_-$

| Parameter | Nitro- | 1,2-Dinitro- | 1,3-Dinitro- | 1,4-Dinitro- |
|---|---|---|---|---|
| $\log k'_w$ (RP-18) | 2.05 | 1.9 | 1.8 | 1.7 |
| $\log k'_w$ (PRP-1) | 3.6 | 3.95 | 4.0 | 4.05 |
| $\log k'_w$ (PGC) | 2.45 | 2.7 | 3.6 | 3.1 |
| $\Delta_1$ | 0.67 | 0.53 | 0.69 | 0.60 |
| $\Delta_2$ | | 0.53 | 0.68 | 0.60 |
| $\Sigma q_+$(ring) | 0.19 | 0.32 | 0.74 | 0.52 |
| $\Sigma q_-$ | −1.08 | −1.04 | −1.79 | −1.50 |

Δ is the difference in the electronic charges borne by the N atom of the nitro group and the adjacent C atom in the ring.

highest local dipolar moment was found between the N atom of the nitro group and the C atom of the ring. Owing to the different locations of the resonance effects, both the $\Delta_1$ and $\Delta_2$ values for 1,2- and 1,4-dinitrobenzene are lower than the Δ value for nitrobenzene, whereas higher values are observed for 1,3-dinitrobenzene. The position of the second nitro group also has a different effect on the increase of the positive ring charge. As shown in Table 4, the retention order on PGC agrees with the sum of the highest local dipolar moments, with the positive charge of the ring and also with the overall negative electron-excess charge density. On $C_{18}$ silica, the retention decreases on adding a second nitro group, whereas on PRP-1, this is an example where the retention increases with increase in the number of substituents, owing to the $\pi-\pi$ interactions between the $\pi$-electron-donor character of PRP-1 and the strong positive electron-excess charge density of the ring of the dinitrobenzenes.

The same data are reported for hydroxybenzenes in Table 5. The field effect of a hydroxy group is negative whereas the resonance effect is positive. Evidently, owing to the much lower positive electron-excess charge density of the ring, no correlation is found between the retention order and the ring charge, so that the interaction cannot be explained in term of $\pi-\pi$ interactions, as on PRP-1. The position on the ring of a second or of a third OH group strongly influences the values of Δ and each of them is the highest where it is in positions 1, 3 and 5. A correlation is observed between the sum of the Δ values and the retention order, indicating that all the polar groups interact at the same time with the PGC surface and should be taken into account in the total interaction. As the solute molecule is planar, the interactions occur be-

Table 5
Values of $\log k'_w$ on PGC for phenol and polyhydroxybenzenes, submolecular polarity parameters Δ, overall positive electronic charge of the benzene ring, $\Sigma q_+$(ring) and overall negative electron-excess charge, $\Sigma q_-$

| Parameter | Phenol | 1,2-Dihydroxy | 1,3-Dihydroxy | 1,4-Dihydroxy | 1,2,3-Trihydroxy | 1,3,5-Trihydroxy |
|---|---|---|---|---|---|---|
| $\log k'_w$ | 1.8 | 2.0 | 2.30 | 2.15 | 2.20 | 2.7 |
| $\Delta_1$ | 0.34 | 0.35 | 0.38 | 0.32 | 0.30 | 0.41 |
| $\Delta_2$ | | 0.27 | 0.40 | 0.32 | 0.34 | 0.44 |
| $\Delta_3$ | | – | – | – | 0.32 | 0.43 |
| $\Sigma q_+$(ring) | 0.90 | 0.16 | 0.13 | 0.13 | 0.20 | 0.18 |
| $\Sigma q_-$ | −0.58 | −0.74 | −0.94 | −0.79 | −0.98 | −1.32 |

Δ is the difference in the electronic charges borne by the oxygen atom and the carbon atom adjacent to it in the ring.

tween the local dipoles and the flat, rigid surface of the layers in the PGC structure, the dispersion interactions thus being favoured in the perpendicular direction to the PGC layers. Kaliszan [44] pointed out that a special form of dispersion interactions can be observed in large molecules containing $\pi$-electrons such as the PGC layers which can simply be described as gigantic aromatic molecules composed entirely of carbon. In these molecules, the length of the fluctuating instantaneous dipole can be so great that the actual interactions are of individual charges changing their position and not the instantaneous dipoles. This form of dispersion interaction is in agreement with the fact that all the polar substituents account for retention, the PGC adapting its fluctuating charges to the different local dipoles in the molecule. Depending on the position of the substituents, local dipoles are not equivalent, as shown by the calculation from the electron density on particular atoms, which is an effective means of quantifying the inter-substituent effect. The local dipolar moments were sometimes difficult to calculate for polar groups such as COOH and some others. The overall negative electron-excess charge density, $\Sigma q_-$, was therefore calculated and we found that the highest resonance effect was always characterized by the highest $\Sigma q_-$ value, as shown for 1,3-dinitrobenzene or 1,3-dihydroxy- and 1,3,5-trihydroxybenzene. A high $\Sigma q_-$ value corresponds also to stronger and/or more numerous local dipoles. Fig. 4 shows that there is good agreement between $\Sigma q_-$ and $\log k'_w$ obtained for phenol and di- and trihydroxybenzenes; the deviation observed for 1,2,3-trihydroxybenzene is certainly due to steric hindrance of the three groups.

The overall negative electron-excess charge density was calculated for all the molecules in Table 1. Fig. 5 shows the variation of $\log k'_w$ with the corresponding $\Sigma q_-$ values. We can observe a trend showing the importance of the overall negative electron-excess charge density for the retention. The more heteroatoms are present in the molecule, the more resonance effects are observed between the ring and the substituents and the higher the retention of the analyte is.

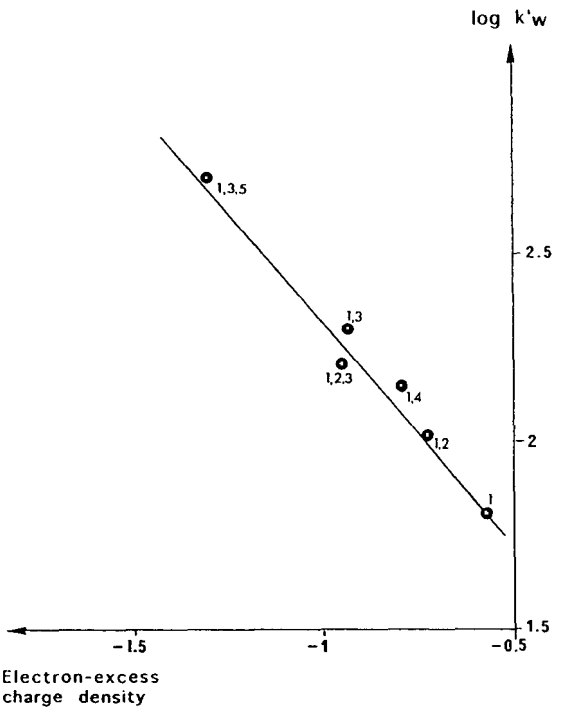


Fig. 4. Relationship between $\log k'_w$ and the overall negative electron-excess charge density, $\Sigma q_-$, of phenol and hydroxybenzenes. The numbers indicate the positions of the hydroxy groups on the benzene ring.

The value of $\Sigma q_-$ is a means of quantifying the electronic characteristics, i.e., the electronic charges of the heteroatom and the induced resonance effects. The correlation in Fig. 5 is similar to that observed between $\log k'_w$ and $\log P_{oct.}$ with $C_{18}$ silicas. It is obtained over a wide variation in $\log k'_w$ from 1 to 4.5 and can be used for obtaining an approximate value of retention. On the basis of instantaneous dipole (or individual charges)-induced dipole interactions, the correlation should be better with the sum of the square of local dipolar moments, taking into account the polarizability of the medium. However, this correlation requires some more complicated calculations.

This result was obtained for very polar compounds. Regarding alkylbenzenes, characterized by similar $\Sigma q_-$ values, the $\log k'_w$ data are situated on a vertical line and do not fit the curves, the retention of these compounds being

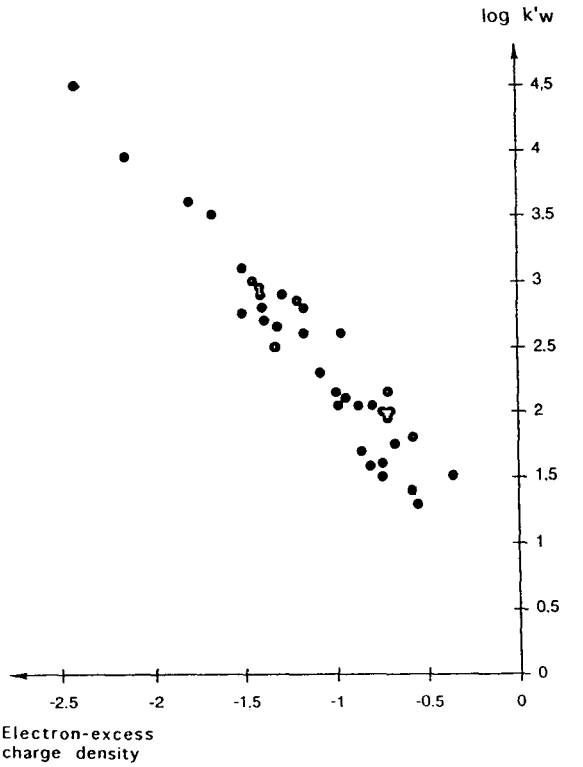


Fig. 5. Relationship between $\log k'_w$ and the overall negative electron-excess charge density, $\Sigma q_-$, of benzene derivatives substituted by polar groups. See Table 1 for compounds.

mainly due to both hydrophobic and small dispersion interactions that are not additive. Comparison between the respective contributions of hydrophobic and electronic interactions would require more data for apolar and moderately polar compounds.

## 4. Conclusion

The porous graphitic carbon retains polar compounds fairly well under reversed-phase conditions. It is obvious now that the retention behaviour of solutes is different from that observed with other reversed-phase sorbents. The prediction of the retention factors of analytes requires a good knowledge of the interactions involved in the retention process. The work presented here is a small contribution, showing that electronic interactions are more important than hydrophobic interactions in the retention mechanism of polar compounds. More data should be collected to widen our knowledge of the PGC behaviour. A better knowledge of the parameters that would allow the characterization of the polarity of molecules is also necessary.

The high retention of some very polar compounds in water confirms the unique potential of PGC as an extraction sorbent for trace analyses for some water-soluble micropollutants.

## Acknowledgement

The authors thank Professor John Knox for fruitful discussions.

## References

[1] K.K. Unger, P. Roumeliotis, H. Mueller and H. Goetz, J. Chromatogr., 202 (1980) 3–14.
[2] K.K. Unger, Anal. Chem., 55 (1983) 361A–375A.
[3] J.H. Knox, K.K. Unger and H. Mueller, J. Liq. Chromatogr., 6 (1983) 1–36.
[4] M.T. Gilbert, J.H. Knox and B. Kaur, Chromatographia, 16 (1982) 138–146.
[5] H. Colin, C. Eon and G. Guiochon, J. Chromatogr., 119 (1976) 41–51.
[6] H. Colin, C. Eon and G. Guiochon, J. Chromatogr., 122 (1976) 223–242.
[7] W. Golkiewicz, C.E. Werkhoven-Goewie, U.A.Th. Brinkman, R.W. Frei, H. Colin and G. Guiochon, J. Chromatogr. Sci., 21 (1983) 27–33.
[8] J.H. Knox and M.T. Gilbert, UK Pat., 7 939 449; US Pat., 4 263 268.
[9] J.H. Knox, B. Kaur and G.R. Millward, J. Chromatogr., 352 (1986) 3–25.
[10] B. Kaur, LC·GC Int. 3, No. 3 (1990) 41–48.
[11] B. Bassler and R.A. Hartwick, J. Chromatogr. Sci., 27 (1989) 162–165.
[12] N. Tanaka, T. Tanigawa, K. Kimata, K. Hosoya and T. Araki, J. Chromatogr., 549 (1991) 29–41.
[13] J. Kriz, E. Adamcova, J.H. Knox and J. Hora, J. Chromatogr. A, 663 (1994) 151–161.
[14] N. Tanaka, K. Kimata, K. Hosoya, H. Miyanishi and T. Araki, J. Chromatogr. A, 656 (1994) 265–287.
[15] C.S. Creaser and A. Al-Haddad, Anal. Chem., 61 (1989) 1300–1302.
[16] R. Fuoco, M.P. Colombini and E. Samcova, Chromatographia, 36 (1993) 65–70.

[17] M.D. Pastor, J. Sanchez, D. Barcelo and J. Albaiges, J. Chromatogr., 629 (1993) 329–337.
[18] L.G. Tuinstra, J.A. Van Rhijn and A.H. Roos, J. High Resolut. Chromatogr., 13 (1990) 797–802.
[19] G. Gu and C.K. Lim, J. Chromatogr., 515 (1990) 183–192.
[20] J.C. Berridge, J. Chromatogr., 449 (1988) 317–321.
[21] R. Kaliszan, K. Osmialowski, B.J. Bassler and R.A. Hartwick, J. Chromatogr., 499 (1990) 333–344.
[22] B.J. Bassler, R. Kaliszan and R.A. Hartwick, J. Chromatogr., 461 (1989) 139–147.
[23] T.M. Engel and S.V. Olesik, J. High. Resolut. Chromatogr., 14 (1991) 99–102.
[24] E. Forgacs, T. Cserhati and K. Valko, J. Chromatogr., 592 (1992) 75–83.
[25] E. Forgacs and T. Cserhati, Chromatographia, 33 (1992) 356–360.
[26] E. Forgacs, K. Valko and T. Cserhati, J. Liq. Chromatogr., 14 (1991) 3457–3573.
[27] V. Coquart and M.-C. Hennion, J. Chromatogr., 600 (1992) 195–201.
[28] M.-C. Hennion and V. Coquart, J. Chromatogr., 642 (1993) 211–224.
[29] S. Guenu and M.-C. Hennion, J. Chromatogr. A, 665 (1994) 243–251.
[30] P.J. Schoenmakers, H.A.H. Billiet and L. de Galan, J. Chromatogr., 282 (1983) 107–121.
[31] M.-C. Hennion and P. Scribe, in D. Barcelo (Editor), Environmental Analysis, Techniques, Applications and Quality Assurance, Elsevier, Amsterdam, 1993, Ch. 2, p. 24–77.
[32] H. Poppe, J. Chromatogr. A, 656 (1993) 19–36.
[33] M.-C. Hennion, C. Picard, C. Combellas, M. Caude and R. Rosset, J. Chromatogr., 210 (1981) 211–228.
[34] P.W. Carr, J. Li, A.J. Dallas, D.I. Eikens and L.C. Choo Tan, J. Chromatogr. A, 656 (1993) 113–133.
[35] R. Kaliszan, J. Chromatogr. A, 656 (1993) 417–435.
[36] T. Braumann, J. Chromatogr., 373 (1986) 191–225.
[37] V. Pichon, L. Chen, S. Guenu and M.-C. Hennion, J. Chromatogr. A, in press.
[38] R.M. Smith, J. Chromatogr. A, 656 (1993) 381–415.
[39] J.J. Sun and J.S. Fritz, J. Chromatogr., 522 (1990) 95–105.
[40] R.M. Smith and D.R. Garside, J. Chromatogr., 407 (1987) 19–35.
[41] J. March, Advanced Organic Chemistry, Wiley, New York, 3rd ed., 1985.
[42] H. Colin, N. Ward and G. Guiochon, J. Chromatogr., 149 (1978) 169–197.
[43] R. Kaliszan, K. Osmialowski, S.A. Tomellini, S.H. Hsu, S.D. Fazio and R.A. Hartwick, J. Chromatogr., 352 (1986) 141–155.
[44] R. Kaliszan, Quantitative Structure–Chromatographic Retention Relationships, Wiley, New York, 1987.

ELSEVIER

Journal of Chromatography A, 712 (1995) 303–309

JOURNAL OF CHROMATOGRAPHY A

# Analysis of taxol, 10-deacetylbaccatin III and related compounds in *Taxus baccata*

Denis R. Lauren[a,*], Dwayne J. Jensen[a], James A. Douglas[b]

[a]*Ruakura Research Centre, The Horticulture and Food Research Institute of New Zealand, Private Bag 3123, Hamilton, New Zealand*

[b]*New Zealand Institute for Crop and Food Research, Private Bag 3123, Hamilton, New Zealand*

First received 20 December 1994; revised manuscript received 1 May 1995; accepted 4 May 1995

**Abstract**

A method is described for the analysis of taxol and related taxanes in the foliage of *Taxus* spp. such as *T. baccata*. The method has been optimised for recovery and analysis of a range of taxanes of differing polarity, namely: taxol, cephalomannine, baccatin III and 10-deacetylbaccatin III (10-DAB-III). Measured recoveries for all these compounds generally exceeded 84%. The reversed-phase high-performance liquid chromatography system developed uses a "sterically protected" $C_8$ column, and allowed analysis of the components of interest with minimum interference from co-extracted compounds. Typical detection limits for routine operation were in the range of 1–10 mg/kg depending on the component and the particular sample. Analysis of test samples of *T. baccata* have shown variations in taxol concentrations in the range 7–510 mg/kg and of 10-deacetylbaccatin III in the range 52–1185 mg/kg.

## 1. Introduction

Taxol is a diterpenoid natural product showing distinct promise as an anti-cancer agent [1]. It is derived from many *Taxus* spp., including *T. brevifolia*, *T. canadensis*, *T. cuspidata*, *T. media* and *T. baccata* [2,3]. The compound has been isolated from bark, needles and small twigs, and more recently, from tissue cultures [4]. Typical concentrations of taxol vary between species, and major differences can be found between samples of the same species and depending on locality and environmental factors [3,5]. The high demand for taxol for clinical use has led to intense study of other forms of production, including the sustainable harvesting of *Taxus* spp. and partial synthesis from related compounds. Numerous related compounds have been identified, including those more commonly cited such as cephalomannine, 10-deacetylcephalomannine, baccatin III and 10-deacetylbaccatin III (10-DAB-III). Structures for taxol and 10-DAB-III are shown in Fig. 1.

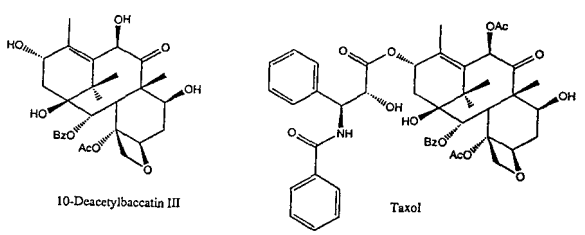


Fig. 1. Structures of two major taxanes found in *T. baccata*.

* Corresponding author.

0021-9673/95/$09.50 
*SSDI* 0021-9673(95)00541-2

As a part of studies of production of taxanes by *T. baccata* from throughout New Zealand, we desired to analyse for taxol, cephalomannine, baccatin III and 10-DAB-III. The main compounds of interest were taxol itself and 10-DAB-III, a useful precursor of the taxol-analogue taxotere and which is reported to be present in *T. baccata* at higher concentrations than taxol [2].

The most commonly used method for analysis of taxanes in plant extracts is high-performance liquid chromatography (HPLC). Methanol [4–8] or methanol–dichloromethane [2,3,9] have been the common solvents of choice for extracting taxanes from plant samples, and earlier published methods [2,5,6] relied on direct analysis of relatively crude plant extracts, generally after simple partition of dried extract between dichloromethane and water. While useful comparative data was presented, problems were reported with high backpressure, short column life and interference from co-extractives. More recent methods have used preliminary hexane washes of the plant material [3,9], or silica [7] or $C_{18}$ solid-phase systems [4,8] for additional clean-up. Our experience was that the more simple procedures, including those with hexane washes, yielded chromatograms with high background baseline absorbance. Accurate quantitation was difficult, especially for samples with low taxane content. Also, the published silica and $C_{18}$ clean-up methods had been optimised for taxol and the closely related cephalomannine, and accordingly were not suitable for other, more polar compounds of interest, such as 10-DAB-III.

The principal purpose of this work was to develop a reliable method for the clean-up of *T. baccata* extracts prior to analysis for taxanes of different polarity. Methanol was chosen as the extraction solvent, and we have adapted a partition clean-up procedure commonly used in our laboratories for the analysis of a number of trace pesticide residues in plant extracts, and combined that with a modification of the silica column clean-up method for taxol described by Castor and Tyler [7]. The analytical system using gradient HPLC developed employs a "sterically protected" $C_8$ reversed-phase column. This is the first report to describe the use of this type of column for analysis of taxanes.

## 2. Experimental

### 2.1. Chemicals and reagents

Standards of taxol, cephalomannine and baccatin III were donated by the Drug Synthesis and Chemistry Branch, Developmental Therapeutics Program, Division of Cancer Treatment, National Cancer Institute (Bethesda, MD, USA). 10-DAB-III was purchased from Sigma (St. Louis, MO, USA). All solvents were either Nanograde (Mallinckrodt) or HPLC grade. Davisil silica (pore size 60 Å, particle size 149–250 $\mu$m) was supplied by Alltech (Deerfield, IL, USA).

### 2.2. Equipment

HPLC was performed on a Shimadzu LC-6A gradient system fitted with a 6AG mixing chamber, SCL-6A autoinjector, CTO-6A column oven, SPD-6AV variable-wavelength UV–Vis absorbance detector and a C-R4AX data system. Multi-wavelength and spectral acquisitions were also obtained for some samples, using a Linear 206 PHD multiple-wavelength detector. The analytical column was a 5-$\mu$m Zorbax SB-$C_8$ (150 × 4.6 mm I.D.) (Rockland Technologies, Newport, DE, USA), and was preceded by a 2-$\mu$m in-line filter (Rheodyne, Cotati, CA, USA).

### 2.3. Sample extraction and clean-up

Foliage samples of *T. baccata* were composed of leaves and small twigs collected around the circumference of individual trees at a height of 1.4 m. The samples were separated into leaf and stem fractions, dried in a forced-air oven at 35°C, finely ground and then stored at −20°C until analysis.

Ground plant material (2 g) was placed in a stoppered 130-ml tube with methanol (100 ml)

and the mixture shaken on a flat-bed orbital shaker for 12–16 h. The mixture was allowed to settle out and clarify, then an aliquot (10 ml) was removed and diluted with 5% saline solution (10 ml). This solution was washed with hexane (2 × 10 ml) and the hexane washes discarded. The solution was then partitioned with dichloromethane (4 × 10 ml). These partition fractions were collected together by filtering each sequentially through anhydrous sodium sulphate (3 g). The combined dichloromethane fraction was evaporated to dryness, redissolved in dichloromethane (2 ml), and then added to a glass column (250 × 10 mm I.D.) dry-packed with silica (1 g). The column was washed with dichloromethane (2 × 2 ml), then with acetone–dichloromethane (4:96) (2 × 5 ml), and each of these washes discarded. Taxanes were eluted from the column with acetone–dichloromethane (50:50) (2 × 5 ml). These eluates were combined and evaporated to dryness ($N_2$, 35°C), and then dissolved in methanol (1 ml) for analysis by HPLC.

### 2.4. HPLC conditions

The analytical column was held at 35°C and the mobile phase flow-rate was 1 ml/min. Separation was achieved with a two-pump gradient programme for pump A (acetonitrile) and pump B (methanol–water, 20:80) as follows: 80% B for 5 min, then jump to 75% B at 5.1 min; hold at 75% B until 14 min then change to 65% B over 10 min and hold at 65% B until 41 min. At this time a column flush-out sequence was commenced by changing to 35% B over 3 min, holding at 35% B from 44 to 55 min, then resetting to 80% B over 5 min, and allowing 20 min for equilibration of the column and stabilisation of the baseline. Thus the total run-time per sample was 80 min. The programme delay through the system was 5–6 min from event to appearance at the detector.

The detector was set at 227 nm. Injection size for standards and samples was 10 μl. Quantitation was by peak height relative to a mixed external standard of 25 μg/ml for each component in methanol. The standard components gave responses of 60–120% of full scale deflection at 0.02 AUFS depending on the compound. The analysis solution concentration was multiplied by a factor of five to convert to mg/kg dry weight. A further multiplication factor of 0.0001 could be used to convert mg/kg to the commonly quoted units of percent of dry weight.

Spectral scanning acquisitions used 31 wavelengths at 4 nm intervals from 201 to 321 nm inclusive. Wavelength response ratios were calculated using 229 and 273 nm.

### 2.5. Recovery tests

Preliminary recovery tests were conducted using a mixed standard solution in methanol. Aliquots equal to 5 μg of each component were processed separately through both the partition and silica clean-up sections of the method. Each of the four partition fractions was collected and analysed separately for these preliminary tests, and silica column recoveries were tested using washes of 4:96, 20:80 and 50:50 acetone–dichloromethane, and 100% acetone. Plant extracts known to contain high levels of taxanes were also tested in these preliminary tests, and the identity of peaks of interest was confirmed by spectral scans and spiking tests.

The final recovery tests were conducted in two identical batches, processed on different days using mixed standard solutions and an extract of a very low taxane content sample of *T. baccata* both with and without spiked taxanes. These five samples plus two samples of high taxane content material were also used to determine the reproducibility of the method. In both batch tests duplicate analyses were performed on the following samples: mixed standard in methanol (5 μg each component per 10 ml), mixed standard in methanol (25 μg each component per 10 ml), low-taxane extract, low-taxane extract plus 5 μg of each component per 10-ml aliquot, low-taxane extract plus 25 μg of each component per 10-ml aliquot, extracts of two different high-taxane materials. Results for the two batches were used as one set for estimation of recoveries and repeatability of the method.

## 3. Results and discussion

Analysis of individual fractions from the partition clean-up step showed that the hexane wash, incorporated to remove potential interfering waxy non-polar components [3], removed less than 1.5% of the compounds of interest. The four dichloromethane extractions were necessary for high recovery of 10-DAB-III. While taxol, cephalomannine and baccatin III were typically 95–100% recovered by two dichloromethane extractions, 10-DAB-III was only 70% recovered, and required an extra two extractions to achieve about 90% recovery. Attempts were made to improve the extraction efficiency for 10-DAB-III by modifying the quantity, concentration and pH of the saline solution, by alternate extraction solvents, or by centrifuging the partition mixture. None of the options tested improved the described method.

Preliminary testing of fractions from the silica clean-up column showed that none of the peaks of interest were removed by the 4:96 acetone–dichloromethane wash, while 20:80 acetone–dichloromethane removed most of the taxol, as reported by Castor and Tyler [7]. This fraction also contained most of the cephalomannine and baccatin III, but only 10–20% of the 10-DAB-III. Washing the silica column with 50:50 acetone–dichloromethane as described in the method, removed all the compounds of interest, and none were found when a subsequent wash with 100% acetone was used. We have found that fractions off silica have a lower background baseline absorbance and are noticeably cleaner than samples through the partition clean-up only, especially in the first 10 min of the chromatogram. This is illustrated by comparing Figs. 2A and 2B.

The HPLC conditions were selected after investigation of a number of gradient options and also the alternative of isocratic analysis in two polarity groupings. Conditions were optimised to give good separation of the two major components, taxol and 10-DAB-III. In some samples interferences occurred for the minor components cephalomannine and baccatin III. For the purpose of our studies, which was to

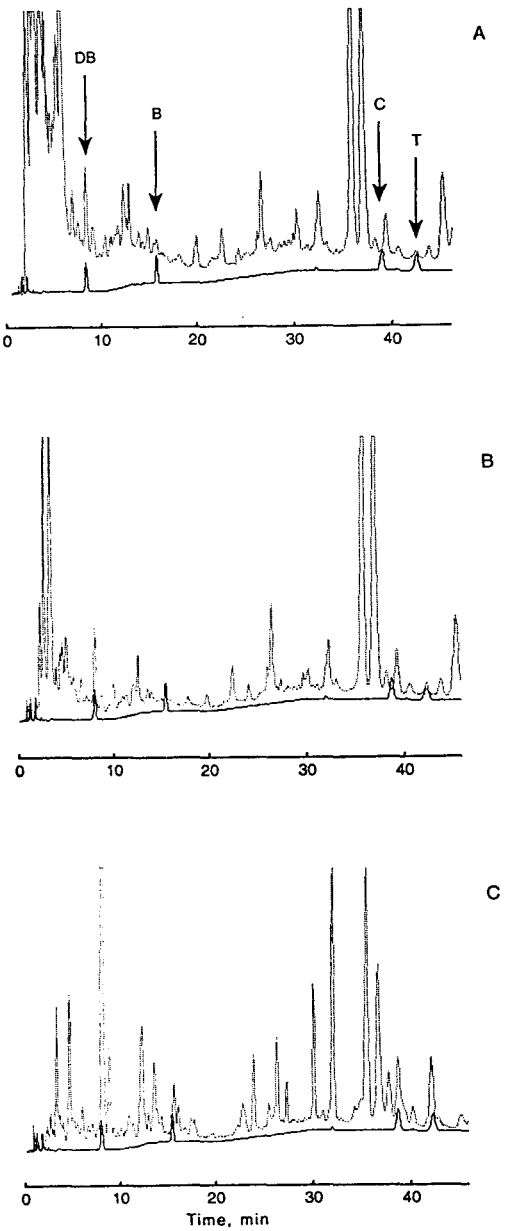


Fig. 2. HPLC chromatograms of (A) low taxane content sample after partition clean-up only and with 5 μg/ml mixed standard as overlay, showing 10-DAB-III (DB), baccatin III (B), cephalomannine (C) and taxol (T). Note that the overlay chromatogram shows the true baseline absorbance of the system. (B) as (A) but after full clean-up of sample. (C) High taxane content extract H1 after full clean-up and with 5 μg/ml mixed standard as overlay. Chromatographic conditions as in Experimental. Figure shows detection at 227 nm with 0.04 AUFS.

identify high-productive plants, it was more important to have accurate values for the major components. Retention times for the peaks of interest were: 8.0 min (10-DAB-III), 15.8 min (baccatin III), 39.0 min (cephalomannine) and 42.5 min (taxol). Sample chromatograms are shown in Fig. 2.

Previous published data suggests that there is no one HPLC column type that will separate or resolve all the taxanes completely. Most recent reports have used specialised columns with phenyl-type phases [2–4,7,8,10]. The present results show that good separations can be achieved using the "sterically protected" $C_8$ column. This column therefore offers another selectivity option to researchers investigating new and known taxanes from *Taxus* species. We have found the SB-$C_8$ column and the separation conditions to be robust. To date over 400 samples, including about 100 partly cleaned up fractions, have been run through the column without any apparent deterioration in the column characteristics or increase in backpressure. The use of an elevated column temperature and a flush-out with each sample may help in this respect.

The integrity of the peaks of interest during method development was confirmed by spiking tests and spectral scans. After development, the assignments were similarly confirmed in selected samples put through the method. These scans showed the two main peaks of interest (taxol and 10-DAB-III) to have spectra very similar to authentic standard materials, with UV maxima at about 230 nm, and little absorbance above 260 nm (see Fig. 3). Similar results were obtained for baccatin III and cephalomannine in some samples, but often these two compounds were present in too low quantities to obtain definite spectra. An alternative approach was to compare chromatograms acquired at 229 and 273 nm. Those acquired at 273 nm showed much lower response for all four peaks of interest, and therefore supported the assignments. For example, measured response ratios ($A_{229}/A_{273}$) in a sample were 14.5, 12.5, 18.8 and 17.0, respectively, for 10-DAB-III, baccatin III, cephalomannine and taxol. These compare with equivalent values for standards of 14.6, 13.9, 20.4 and 15.5. Wavelength response ratios have been used elsewhere [7,10] to estimate taxane peak purity in the presence of potential interfering co-extractive compounds that have strong absorbance near 280 nm.

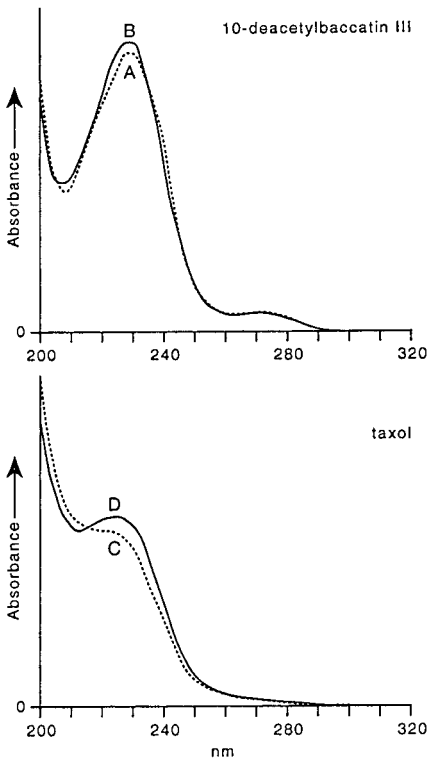


Fig. 3. Spectra for 10-DAB-III and taxol acquired during chromatography of a standard mixture (A and C) and a cleaned up sample of *T. baccata* (B and D).

The effectiveness and reproducibility of the chosen method was confirmed by replicate recovery tests on standards, on a low taxane content *T. baccata* extract with and without spikes, and on two *T. baccata* extracts containing moderately high levels of taxol and 10-DAB-III. The results are given in Table 1, and show good repeatability of results. Standard deviations are typically less than 10% of the mean value obtained. Also, the results represent recoveries better than 76% and generally better than 84%.

Detection limits for standards under routine operating conditions were below 0.13 $\mu$g/ml

Table 1
Reproducibility ($n = 4$) and recovery data for taxanes through the method[a]

| Sample | Mean concentration ($\mu$g/ml in final analysis solution) for taxanes | | | |
|---|---|---|---|---|
| | 10-DAB-III | Baccatin-III | Cephalomannine | Taxol |
| *Tests for recovery and reproducibility* | | | | |
| 5 $\mu$g/10 ml standard in methanol | 4.2 (0.2) | 4.8 (0.1) | 4.5 (0.2) | 4.6 (0.3) |
| 25 $\mu$g/10 ml standard in methanol | 19.2 (1.9) | 21.5 (2.0) | 22.4 (0.5) | 22.3 (0.6) |
| Extract L (low taxane content) | 10.4 (1.0) | 1.1 (0.2) | n.d. | 1.4 (0.2) |
| 5 $\mu$g/10 ml spike in extract L | 15.0 (0.9) | 5.1 (0.1) | br. | 6.2 (0.2) |
| 25 $\mu$g/10 ml spike in extract L | 32.2 (3.0) | 24.6 (1.5) | 24.5 (1.2) | 25.1 (0.9) |
| *Tests for reproducibility only* | | | | |
| Extract H1 (high taxane content) | 126.1 (6.3) | 8.9 (0.4) | 14.7 (1.3) | 21.3 (2.1) |
| Extract H2 (high taxane content) | 70.6 (2.5) | 9.0 (0.25) | 22.0 (1.1) | 48.0 (5.4) |

[a] Samples of 10 ml of *T. baccata* extracts or standard solutions in methanol were processed through the method and then made up in 1 ml of methanol for analysis by HPLC. Expected concentrations for the two levels of standards are 5 and 25 $\mu$g/ml. The four replicates represent results from two batches of duplicate samples processed on different days. Values in parentheses represent the standard deviation.
n.d. = not detected at detection limit.
br. = broad peak. Component not resolved from adjacent co-extractive. Accurate analysis not possible.

(equivalent to 0.66 mg/kg) (signal to noise ratio at least 5), while detection limits in low-taxane samples of *T. baccata* were more likely to be in the range 1–10 mg/kg depending on the component and the particular sample. In samples analysed to date, taxol concentrations have varied from 7 to 510 mg/kg, while 10-DAB-III levels have been in the range 52–1185 mg/kg.

## 4. Conclusion

The method developed gives clean analytical samples and allows reliable analysis of four taxanes with very different polarity in extracts of *T. baccata*. Recently, another method was reported for the analysis of taxanes with a range of polarity in extracts cleaned up by a combination of partition and selective solubility off a solid-phase (celite) column [10]. We had earlier investigated using celite in a similar manner, and although promising results were obtained, considered that silica clean-up was potentially more adaptable. Clean-up efficiency by the two methods was similar but there were selectivity differences. Therefore, it is probable that investigation of combinations of the two phases would be useful for samples found to be intractable by either method alone.

## Acknowledgements

We thank Dr. G. Cragg, National Cancer Institute, Frederick, MD, USA for arranging a supply of taxanes, and also J.M. Follett for collection, drying and grinding of the *T. baccata* samples used for this study, and M.P. Agnew for technical assistance.

## References

[1] P.F. Heinstein and C.-J. Chang, Annu. Rev. Plant Physiol. Plant Mol. Biol., 45 (1994) 663.
[2] K.M. Witherup, S.A. Look, M.W. Stasko, T.J. Ghiorzi and G.M. Muschik, J. Nat. Prod., 53 (1990) 1249.
[3] N.C. Wheeler, K. Jech, S. Masters, S.W. Brobst, A.B. Alvarado, A.J. Hoover and K.M. Snader, J. Nat. Prod., 55 (1992) 432.
[4] E.R.M. Wickremesinhe and R.N. Arteca, J. Liq. Chromatogr., 16 (1993) 3263.
[5] R.G. Kelsey and N.C. Vance, J. Nat. Prod., 55 (1992) 912.

[6] K.M. Witherup, S.A. Look, M.W. Stasko, T.G. McCloud, H.J. Issaq and G.M. Muschik, J. Liq. Chromatogr., 12 (1989) 2117.
[7] T.P. Castor and T.A. Tyler, J. Liq. Chromatogr., 16 (1993) 723.
[8] M.J.I. Mattina and G.J. MacEachern, J. Chromatogr. A., 679 (1994) 269.
[9] A.G. Fett Neto and F. DiCosmo, Planta Med., 58 (1992) 464.
[10] W.J. Kopycki, H.N. ElSohly and J.D. McChesney, J. Liq. Chromatogr., 17 (1994) 2569.

ELSEVIER

Journal of Chromatography A, 712 (1995) 311–320

JOURNAL OF CHROMATOGRAPHY A

# Chromium speciation by anion-exchange high-performance liquid chromatography with both inductively coupled plasma atomic emission spectroscopic and inductively coupled plasma mass spectrometric detection☆

Francine A. Byrdy, Lisa K. Olson, Nohora P. Vela, Joseph A. Caruso*

*Department of Chemistry, University of Cincinnati, Cincinnati, OH 45221-0172, USA*

First received 22 November 1994; revised manuscript received 20 April 1995; accepted 1 May 1995

**Abstract**

Development of a new method for the determination of Cr(III) and Cr(VI) is described. Anion-exchange high-performance liquid chromatography (HPLC) was used to separate Cr(III) and Cr(VI) with on-line detection by inductively coupled plasma atomic emission spectroscopy (ICP-AES) at 2766 Å in preliminary studies, and inductively coupled plasma mass spectrometry (ICP-MS) with single-ion monitoring at $m/z$ 52 and $m/z$ 53 for final work. A mobile phase consisting of ammonium sulfate and ammonium hydroxide was used, and a simple chelation procedure with EDTA was followed to stabilize the Cr(III) species in standard solutions. ICP-MS results indicated the feasibility of using chromium isotope $m/z$ 53 instead of the more abundant $m/z$ 52 isotope due to a high mobile-phase background most significantly from the $SO^+$ polyatomic interference. The absolute detection limits based on peak-height calculations were 40 pg for Cr(III) and 100 pg for Cr(VI) in aqueous media by HPLC–ICP-MS. The linear dynamic range extended from 5 ppb (ng/ml) to 1 ppm ($\mu$g/ml) for both species. By HPLC–ICP-AES, detection limits were 100 ng for Cr(III) and 200 ng for Cr(VI). Cr(III) was detected in NIST-SRM 1643c (National Institute of Standards and Technology-Standard Reference Material, Trace Elements in Water) by HPLC–ICP-MS at the 20 ppb level.

## 1. Introduction

In May 1988, a symposium was held entitled "The Chromium Paradox in Modern Life [1]". The symposium title not only illustrates the current interest in chromium, but aptly describes the element as a "paradox" as well. Chromium is naturally-occurring, commonly found in rocks and minerals, and is used in numerous industrial processes including steel alloying and textile production. Known to exist in all oxidation states from 0 to VI, Cr(III) and Cr(VI) are the forms most commonly found [2]. There are a number of predominant chromium species which may exist depending on solution pH [2–4].

Chromium is a "paradox" since it is classified as both biologically important and also as a toxic industrial hazard depending upon its oxidation state. Cr(III) is known to be an essential trace nutrient involved in the mechanism of the action

* Corresponding author.

☆ Presented in part at the *1994 Winter Conference on Plasma Spectrochemistry*, San Diego, CA, Jan. 10–15, 1994.

0021-9673/95/$09.50 
*SSDI* 0021-9673(95)00528-5

of the pancreatic hormone insulin and/or glucose metabolism [5]. No minimum daily requirement of chromium has yet been established, but 50–200 μg per day is considered adequate. Cr(III) is found in fruits, vegetables, meats, cereals and various other foods. A deficiency of this nutrient may lead to glucose intolerance [6]. Conversely, Cr(VI) is known to be carcinogenic and mutagenic. Unlike Cr(III), Cr(VI) may cross cellular membranes by way of non-specific anion carriers [7], causing skin ulcerations, nasal perforations, and lung cancer [2]. The subsequent reduction of Cr(VI) to intermediates such as Cr(IV) and Cr(V) is thought to play a role in its toxicity [7].

It is obvious that speciation (the determination and quantitation of different chemical forms) is necessary to obtain an adequate toxicological sample assessment for chromium. As a result, several methods for inorganic chromium speciation have been described. Non-chromatographic methods are generally labor and time-intensive. In general, flow-injection and HPLC procedures appear to be simpler and more rapid. A summary of some of these methods with UV, FAAS (flame atomic absorption spectroscopy), ETAAS (electrothermal atomic absorption spectroscopy), DCP (direct current plasma)-AES, and ICP-AES detection may be found in Ref. [8]. Often, Cr(III) is calculated by subtraction of Cr(VI) from total chromium. This type of calculation may involve some uncertainty. Simultaneous determination would not only be less time-consuming, but would pose less risk of calculation errors [9]. In some studies, a conversion step with Ce(IV) was necessary, but this may introduce contaminants [10,11]. Preconcentration is commonly done on-column to improve detection limits. However, poor sensitivity, low sampling frequency [12,13], and incomplete recovery [12] may result anyway. In another study spectral interferences from low selectivity posed a problem [14].

There are only a few HPLC techniques which have employed ICP-AES or DCP-AES detection for the speciation of chromium [15–21]. Various advantages may be obtained using ICP-MS detection over these optical techniques. ICP-MS provides excellent sensitivity, selectivity, and the potential for isotope determinations. Plasma-MS detection limits are generally two to three orders of magnitude lower than those attainable using AES, and new advances in software programs allow the user to acquire data simultaneously for several elements over time. In addition, elemental MS spectra are relatively simple compared to optical spectra.

Roehl and Alforque [22] have compared colorimetric with ICP-MS detection for the determination of Cr(VI) by ion chromatography (IC). Detection limits for both methods were in the 1–2 ppb range for Cr(VI). Total chromium was determined without IC and Cr(III) may be calculated from the difference. As stated earlier, this type of calculation is unfavorable. Arar et al. [23] have reported the off-line determination of Cr(VI) in sludge incinerator emissions using an ion chromatographic method from Ref. [3]. A preconcentration scheme and post-column reaction were used, followed by the collection, acidification, and dilution of samples prior to ICP-MS detection. On-line detection of both Cr(III) and Cr(VI) in one step would be less time-consuming. Jakubowski et al. [24] have speciated chromium using ion-pair chromatography and hydraulic high-pressure nebulization with ICP-MS detection. Since the eluent contained 25% methanol, polyatomic interferences from carbon were a problem.

As indicated in the previous paragraph, problems may be encountered when an HPLC method is developed for ICP-MS detection. The coupling of HPLC with plasma MS is not always straightforward. Restrictions are placed on the types of mobile phases which may be employed in order to achieve overall simplicity of the interface. Particular areas of concern include the salt and organic content of the mobile phase. Clogging of the torch tip and orifices of the ICP-MS may result from salt deposition when mobile phases with total dissolved salt concentrations greater than 0.2% are used. Clogging can lead to decreased sensitivity and unsatisfactory detection limits. Organic mobile phases tend to cause plasma instability as well as carbon deposition on the sampler and skimmer cones which can lead to decreased sensitivity. Additionally, the polyatomic ion $^{40}Ar^{12}C^{+}$ may form when organic mobile phases such as those com-

monly employed in reversed-phase or ion-pairing techniques are used, and interference problems may ensue.

The method chosen was adapted from a Technical Note by Dionex Corporation [3]. This anion-exchange method was described for the determination of Cr(VI) in water, wastewater, and solid waste extracts employing a post-column reaction scheme using diphenylcarbohydrazide (DPC) in an acidic medium with visible detection at 520 nm. Bulk sample analysis may be done using DPC. There are, however, potential interferences from other colored species such as Fe(III) or Cu(II) complexes. Additionally, V, Mo, and Hg may form colored reaction products with DPC and interfere with the detection of Cr [8]. This technical note has been modified and extended to the determination of both Cr(III) and Cr(VI) by utilizing a very simple chelation procedure to stabilize the former species [9]. No post-column reaction was necessary with either ICP-AES or ICP-MS detection. The accuracy of the final method was assessed by analyzing a certified reference material, and the experimental results were compared with the certified reference value.

## 2. Experimental

### 2.1. Instrumentation

A Dionex metal-free HPLC system (Model DX-300, Sunnyvale, CA, USA) consisting of an advanced gradient pump with an eluent degas module was used. A Rheodyne (Cotati, CA, USA) Model 9125 metal-free injector was employed with a 100-$\mu$l injection loop. The temperature of the analytical column was controlled at 25°C with an Alltech water jacket (Alltech Associates, Deerfield, IL, USA). The outlet of the analytical column was connected directly to a type C1 concentric nebulizer (Precision Glassblowing of Colorado, Parker, CO, USA) by means of Teflon tubing of 0.012 mm I.D. and 68 cm in length. A double-pass spray chamber was used.

For preliminary work, the ICP-AES instrument used was a Plasma-Therm HFS-2500D (Kreeson, NJ, USA). All gas flow-rates were regulated with a needle valve flowmeter which was calibrated before experiments were begun. A 1.26 m Czerny-Turner Model 1269 (Spex Industries, Metuchen, NJ, USA) monochromator with a 2400 lines/mm grating was used. A potential of 750 V was applied for detection with the photomultiplier tube. The data acquisition was done with a Datamate microcomputer (Spex Industries) and spectra were plotted using a Houston Instrument's HI Plotter. Operating conditions for the ICP-AES set-up are given in Table 1.

The ICP-MS instrument was a VG PlasmaQuad PQII + Turbo equipped with a high-performance interface (VG Instruments, Winsford, Cheshire, UK). A nickel sampler and skimmer, each with a 1.0-mm orifice, were used. Adjustment of the sampling position and ion lenses for the optimum chromium signal at $m/z$ 52 and $m/z$ 53 was done using solution nebulization of a 10 ppb standard of both chromium species in distilled, deionized water. Operating conditions for the ICP-MS set-up are given in Table 1.

### 2.2. Reagents

The mobile phase was prepared from 99.999% ammonium sulfate (Aldrich, Milwaukee, WI, USA), double distilled ammonium hydroxide (Aldrich), and distilled, deionized 18 MΩ water (Barnstead, Boston, MA, USA). The mobile

Table 1
Typical ICP-AES and ICP-MS operating conditions

| Conditions | ICP-AES | ICP-MS |
|---|---|---|
| Rf power | | |
| Forward | 1.35 kW | 1.45 kW |
| Reflected | <5 W | <5 W |
| Gas flow-rates | | |
| Auxiliary | 1 l/min | 1.2 l/min |
| Coolant | 16 l/min | 12 l/min |
| Nebuliser | 1 l/min | 1 l/min |
| Spray chamber | double-pass | double-pass |
| Nebuliser | concentric | concentric |

phase was degassed prior to use and an in-line filter was employed. For ICP-AES work, Cr(III) stock solutions (1000 ppm) were made from $CrCl_3 \cdot 6H_20$ (Fisher Scientific, Fair Lawn, NJ, USA) in 5% (v/v) redistilled nitric acid (GFS Chemicals, Columbus, OH, USA) (in distilled, deionized 18 MΩ water). For the ICP-MS method, a chelation procedure was followed as given below.

For both ICP-AES and ICP-MS work, a Cr(VI) stock solution (1000 ppm) was prepared after drying $K_2Cr_2O_7$ (99.95–100.05%, Aldrich) in a 90°C oven for 2 h. Distilled, deionized 18 MΩ water was used for dilutions. All working solutions were prepared fresh daily from stock solutions filtered through sterile 0.2-μm hydrophilic nylon membranes (Alltech Associates). Standards ranging in concentration from 1 ppm to 100 ppm were employed in the ICP-AES study. With ICP-MS detection, standards ranged from 1 ppb to 1 ppm. Stock solutions were made separately and then mixtures of Cr(III) and Cr(VI) were prepared fresh on the day of analysis. The mixtures were naturally at a pH of 5.

### 2.3. Chelation procedure

To stabilize the Cr(III) species and guard against the potential oxidation of Cr(III) to Cr(VI), a chelation procedure found in the literature was employed in the ICP-MS method only [9]. For the stock standard (600 ppm), Cr(III) as $CrCl_3 \cdot 6H_2O$ was dissolved in distilled, deionized 18 MΩ water, and the disodium salt of EDTA (Fisher Scientific) was added to the 600 ppm Cr(III) stock standard. The mixture was heated for 1 h at 50°C and the pH of the solution was adjusted to 4.0 with $NH_4OH$. A blank solution was prepared with an amount of EDTA corresponding to that present in a mixture of chelated Cr(III) and Cr(VI) at a concentration of "1 ppm" which was the highest standard concentration employed.

### 2.4. Chromatography

For this study, a 250 × 4 mm I.D. IonPac AS7 10 μm column (Dionex Corp.) was used. In addition, an IonPac AG7 guard column (50 × 4 mm I.D.) was employed in the ICP-AES method, and an IonPac NG1 guard column (35 × 4 mm I.D.) in the ICP-MS method. Both guard columns were purchased from Dionex. The IonPac NG1 is a polymeric reversed-phase column, while the IonPac AS7 and IonPac AG7 are mixed-mode columns. This means that although the AS7 and AG7 columns are primarily used as anion-exchangers, they do have some cation-exchange sites.

Two mobile phase conditions were studied. The chromatography for the ICP-AES method was taken from Ref. 3 with a few modifications: (1) the corresponding guard column to the AS7, the AG7, was used instead of the NG1 as proposed in the publication; (2) no post-column reaction scheme was employed; and (3) standards were made in doubly distilled 5% $HNO_3$ since this matrix was found to be optimal for the study. The ICP-MS method utilized a weaker mobile phase, the NG1 guard column, and a flow-rate of 2.0 ml/min to reduce the analysis time by 1/3. A comparison of the method conditions is given in Table 2. Prior to use, both the analytical and guard columns (Dionex AS7 and AG7 or NG1) were conditioned by pumping the mobile phase through the columns at a flow-rate of 2 ml/min for at least 1 h.

Chromatography data were collected at 2677.16 Å for ICP-AES detection and using single-ion monitoring at $m/z$ 52 and $m/z$ 53 with a 1.3-s integration time for ICP-MS detection. Data were transferred to an in-house program so that results could be easily imported into a spreadsheet.

## 3. Results and discussion

In anion-exchange chromatography, the column contains cationic sites to which solute anions are attracted. In the simplest case, an anion should be retained on an anion-exchange column, while a cationic species should be unretained and elute with the void volume or the solvent front. At acidic pH, Cr(III) exists pri-

Table 2
HPLC method conditions for ICP-AES and ICP-MS detection

| Conditions | ICP-AES Method | ICP-MS Method |
|---|---|---|
| Eluent | 250 m*M* $(NH_4)_2SO_4$<br>100 m*M* $NH_4OH$<br>pH 9.2 | 35 m*M* $(NH_4)_2SO_4$<br>pH 9.2 with $NH_4OH$ |
| Column | Dionex IonPac AS7<br>Dionex IonPac AG7 | Dionex IonPac AS7<br>Dionex NG1 |
| Dimensions | 250 × 4 mm<br>10 μm particle size | 250 × 4 mm<br>10 μm particle size |
| Injection loop | 100 μl | 100 μl |
| Flow-rate | 1.5 ml/min | 2.0 ml/min |
| Detector | ICP-AES 2677.16 Å<br>ICP-MS *m/z* 52 and 53 | ICP-MS *m/z* 52 and 53 |

marily as a cation, while Cr(VI) exists as an anion from pH 2 and beyond pH 6. Since the AG7 column has some cation-exchange sites, the elution of both species proved to be more complicated than originally expected.

### 3.1. ICP-AES method

Fig. 1 shows a chromatogram obtained from a mixture injection of 5 μg of each chromium species with ICP-AES detection using the sulfate

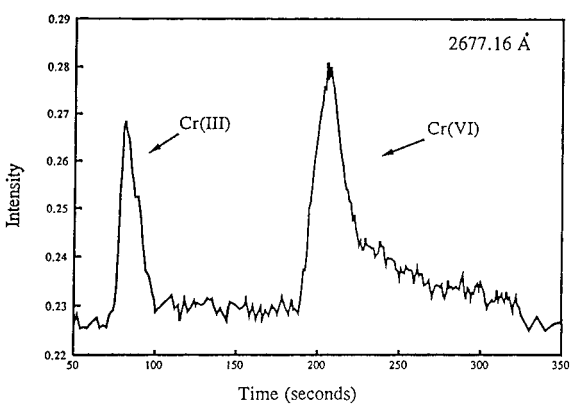


Fig. 1. Chromatogram of a 5- μg injection of a chromium mixture at 2677 Å using the HPLC–ICP-AES conditions outlined in Table 2.

mobile phase. Tailing was evident on the Cr(VI) peak, and the retention time of the Cr(VI) species was slightly longer than that found in Ref. [3]. Table 3 gives the analytical figures of merit obtained utilizing this method with the emission system. Absolute detection limits were 100 ng for Cr(III) and 200 ng for Cr(VI). From the %R.S.D. (>10%), however, it became clear that Cr(III) was not eluting reproducibly from the column. Most likely, Cr(III) was strongly attracted to the cation-exchange sites on the column.

Table 3
Analytical figures of merit for HPLC–ICP-AES data

| Figures of merit | Cr(III) | Cr(VI) |
|---|---|---|
| $R^2$ (cal. curve) | 0.9987 | 0.9996 |
| Slope of log–log curve | 1.205<br>(10–50 ppm) | 0.9131<br>(25–100 ppm) |
| Linear dynamic range | 0.5 | 1 |
| Relative detection limit | 1 ppm | 2 ppm |
| Absolute detection limit | 0.1 μg | 0.2 μg |

### 3.2. ICP-MS method

The ICP-AES method was next applied to the ICP-MS system. A chromatogram showing the injection of 0.1 $\mu$g of each chromium species at $m/z$ 53 is given in Fig. 2. As seen in the figure, tailing was now evident on the Cr(III) peak. The retention of Cr(III) was the same as that observed in the ICP-AES study, but Cr(VI) had shifted to a slightly longer retention time. Ultimately, the method as developed for AES detection was not suitable for MS detection due to the behavior of Cr(III) as well as the high mobile phase concentration which led to salt deposition and high background signals.

Additionally, it was discovered that the NG1 column used in Ref. [3] was employed to remove non-ionic organic compounds from the sample matrix which appear to complicate chromate analyses with the AS7 column. In order to adapt the method to ICP-MS detection, a new AS7 column and an NG1 guard column were used. To stabilize the Cr(III) species, a chelation procedure was followed. Finally, the concentration of ammonium sulfate in the mobile phase was decreased.

Using the new columns, the first parameter evaluated was the mass to use for single-ion monitoring. At $m/z$ 52, chromium is 83.76% abundant, while at $m/z$ 53 it is 9.55% abundant.

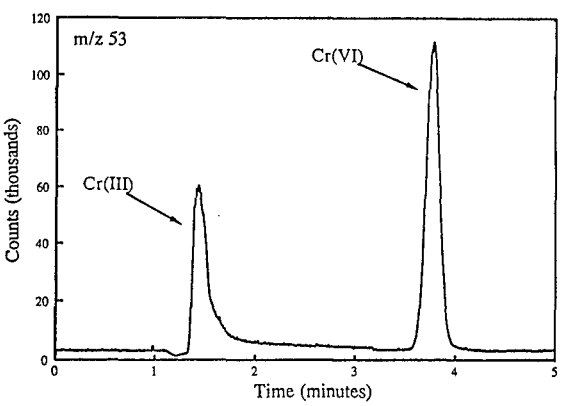


Fig. 2. Chromatogram of a 0.1-$\mu$g injection of a chromium mixture at $m/z$ 53 using the HPLC–ICP-AES conditions outlined in Table 2.

Preliminary studies at $m/z$ 52 showed a substantially high background ( > 100 000 counts) from the 250 m$M$ mobile phase alone. The background increased at both $m/z$ values as the ammonium sulfate concentration was increased; presumably as a result of the formation of $^{36}S^{16}O^{+}$ and $^{36}S^{16}O^{1}H^{+}$ at $m/z$ 52 and $m/z$ 53, respectively. The effect was more pronounced at the former $m/z$ value. Although $^{36}S$ only has a relative abundance of 0.02%, it can be present in a concentration equivalent to roughly 2 ppm in the 250 m$M$ mobile phase. This is a substantial quantity for the very sensitive ICP-MS instrument. Roehl and Alforque [22] stated that the formation of this interference would "probably preclude the use of $^{52}Cr$ for the determination of chromium by ICP-MS" using a sulfate-containing mobile phase. Neither $m/z$ 50 nor $m/z$ 54 were used since the polyatomic interferences from argon and sulfate at these $m/z$ values would be more abundant (i.e. $^{34}S^{16}O^{+}$ and $^{36}Ar^{14}N^{+}$ at $m/z$ 50, and $^{38}Ar^{16}O^{+}$ at $m/z$ 54).

As a result of the extremely high background at $m/z$ 52, signal-to-background ratios were degraded. A comparison of the chromatograms in Fig. 3 shows improved ratios at $m/z$ 53. Hence, this $m/z$ value was chosen for the remainder of the studies. The abundance advantage at $m/z$ 52 is largely offset by the high background signal.

Fig. 4 shows the effect of the mobile phase concentration on the retention of both Cr(III) and Cr(VI) at $m/z$ 53. Since values for capacity factors between 2 and 10 are considered optimal for a given separation, it is immediately obvious from the figure that mobile phase concentrations below 35 m$M$ are not ideal for the elution of Cr(VI). The capacity factor was calculated using a dip in the baseline at 78 s (corresponding to the solvent front) as the $t_0$ value. Ordinarily, one does not see the void volume using ICP-MS since one is detecting by mass. Sometimes, however, a baseline disturbance may be observed if the solvent plug briefly alters the plasma conditions.

Mobile phases containing high salt concentrations and the resulting clogging of parts of the ICP-MS system generally lead to decreased sensitivity. To circumvent this complication, the

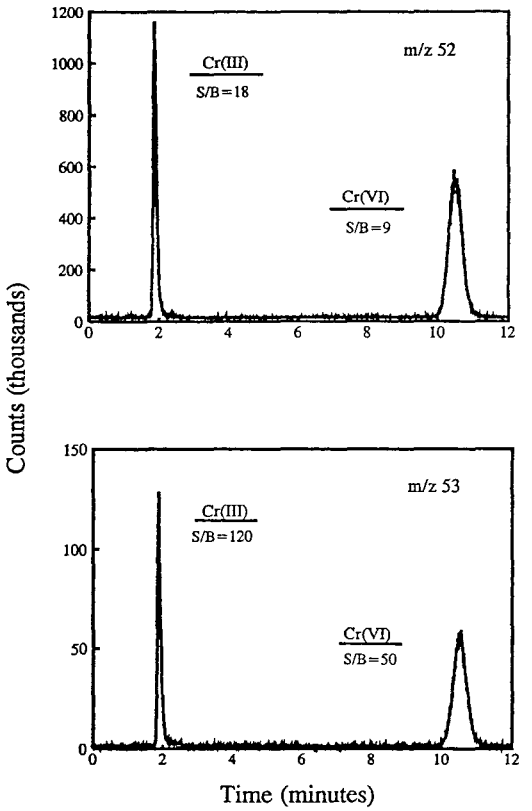


Fig. 3. Chromatograms of a mixture of Cr(III) (60 ng) and Cr(VI) (100 ng) with single-ion monitoring at *m/z* 52 and *m/z* 53 showing improved signal-to-background ratio at the latter *m/z* value. Conditions: pH 9.2, flow-rate 2 ml/min, 35 m*M* $(NH_4)_2SO_4$.

forward Rf power was initially increased to 1450 W and a nitric acid wash was employed when using the 250 m*M* mobile phase (containing 3.3% total dissolved salt). Both helped slightly, but because the background was very unstable at high concentrations, lowering the buffer concentration had the most significant effect. The best compromise between *k'* values for both chromium species and the mobile phase concentration was found using 35 m*M* $(NH_4)_2SO_4$ (containing 0.5% total dissolved salt).

Next, the effect of the mobile phase pH on the retention of both Cr(III) and Cr(VI) was evaluated using 35 m*M* ammonium sulfate and a flow-rate of 1.5 ml/min. No significant change was noted between pH 8.6 and 9.8. As a result, pH

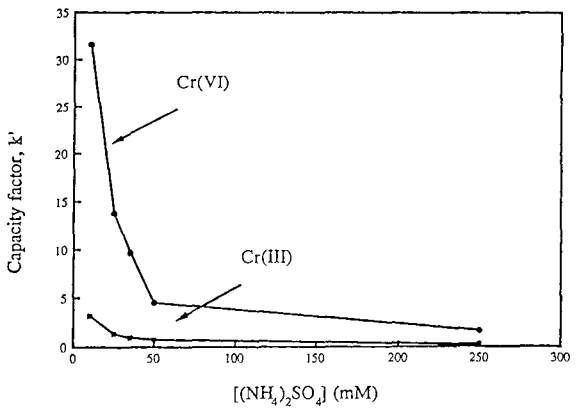


Fig. 4. Effect of mobile phase concentration on the retention of Cr(III) (6 ng) and Cr(VI) (10 ng) based on injection of a mixture at a flow-rate of 1.5 ml/min, mobile phase pH 9.2, and single-ion monitoring at *m/z* 53.

9.2 was chosen, corresponding to the pH used in the initial work [3].

Interconversion between the Cr(III) and Cr(VI) species was not observed in fresh solutions. No peaks corresponding to the elution of Cr(VI) or Cr(III) were observed in chromatograms when solutions of Cr(III) or Cr(VI), respectively, were injected onto the column. Some researchers have expressed concern that Cr(VI) could be converted to Cr(III) at low pH values [25], and that interconversion may also occur under other conditions [26]. The pH value and chelation procedure used here, however, did not facilitate Cr(VI) to Cr(III) conversion, thus indicating the stability of the chromium species under these conditions. Gjerde et al. have observed the same [18].

Analytical figures of merit for the ICP-MS method are given in Table 4. The method was linear over 2.5 orders of magnitude and the %R.S.D. values were found to be less than 5% for 7 replicate injections of a 50 ppb mixture. A significant improvement in the linear dynamic range is found when ICP-MS results are compared with ICP-AES data. This is more likely a result of initial problems with the chromatography rather than differences between the detection schemes. As expected, an improvement in detection limits of over 3 orders of magnitude from ICP-AES to ICP-MS detection was ob-

Table 4
Analytical figures of merit for HPLC–ICP-MS data

| Figures of merit | Peak area | | Peak height | |
|---|---|---|---|---|
| | Cr(III) | Cr(VI) | Cr(III) | Cr(VI) |
| $R^2$ (cal. curve) | 0.9998 | 0.9990 | 0.9999 | 0.9990 |
| Slope of log–log curve | 1.081 (3–600 ppb) | 0.9320 (5–1000 ppb) | 1.072 (3–600 ppb) | 0.9346 (5–1000 ppb) |
| Linear dynamic range | 2.5 | 2.5 | 2.5 | 2.5 |
| %R.S.D. | 4 | 3 | 4 | 4 |
| Relative detection limit | 3 ppb | 3 ppb | 0.4 ppb | 1 ppb |
| Absolute detection limit | 0.3 ng | 0.3 ng | 0.04 ng | 0.1 ng |

served. Detection limits were calculated using 3 times the standard deviation of the blank divided by the slope of the calibration curve. Peak-height values for absolute detection limits were improved over peak-area values as a result of the way in which they were calculated. Since 12 blank values were used in the calculations for peak height as opposed to 6 blank values for the peak-area calculations, standard deviations were lower for the peak-height calculations and hence, detection limits were better. These limits are slightly lower than those found by Jakubowski et al. [24]. Additionally, the method presented here does not require a complex nebulization system.

### 3.3. Reference material

Since the method proposed in Ref. [3] is used for the analysis of chromium in water, wastewater, and solid waste extracts, a NIST-SRM 1643c (Trace Elements in Water) was chosen to assess the applicability of this method. The certified value for total chromium in the SRM is $19.0 \pm 0.6$ ppb. A standard curve was prepared using direct nebulization of the standards without chromatography, and a value of $21.0 \pm 1.0$ ppb was obtained for total chromium in the SRM. Only one peak corresponding to Cr(III) was found in the SRM (a chromatogram of unchelated SRM 1643c is given in Fig. 5). This is in agreement with the results obtained by others for this standard reference material [8,17]. A peak-area calculation for the single peak ($18.5 \pm 2.2$ ppb) falls within the range for the certified value.

SRM 1643c was chelated with the disodium salt of EDTA. The complex was only slightly retained on the column, and a large baseline disturbance was observed after the peak. There is likely some carbon in the sample from excess free EDTA which gives rise to a rather broad

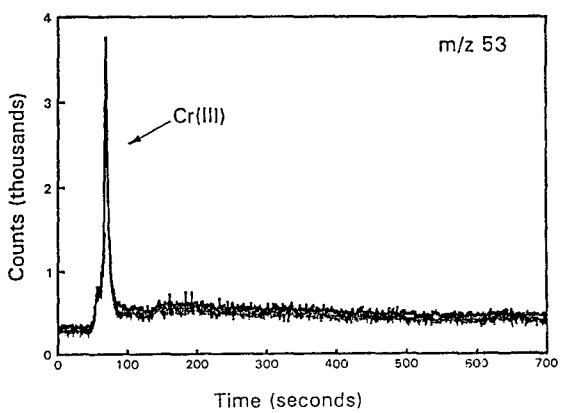


Fig. 5. Injection of 100 $\mu$l of NIST-SRM 1643c (Trace Elements in Water) using the HPLC–ICP-MS conditions outlined in Table 2 with single-ion monitoring at $m/z$ 53.

peak as the EDTA elutes from the column. This is evident in chromatograms from the formation of $ArC^+$ in the plasma. Future work will include an investigation of alternative chelation procedures.

Unfortunately, at this time there are no commercially available standard reference materials for chromium which are certified to contain certain amounts of different species. Admittedly, developing these types of standards is a challenge since maintaining the integrity of the individual species may be difficult in certain matrices. Until a way is found to reliably produce these samples, researchers will have to continue to look at spiked samples, total elemental concentration standards, and interlaboratory results to assess the viability of a method.

## 4. Conclusions

In summary, it was concluded that chromium isotope $m/z$ 53 will provide lower detection limits than the use of $m/z$ 52 due to a high $SO^+$ mobile phase background. However, if one wishes to, the analysis may be performed successfully at $m/z$ 52 in order to avoid a possible chlorine interference at $m/z$ 53. Chlorine polyatomic interferences which may occur at $m/z$ 53 include $^{37}Cl^{16}O^+$ and $^{35}Cl^{18}O^+$. Additionally, a "quick and dirty" sample analysis may be done at $m/z$ 53 using a concentration of 50 m$M$ $(NH_4)_2SO_4$ in the mobile phase to reduce the analysis time. Long analyses at this condition are poor due to salt deposition on the ICP-MS glassware over time.

One future possibility which could be explored is the use of a concentration gradient which could lead to a reduction in the analysis time. The method presented here, with absolute detection limits at the picogram level, should prove to be a viable alternative to other speciation techniques for chromium. Ultra-trace level detection by ICP-MS will be advantageous to various researchers. The use of this method for the evaluation of the purity of chromium in dietary supplements [27], the speciation of chromium in a urine standard reference material [28], and the determination of chromium in dyes has been presented elsewhere [29].

## Acknowledgements

The authors wish to thank Drs. John Dorsey (University of Florida) and Doug Heitkemper (U.S. FDA, Cincinnati, OH, USA) for helpful suggestions during the course of this work. Additionally, we would like to acknowledge Jackie Richards of Dionex Corp. for her technical assistance. We are grateful to the National Institute of Environmental Health Sciences for partial support of this work through grant numbers ES03321 and ES04908. We acknowledge the NIH-BRS Shared Instruments Grants program for providing the VG PlasmaQuad through grant number S10RR02714, and the U.S. Environmental Protection Agency for partial support of this work through grant number CR-818301.

## References

[1] H. Salem and S.A. Katz (Editors), Sci. Total Environ., 86 (1989) 1–206 (special issue).
[2] D.T. Gjerde and H.C. Mehra, Trace Metal Analysis and Speciation, Elsevier Science, New York, 1991, p. 213.
[3] Technical Note 26, Dionex Corp., Sunnyvale, CA (May 1990).
[4] S.I. Shupack, Env. Health Perspec., 92 (1991) 7.
[5] C. Veillon, Sci. Total Environ., 86 (1989) 65.
[6] H. Salem, Sci. Total Environ., 86 (1989) 1.
[7] P. O'Brien and G. Wang, Env. Geochem. Health, 11 (1989) 77.
[8] M. Sperling, S. Xu and B. Welz, Anal. Chem., 64 (1992) 3101.
[9] Y. Suzuki and F. Serita, Ind. Health, 23 (1985) 207.
[10] J.C. de Andrade, J.C. Rocha and N. Baccan, Analyst, 109 (1984) 645.
[11] J. Ruz, A. Rios, M.D. Luque de Castro and M. Valcarcel, Fresenius' Z. Anal. Chem., 322 (1985) 499.
[12] T.P. Lynch, N.J. Kernoghan and J.N. Wilson, Analyst, 109 (1984) 839.
[13] A. Shah and S. Devi, Anal. Chim. Acta, 236 (1990) 469.
[14] S. Hirata, Y. Umezaki and M. Ikeda, Anal. Chem., 58 (1986) 2603.
[15] I.S. Krull, K.W. Panaro and L.L. Gershman, J. Chromatogr. Sci., 21 (1983) 460.

[16] I.S. Krull, D. Bushee, R.N. Savage, R.G. Schleicher and S.B. Smith, Anal. Lett., 15 (1982) 267.
[17] I.T. Urasa and S.H. Nam, J. Chromatogr. Sci., 27 (1989) 30.
[18] D.T. Gjerde, D.R. Wiederin, F.G. Smith and B.M. Mattson, J. Chromatogr., 640 (1993) 73.
[19] S.B. Roychowdhury and J.A. Koropchak, Anal. Chem., 62 (1990) 484.
[20] K.E. Lawrence, G.W. Rice and V.A. Fassel, Anal. Chem., 56 (1984) 289.
[21] K.E. LaFreniere, V.A. Fassel and D.E. Eckels, Anal. Chem., 59 (1987) 879.
[22] R. Roehl and M.M. Alforque, At. Spectros., 11 (1990) 210.
[23] E.J. Arar, S.E. Long, T.D. Martin and S. Gold, Environ. Sci. Technol., 26 (1992) 1944.
[24] N. Jakubowski, B. Jepkens, D. Stuewer and H. Berndt, J. Anal. Atom. Spectrom., 9 (1994) 193.
[25] F.A. Cotton and G. Wilkinson, Advanced Inorganic Chemistry, Wiley, New York, 3rd ed., 1972.
[26] U.S. EPA Method 218.6. E.J. Arar, S.E. Long and J.D. Pfaff, Determination of Dissolved Hexavalent Chromium in Drinking Water, Groundwater and Industrial Wastewater Effluents by Ion Chromatography. U.S. EPA: Environmental Monitoring and Systems Laboratory, Cincinnati, OH, Revision 3.0, Nov. 1991.
[27] H. Ding, L.K. Olson, J.A. Caruso and F.A. Byrdy, 1995 Pittsburgh Conference, New Orleans, LA, March 5–10, 1995, Paper 615.
[28] L.K. Olson, J. Wang, J.A. Caruso and B.S. Sheppard, 1994 Pittsburgh Conference, Chicago, IL, Feb. 27–March 4, 1994, Paper 390.
[29] G. Zoorob, M.J. Tomlinson, J. Wang and J.A. Caruso, 1995 Pittsburgh Conference, New Orleans, LA, March 5–10, 1995, Paper 1170.

ELSEVIER

Journal of Chromatography A, 712 (1995) 321–343

JOURNAL OF CHROMATOGRAPHY A

# Differentiation of the source of spilled oil and monitoring of the oil weathering process using gas chromatography–mass spectrometry

Zhendi Wang*, Merv Fingas

*Emergencies Science Division, ETC, Environment Canada, 3439 River Road, Ottawa, Ont. K1A 0H3, Canada*

First received 6 March 1995; revised manuscript received 1 May 1995; accepted 8 May 1995

**Abstract**

Methods described use high-performance capillary gas chromatography–mass spectrometry (GC–MS) operating mainly in the selected-ion monitoring (SIM) mode for oil analysis. The methods have been applied to the characterization of crude oils, weathered oils, biodegradation oils, and oil-spill-related environmental samples with different compositions, nature, and concentrations. Using GC–MS enables the identification and quantitation of specific target petroleum hydrocarbons including $C_8$ through $C_{40}$ normal alkanes, the isoprenoids, BTEX and alkyl benzene, target polycyclic aromatic hydrocarbons (PAHs) and their alkylated homologues, and biomarker triterpanes and steranes. The analysis of these target compounds and/or compound groups is important and essential for oil-spill monitoring. The analytical data have been successfully used for the differentiation of oils, tracking the source of long-term spilled oils, monitoring the oil weathering and biodegradation process under variable environmental conditions, and the determination of the weathering percentages of very heavily weathered oil samples by the selective use of biomarker parameters. Compared to some other traditional methods which were originally designed for industrial waste and hazardous waste, the methods described here are more selective and give a better representation of the true oil composition, and hence are more defensible.

## 1. Introduction

Oil contamination of soil and water caused by transportation accidents and leakages is a consequence of the growing industrialization and demands for energy. Incidents of this type have created a global public awareness of the risks and danger associated with oil spills and driven the search for effective and environmentally safe cleanup treatments. During the last decade, a large progress has been made in oil-spill cleanup techniques including physical, chemical and biological methods [1]. Among these techniques, bacterial degradation of petroleum hydrocarbons has been widely recognized. For example, biodegradation was used for the 1989 EXXON VALDEZ spill cleanup [2,3]. Appropriate selection and application of standardized and comparable analytical methods are required to assess the damage to the environment and natural resources caused by the released petroleum, to

* Corresponding author.

0021-9673/95/$09.50 
*SSDI* 0021-9673(95)00546-3

provide an effective cleanup strategy, to evaluate the efficacy of bioremediation products and other oil-spill treating products, and to understand the behaviour and fate of spilled oil in the environment and to predict the potential long-term impact of the spilled oil.

Crude oil and oil-spill-related samples are extremely complex mixtures in which the components range from simple alkanes to complex asphaltic components, the boiling points of which vary over a wide range from a few to several hundred degrees. As soon as oil is spilled into the environment the processes of volatilization, dissolution, microbial and photochemical degradation act to change its composition. Consequently, the chemical analysis methods employed should yield sufficient accuracy and compositional detail (especially with respect to the key toxic compounds, because the effects of spilled oil on the environment are strongly related not only to the gross amount of oil, but also to the levels of those key toxic compounds) to answer the specific questions to be answered in an environmental assessment study.

In recent years, major advances have been achieved in the analytical methods and techniques used for oil analysis. Various adsorbents (including silica gel, alumina, florisil, combination of silica and alumina, and solid-phase extraction) and various eluting solvents have been used to fractionate oil into saturated, aromatic, and polar groups [4,5]. The fractions are then analyzed using techniques, e.g. gravimetric methods, gas chromatography (GC), infrared spectroscopy (IR), ultraviolet (UV) and fluorescence spectroscopy, and mass spectrometry (MS). Among these techniques, capillary GC is most widely used. Over the last decade GC with flame ionization detection (FID) has been employed in oil-spill studies for the determination of *n*-alkanes, isoprenoids, and the total petroleum hydrocarbons. However, because of its nonspecificity FID may produce erroneous results, due to e.g. analyte coelution and matrix interference, when it is used for the determination of polycyclic aromatic hydrocarbon compounds (PAHs). Thus, the compound-specific data and information obtained from GC–FID is limited: quantitation of aromatic compounds can be only partially achieved, and identification and quantitation of biomarker compounds would be almost impossible. As for the gravimetric, IR, and UV methods, they only provide estimates of the whole fractions.

For weathering studies, monitoring the changes in the chemical composition of the spilled oil is of crucial importance, especially when there is a prolonged period of weathering. Also for oil source identification, detailed knowledge of the chemical composition is needed, since each type of oil has a different component distribution. Therefore, positive conclusions about oils sources and the fate of the oil in the environment can only be obtained through comparison of their chemical composition, especially through the so called "pattern-recognition" plots involving more than 100 important individual oil components and component groupings [6]. All of these demands point to GC–MS fingerprinting as the most appropriate technique.

High-performance capillary GC–MS, which combines chemical separation by GC with spectral resolution by MS, allows for specific target compound determination. This is especially important for the determination of the alkyl aromatic homologous compounds ($C_1$- through $C_6$-alkyl groups of benzene, naphthalene, and other PAHs) and biomarker compounds (triterpanes and steranes) in oil. For quantitation of target compounds, the selected-ion monitoring (SIM) mode of GC–MS is mostly selected. GC–MS operating in the SIM mode shows several distinct advantages. The method detection limits for the target analytes are generally lower by almost an order of magnitude than those produced by conventional full-scan GC–MS. The reduction in number of ions per scan in GC–SIM-MS analysis increases the sensitivity of the instrument, thereby lowering the instrument detection limit. Furthermore, the use of GC–SIM-MS often increases the linear range of the instrument for low-concentration analytes. Over the past several years, new low-cost GC–MS systems have made GC–MS analysis feasible and attractive for

many analytical laboratories, and this trend will continue.

In recent years, the Emergencies Science Division (ESD) of Environment Canada in cooperation with the US Minerals Management Service has conducted projects to investigate various countermeasures in responding to oil spills. The goal of one such project is to develop analytical methods to identify, characterize and quantify oil samples with respect to their composition, nature and concentrations. Using this method, Alberta Sweet Mix Blend (ASMB) oil has been extensively characterized [7]; long-term weathered oil samples have been identified and their fate and persistence in the environment have been studied through pattern recognition of biomarker compounds [8,9]; the effects of weathering on the chemical composition of oil have been quantitatively understood [6] and determination of weathering percentages of oil in highly-weathered oil sediment samples has been achieved using $C_{29}$-$\alpha\beta$- and $C_{30}$-$\alpha\beta$-hopane in the source oil as internal oil references [9]; screening procedures have been developed for assessing the efficacy and toxicity of oil-spill bioremediation agents by analyzing hundreds of biodegradated oil samples [10], and identification of alkyl benzenes in oil and direct determination of BTEX (the collective name for benzene, toluene, ethylbenzene, and the xylene isomers) and (BTEX + $C_3$-benzenes) using GC–MS has been achieved [11]. The high chemical and spectral separation power of GC–MS allows us to identify, characterize and quantify over 100 saturated hydrocarbons, over 50 alkyl benzene homologues and over 60 PAH compounds, and over 50 biomarker compounds in crude oils, weathered oils, biodegradation oils, and various oil-spill-related environmental samples. The focus of this analytical technique is to identify and quantify target compounds as accurately as possible with minimal interference so that more complete and precise information on the changes in chemical composition and the effects of various factors on oil degradation can be monitored and assessed as the oils undergo weathering and degradation processes.

## 2. Experimental

### 2.1. Capillary gas chromatography–mass spectrometry

Analyses were performed on a HP 5890 GC–5972 MSD. System control and data acquisition was achieved by HP G1034C MS ChemStation (DOS series). The MSD was operated in the scan and selected-ion monitoring (SIM) modes to obtain spectral data for the identification of the components, and in the SIM mode for quantitation of target compounds. The SIM mode involves monitoring those specific, preselected ions which are useful for identifying, characterizing, and quantifying the oil components of interest. Table 1 lists important oil fingerprinting compounds and compound classes. As shown, the target compounds include: *n*-alkanes (*n*-$C_8$ to *n*-$C_{40}$) plus five selected–and often the most abundant–isoprenoids (2,6,10-trimethyldodecane, 2,6,10-trimethyltridecane, norpristane, pristane and phytane); PAHs and their alkylated homologues; biomarker compounds triterpanes and steranes. Sometimes the volatile aromatic hydrocarbons BTEX and $C_2$- through $C_5$-benzenes and polar compounds may be included as well, depending on the type of oil spilled and on the environmental assessment requirement. The columns used were 30 m × 0.25 mm I.D., 0.25 $\mu$m HP-5 fused-silica columns. The chromatographic conditions were as follows: carrier gas, helium (1.0 ml/min); injection mode, splitless; injector and detector temperature, 290°C and 300°C, respectively; temperature program for *n*-alkane distribution, alkylated PAHs and biomarker compounds, 50°C for 2 min, then 6°C/min to 300°C, hold 16 min; temperature program for BTEX and target alkyl benzenes, 35°C for 2 min, then ramp at 10°C/min to 300°C and hold 10 min.

### 2.2. Oil and oil samples

Alberta Sweet Mix Blend (ASMB) oil is the reference oil used for dispersant testing in ESD. This oil has been extensively characterized and

Table 1
Petroleum fingerprinting analytes of interest

| Aliphatics hydrocarbons | Target ions | Target PAHs | Target ions | Biomarkers compounds | Target ions |
|---|---|---|---|---|---|
| *n*-C8 | 85, 71 | Naphthalene | 128 | *Triterpanes* | |
| *n*-C9 | 85, 71 | C1-naphthalene | 142 | Tricyclic terpanes | 191 |
| *n*-C10 | 85, 71 | C2-naphthalene | 156 | Tetracyclic terpanes | 191 |
| *n*-C11 | 85, 71 | C3-naphthalene | 170 | Pentacyclic terpanes | 191 |
| *n*-C12 | 85, 71 | C4-naphthalene | 184 | $C_{27}H_{46}$(Ts) | 191 |
| *n*-C13 | 85, 71 | Phenanthrene | 178 | $C_{27}H_{46}$(Tm) | 191 |
| *n*-C14 | 85, 71 | C1-phenanthrene | 192 | $C_{28}H_{48}$ | 191 |
| *n*-C15 | 85, 71 | C2-phenanthrene | 206 | $C_{29}H_{50}$ $\alpha\beta$- | 191 |
| *n*-C16 | 85, 71 | C3-phenanthrene | 220 | $C_{30}H_{52}$ $\alpha\beta$- | 191 |
| *n*-C17 | 85, 71 | C4-phenanthrene | 234 | $C_{31}H_{54}$ 22*S*/22*R* | 191 |
| Pristane | 85, 71 | Dibenzothiophene | 184 | $C_{32}H_{56}$ 22*S*/22*R* | 191 |
| *n*-C18 | 85, 71 | C1-dibenzothiophene | 198 | $C_{33}H_{58}$ 22*S*/22*R* | 191 |
| Phytane | 85, 71 | C2-dibenzothiophene | 212 | $C_{34}H_{60}$ 22*S*/22*R* | 191 |
| *n*-C19 | 85, 71 | C3-dibenzothiophene | 226 | $C_{35}H_{62}$ 22*S*/22*R* | 191 |
| *n*-C20 | 85, 71 | Fluorene | 166 | | |
| *n*-C21 | 85, 71 | C1-fluorene | 180 | *Steranes* | |
| *n*-C22 | 85, 71 | C2-fluorene | 194 | $C_{27}$20 *R*/*S*-cholestanes | 217, 218 |
| *n*-C23 | 85, 71 | C3-fluorene | 208 | $C_{28}$20 *R*/*S*-ergostanes | 217, 218 |
| *n*-C24 | 85, 71 | Chrysene | 228 | $C_{29}$20 *R*/*S*-stigmastanes | 217, 218 |
| *n*-C25 | 85, 71 | C1-chrysene | 242 | | |
| *n*-C26 | 85, 71 | C2-chrysene | 256 | *Surrogates and standards* | |
| *n*-C27 | 85, 71 | C3-chrysene | 270 | 1. Surrogates | |
| *n*-C28 | 85, 71 | Biphenyl | 154 | d10-Acenaphthene | 164 |
| *n*-C29 | 85, 71 | Acenaphthylene | 152 | d10-Phenanthrene | 188 |
| *n*-C30 | 85, 71 | Acenaphthene | 153 | d12-Benz[*a*]anthracene | 240 |
| *n*-C31 | 85, 71 | Anthracene | 178 | d12-Perylene | 264 |
| *n*-C32 | 85, 71 | Fluoranthene | 202 | | |
| *n*-C33 | 85, 71 | Pyrene | 202 | 2. Internal Standards | |
| *n*-C34 | 85, 71 | Benz[*a*]anthracene | 228 | d14-Terphenyl | 244 |
| *n*-C35 | 85, 71 | Benzo[*b*]fluoranthene | 252 | $C_{30}$-$\beta\beta$-Hopane | 191 |
| *n*-C36 | 85, 71 | Benzo[*k*]fluoranthene | 252 | | |
| *n*-C37 | 85, 71 | Benzo[*e*]pyrene | 252 | 3. QC Standards | |
| *n*-C38 | 85, 71 | Benzo[*a*]pyrene | 252 | *n*-alkane standards | |
| *n*-C39 | 85, 71 | Perylene | 252 | SRM 1491 | |
| *n*-C40 | 85, 71 | Indeno(1,23-cd)pyrene | 276 | alkyl-benzene std | |
| | | Dibenz[*a*,*h*]anthracene | 278 | triterpane and sterane std | |
| BTEX and C3-benzenes | 78,91,105 | Benzo[*ghi*]perylene | 276 | | |

detailed identification and quantitation results have been reported elsewhere [4,7]. Other oils were obtained from various sources during the period 1985–1994 and stored in the cold room of this laboratory.

BIOS (Baffin Island Oil Spill, 12 year old) and 22-year-old Arrow oil sediment samples (except the sample BIOS No. 8 which was a water sample) were collected from Baffin Island and the north shore of Chedabucto Bay of Canada, respectively. The sediment and water sample preparation, extraction, cleanup, and fractionation have been described elsewhere [4,7–9].

### 2.3. Quantitation and analysis quality control

Initially, five-point calibration curves were established for analytes and internal standards, demonstrating the linear range of the analysis. The relative response factor (RRF) and relative

standard deviation (R.S.D.) for each hydrocarbon component was calculated relative to the internal standard. The GC–MS instrument was carefully maintained and tuned daily to achieve the required sensitivity. An instrument blank and standard solutions (which were composed of authentic *n*-alkanes plus isoprenoids, or authentic target PAH compounds, or authentic alkyl benzenes, or authentic hopanes and steranes, depending on the analysis requirement) were analyzed before and after each sample batch (approximately 10 samples) to monitor accuracy and precision. The RRFs obtained from the daily calibration standards should fall within 25% of the corresponding initial calibration curve values [8,12]. If not, a five-point calibration curve would be repeated for that compound prior to sample analysis.

The calibration standard for *n*-alkane analysis was composed of $C_8$- through $C_{40}$-*n*-alkanes, pristane, and phytane. 5-$\alpha$-Androstane was used as the internal standard.

Quantitation of BTEX and $C_3$-benzenes, target PAHs, alkylated PAH homologues was performed in the SIM mode with RRFs for each compound determined during instrument calibration. PAH alkyl homologues were quantified by using the straight baseline integration of each level of alkylation. Although the alkylated homologue groups can be quantitated using the RRF of the respective unsubstituted parent PAH compounds, it is preferable to obtain the RRFs directly from alkylated PAH standards, when commercially available. In this work, the RRFs obtained for 1-methyl-naphthalene, 2-methyl-naphthalene, 2,6-dimethyl-naphthalene, 2,3,5-trimethyl-naphthalene, and 1-methyl-phenanthrene were used for quantitation of 1-methyl-naphthalene, 2-methyl-naphthalene, $C_2$-naphthalene, $C_3$-naphthalene, and $C_1$-phenanthrene in oil, respectively. The RRFs of 2,3,5-trimethyl-naphthalene and 1-methyl-phenanthrene were used for quantitation of $C_4$-naphthalene, and $C_2$-, $C_3$-, and $C_4$-phenanthrenes, respectively. The selection criteria for the integration and reporting of each alkylated homologue were based primarily on pattern recognition and the presence of selected confirmation ions.

The average RRF for the biomarker compound $C_{30}$-17$\beta$(H)21$\alpha$(H)-hopane was determined relative to the internal standard $C_{30}$-17$\beta$(H)21$\beta$(H)-hopane. The average RRF for $C_{30}$-17$\beta$(H)21$\alpha$(H)-hopane (*m/z* 191) was used for quantitation of $C_{30}$-17$\alpha$(H)21$\beta$(H)-hopane and other triterpanes (in the range $C_{19}$–$C_{35}$) in the oil sample. For quantitation of steranes, due to the lack of availability of appropriate deuterated steranes, $C_{29}$-20*R*-$\alpha\alpha\alpha$-ethylcholestane was used and monitored at *m/z* 217 to obtain the RRF relative to $C_{30}$-17$\beta$(H)-21$\beta$(H)-hopane monitored at *m/z* 191, and then the average RRF of $C_{29}$-20*R*-$\alpha\alpha\alpha$-ethylcholestane was used for estimation of sterane compounds in the oil.

## 3. Results and discussion

### 3.1. Saturated hydrocarbons

The types and concentrations of specific oil constituents in environmental samples are dictated by the origin and nature of the spilled oil. Each oil has a different "fingerprint" and compound distribution. For crude oil, the distribution depends greatly on its geological source; for weathered oil, the distribution depends not only on the weathering conditions, but also on the time of weathering (short-term or long-term). The low-molecular-mass ($M_r$) saturated hydrocarbons in weathered oil samples may be lost and some degradation-resistant compounds may at the same time increase in relative concentration because of the weathering effects. This results in significant changes in the chemical composition and concentration of the oil.

Saturated hydrocarbons are major constituents of petroleum. Although the *n*-alkanes and isoprenoids are generally not of toxicological concern, identification and quantitation of these target analytes would be valuable to serve the following purposes [6,9,13,14]: tracer of the presence of spilled oil; basic spilled-oil fingerprints; indicator of the fate of the spilled oil and the changes in chemical composition due to weathering; and monitoring the loss of spilled-oil components by evaporation and/or biodegrada-

tion in environmental samples. In addition, these chemical data can also be used to differentiate the specific spilled oil from pre-spill or background pollution sources in environmental samples. Some biodegradation indicators relative to the spilled source oil (such as the $n$-$C_{17}$/pristane, and $n$-$C_{18}$/phytane ratios) can provide information on the effect of microbial biodegradation on the loss of hydrocarbons in an impacted area. Fig. 1 shows $n$-alkane distribution chromatograms of three different oils obtained by GC–MS ($m/z$ 85) measurement: ASMB oil (B), California oil (D), and Orimulsion (F). For comparison purposes, the GC–FID chromatograms (A, C, and E) are also presented in Fig. 1. The GC–MS chromatograms of saturated hydrocarbons ($m/z$ 85, 71, and 57) show very neat profiles of $n$-alkanes including isoprenoids with minimal interference from other petroleum hydrocarbons. Also, they give clear information on the large differences in the saturated-compound distribution between oils, which is indicated by the distribution of the $n$-alkanes and by the profile of the hump. It can be readily seen from Fig. 1 that these three oils are very different, not only because of their different distribution patterns and profiles, but also because of the significantly higher concentration of branched saturates relative to normal alkanes in California oil. As for Orimulsion, no noticeable $n$-alkanes are seen from its GC–FID and GC–MS chromatograms.

Fig. 2A–F shows the $n$-alkane distribution of the ASMB oils (determined by GC–FID) which were artificially weathered to varying percentages of weight loss (w/w) using a lab-scale rotary evaporation technique [6]. For the source ASMB oil, the most abundant $n$-alkanes are found in the $n$-$C_8$ to $n$-$C_{17}$ region (Fig. 2A), and the abundance of $n$-alkanes gradually decreases as the carbon number increases. As weathering increases, the abundance of aliphatic components shifts to higher carbon numbers. For example, the $n$-alkane with the highest concentration is $n$-$C_9$ in 0% weathered oil (4.8 mg/g oil) and $n$-$C_{17}$ in 44.5% weathered oil (6.7 mg/g oil), respectively. It is noted that even though the ASMB oil was weathered from 0% to 45%, the sum of the $n$-alkanes for the six weathered ASMB oil samples did not change significantly (range, 70–76 mg/g oil). This can be explained by the combination of two opposite effects: one being the loss of low-$M_r$ aliphatic components by evaporation, the another the buildup of high-$M_r$ aliphatic components by oil volume reduction. The ratios of $n$-$C_{17}$/pristane, $n$-$C_{18}$/phytane, and pristane/phytane are virtually unaltered because these compounds have about the same volatility. It has been demonstrated, however, that the ratios of $n$-$C_{17}$/pristane and $n$-$C_{18}$/phytane significantly decreased when biodegradation was involved [8,9,15,16]. This is because biodegradation preferentially removes $n$-$C_{17}$, $n$-$C_{18}$ and other normal alkanes from oil samples. Therefore, for less weathered or short-term weathered oil, the traditional diagnostic ratios such as $n$-$C_{17}$/pristane, $n$-$C_{18}$/phytane, and pristane/phytane are useful to identify the source of the oil and to assess the effect of microbial degradation and weathering of the oil, but they would be of less value for highly weathered and degraded oil samples (usually under long-term environmental exposures) due to the nearly complete loss of not only $n$-alkanes, but also of isoprenoids and most PAH compounds. Fig. 3 illustrates this case well. Fig. 3 (top) shows the GC–MS chromatogram of the $m/z$ 85 fragment of weathered Arrow oil, which shows a mixture dominated by a homologous series of $n$-alkanes ranging from $n$-$C_9$ to $n$-$C_{40}$ with a maximum around $n$-$C_{20}$ to $n$-$C_{22}$. Isoprenoids are also present, with pristane and phytane being the most abundant. In sharp contrast, the $n$-alkanes, including the five isoprenoids, were nearly completely lost in a 22-year-old Arrow oil sample. The unresolved complex mixture (UCM) dominates the total peak area (Fig. 3, bottom). This dominated UCM indicates the sample has been very heavily weathered (indicator of weathering degree) and its chemical composition has undergone extreme alteration. Definitely, this kind of chromatogram cannot provide much information on the source of the spilled oil.

### 3.2. BTEX and alkyl benzenes

The composition and concentration of BTEX and alkyl benzene compounds (being important constituents of oil and probably the most volatile

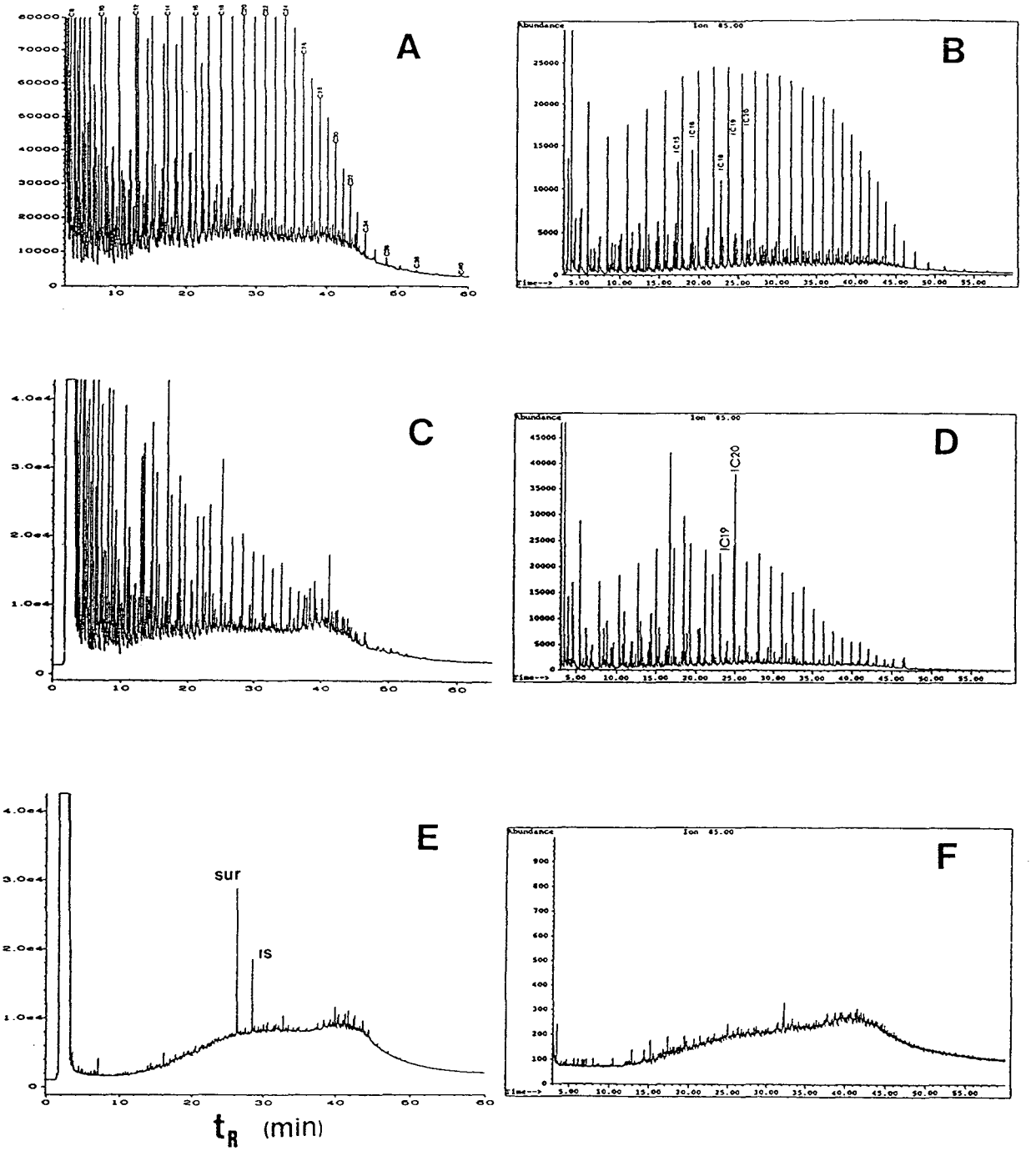


Fig. 1. Comparison of alkane distribution chromatograms (GC–FID and GC–MS at $m/z$ 85) of ASMB oil (A and B), California oil (C and D), and Orimulsion oil (E and F). Numbers represent carbon numbers of $n$-alkanes.

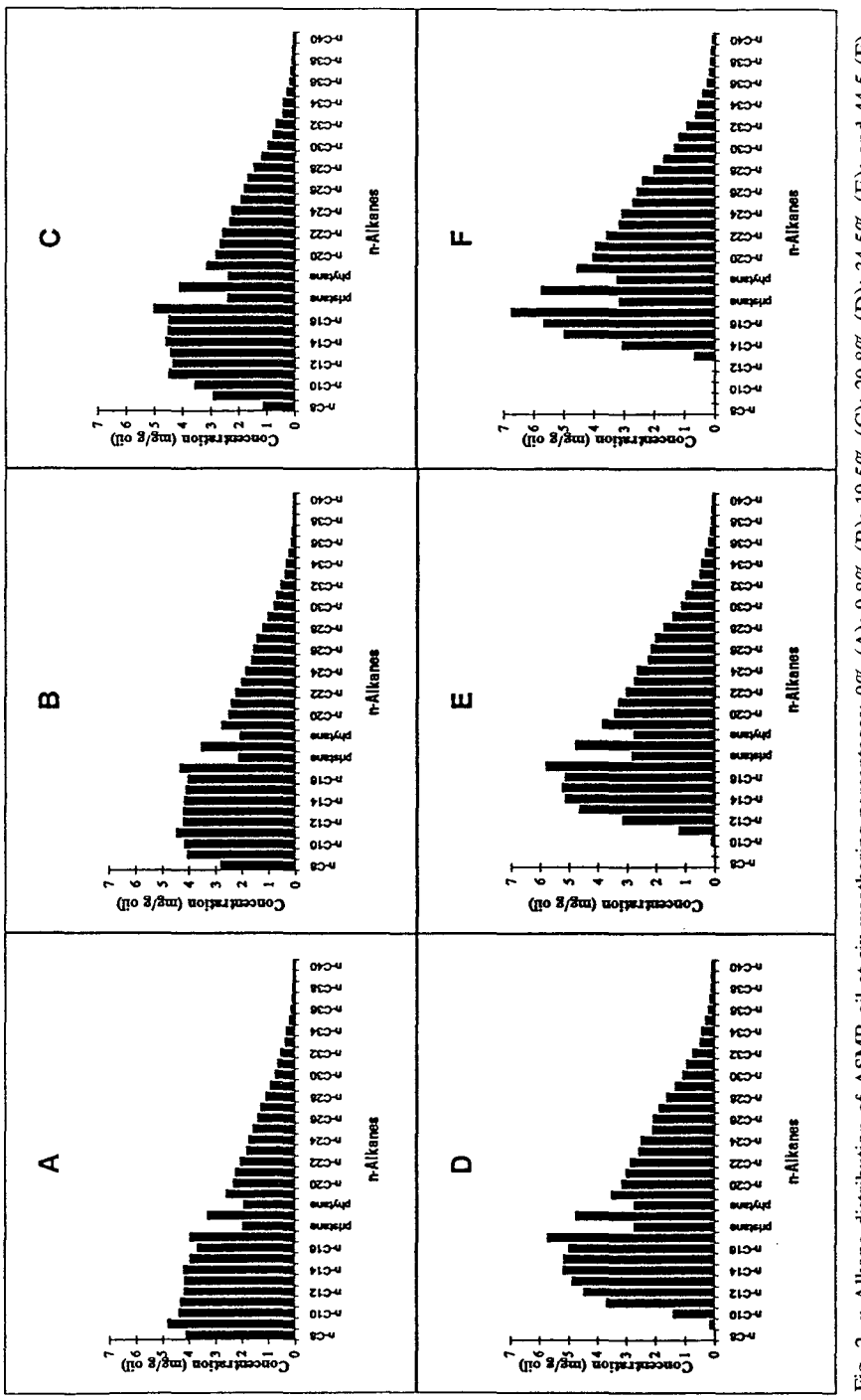


Fig. 2. *n*-Alkane distribution of ASMB oil at six weathering percentages: 0% (A); 9.8% (B); 19.5% (C); 29.8% (D); 34.5% (E); and 44.5 (F).

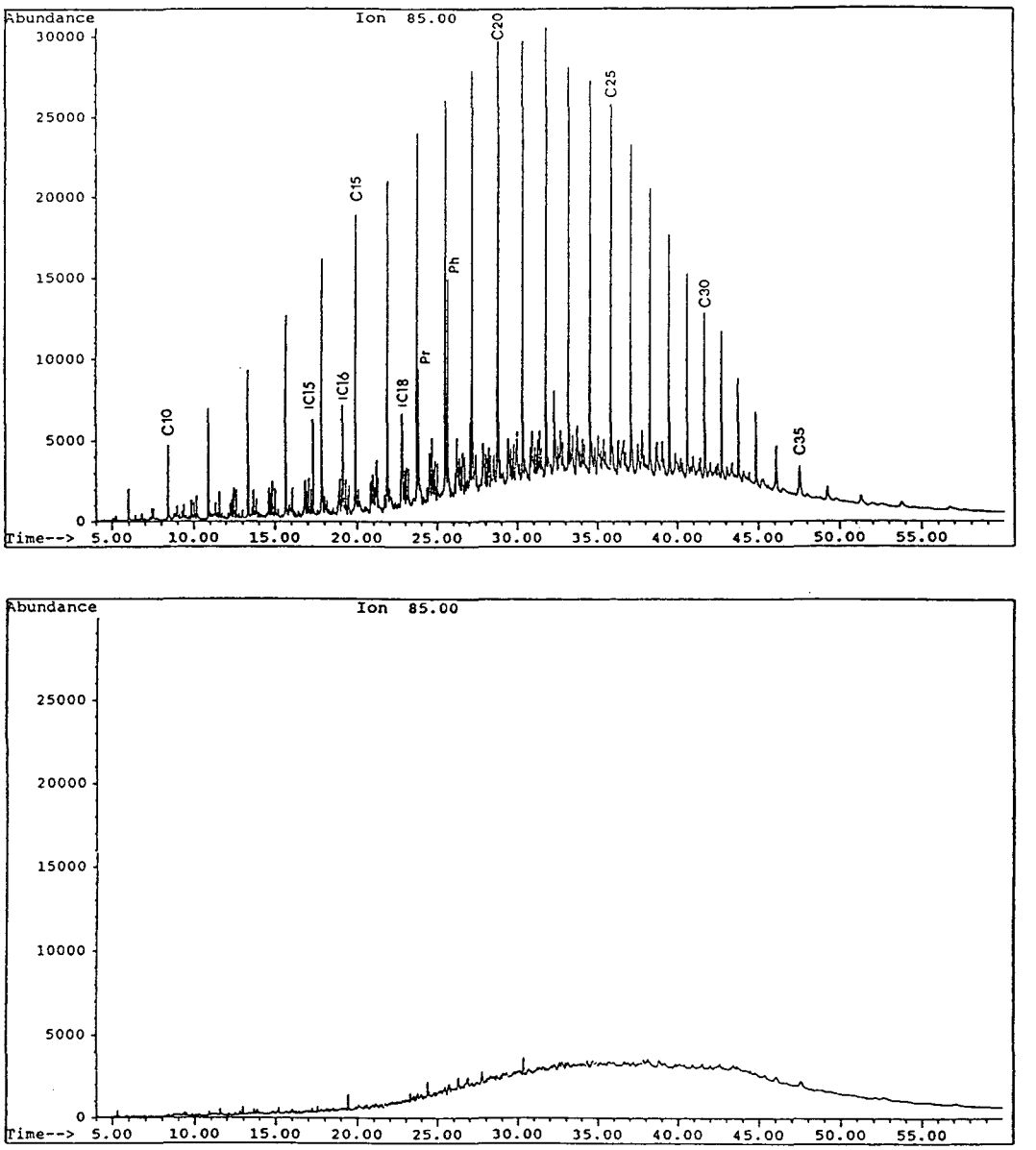


Fig. 3. GC–MS chromatograms of saturated hydrocarbons ($m/z$ 85) for the weathered source Arrow oil (top) and the sample S-4 (bottom). Numbers represent carbon numbers of $n$-alkanes. iso-C15, iso-C16, iso-C18, Pr, and Ph represent the five most abundant isoprenoids: 2,6,10-trimethyldodecane, 2,6,10-trimethyltridecane, norpristane, pristane, and phytane, respectively.

aromatic compounds) in oil can directly affect the physical and chemical properties of petroleum. The immediate toxic effects of this group of compounds following a spill emphasize the usefulness of analytical data on these groups in biological assessment studies.

The structural identification and characterization of alkyl benzenes are based on mass data in

both scan and SIM modes, comparison of GC retention data with reference standards, and calculation of retention index ($I$) values verified by comparison with literature $I$-values. Comparison of the $I$-values with those reported in the literature enables the assignment of some positional isomers. As an example, Figs. 4A and 4B show the GC–MS scan and SIM chromatograms of alkyl benzene compounds in the retention-time range 2.5–11.5 min obtained from the aromatic fraction of the ASMB oil. Table 2 lists 58 positively identified alkyl benzene compounds with the alkyl group ranging from $C_1$ to $C_8$. It is evident from Table 2 that the three series of $I$-values [the calculated $I$-values, the literature $I$-values [17], and the $I$-values calculated from the chromatographic data of the BTEX and alkyl-benzene (from $C_3$- to $C_6$-benzene) standards] are in excellent agreement.

Quantitation of BTEX and alkyl benzenes was achieved by operating GC–MS in the SIM mode and by direct injection of oil in $n$-pentane solution. It has been noticed that sample handling can greatly affect the analytical precision and accuracy of the determination of alkyl benzene compounds in oil due to the volatility of the lighter alkyl benzenes. In order to achieve improved analytical precision and accuracy, the following refinements were implemented in addition to the routine quality control measures:

(1) Oil was precisely weighed, directly dissolved in $n$-pentane, and tightly sealed to avoid any possible loss of alkyl benzene compounds, especially the BTEX compounds

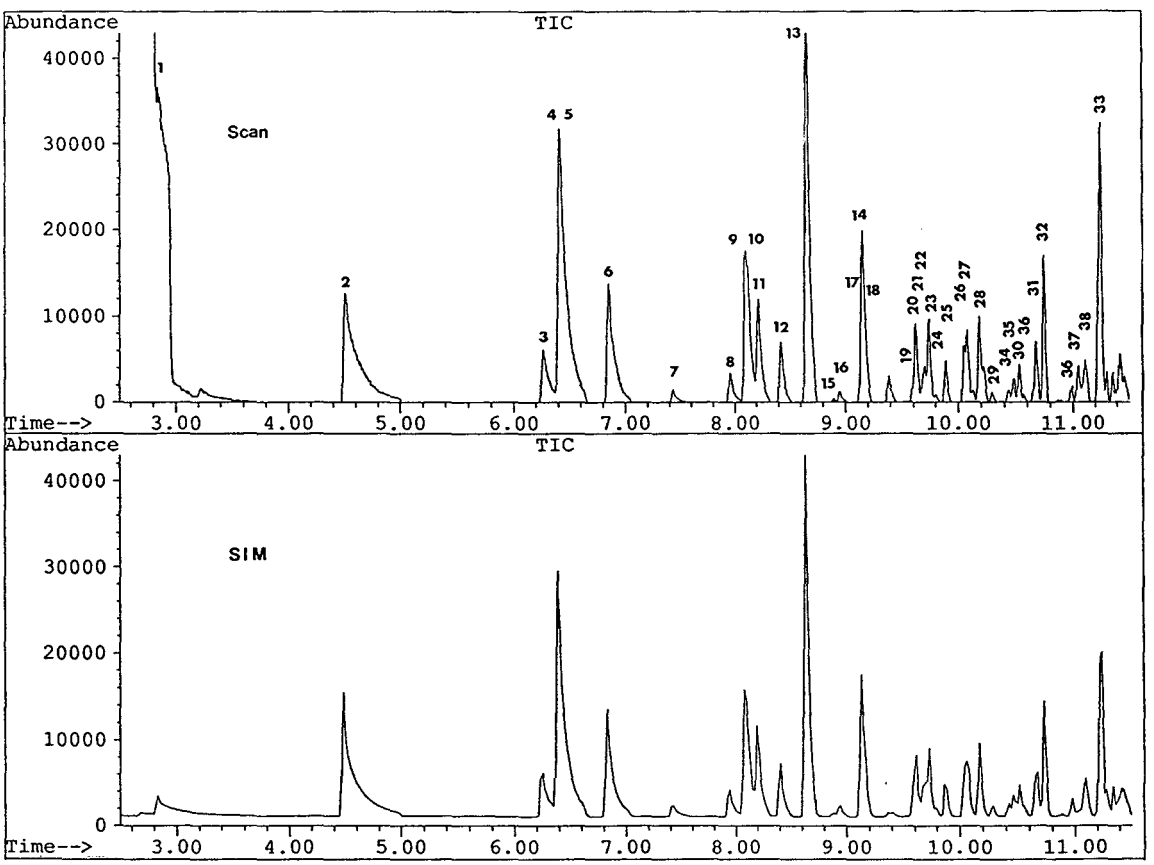


Fig. 4. GC–MS scan (A) and SIM (B) chromatograms of alkyl benzene compounds in the retention time range of 2.5–11.5 min. See Table 2 for component identification.

Table 2
Alkyl-substituted benzene compounds identified in ASMB oil

| Peak no. | $t_R$ (min) | Compound identified | $M_r$ | Cal. $I$ | Lit. $I$ | Std. $t_R$ (min) | Std. $I$ |
|---|---|---|---|---|---|---|---|
| | | C0-Benzene | | | | | |
| 1 | 2.840 | benzene | 78 | 671.3 | 670.6 | 2.836 | 671.0 |
| | | C1-Benzene | | | | | |
| 2 | 4.490 | toluene | 92 | 771.2 | 772.7 | 4.492 | 771.3 |
| | | C2-Benzene | | | | | |
| 3 | 6.268 | ethyl-benzene | 106 | 868.1 | 867.4 | 6.264 | 867.9 |
| 4 | 6.411 | *m*-xylene | 106 | 875.3 | 874.8 | 6.405 | 875.0 |
| 5 | 6.421 | *p*-xylene | 106 | 875.8 | 875.4 | 6.410 | 875.3 |
| 6 | 6.852 | *o*-xylene | 106 | 896.5 | 898.7 | 6.847 | 896.3 |
| | | C3-Benzene | | | | | |
| 7 | 7.430 | iso-propyl-benzene | 120 | 930.7 | 931.4 | 7.437 | 931.1 |
| 8 | 7.956 | propyl-benzene | 120 | 960.7 | 959.9 | 7.959 | 960.8 |
| 9 | 8.080 | 1-ethyl-3-methyl-benzene | 120 | 967.4 | 967.2 | 8.086 | 967.8 |
| 10 | 8.100 | 1-ethyl-4-methyl-benzene | 120 | 968.5 | 969.0 | 8.096 | 968.3 |
| 11 | 8.214 | 1,3,5-trimethyl benzene | 120 | 974.7 | 974.0 | 8.214 | 974.6 |
| 12 | 8.420 | 1-ethyl-2-methyl-benzene | 120 | 985.5 | 985.7 | 8.423 | 985.7 |
| 13 | 8.653 | 1,2,4-trimethyl benzene | 120 | 997.5 | 998.8 | 8.655 | 997.6 |
| 14 | 9.137 | 1,2,3-trimethyl benzene | 120 | 1028.2 | >1000 | 9.135 | 1028.1 |
| | | C4-Benzene | | | | | |
| 15 | 8.886 | iso-butyl-benzene | 134 | 1012.1 | >1000 | 8.868 | 1010.9 |
| 16 | 8.934 | *sec.*-butyl-benzene | 134 | 1015.2 | >1000 | 8.920 | 1014.3 |
| 17 | 9.120 | *m*-cymene | 134 | 1027.1 | | 9.122 | 1027.3 |
| 18 | 9.170 | *p*-cymene | 134 | 1030.3 | | 9.162 | 1029.8 |
| 19 | 9.590 | 1,3-diethyl-benzene | 134 | 1056.3 | | 9.573 | 1055.3 |
| 20 | 9.620 | 1-methyl-3-propyl-benzene | 134 | 1058.1 | | 9.613 | 1057.7 |
| 21 | 9.674 | 1-methyl-4-propyl-benzene | 134 | 1061.3 | | 9.685 | 1062.0 |
| 22 | 9.700 | butyl-benzene | 134 | 1062.9 | | 9.710 | 1063.5 |
| 23 | 9.750 | 1-ethyl-3,5-dimethyl-benzene | 134 | 1065.9 | | 9.746 | 1065.6 |
| 24 | 9.800 | 1,2-diethyl-benzene | 134 | 1068.8 | | 9.793 | 1068.4 |
| 25 | 9.890 | 1-methyl-2-propyl-benzene | 134 | 1074.1 | | 9.885 | 1073.8 |
| 26 | 10.050 | 1-ethyl-2,4-dimethyl-benzene | 134 | 1083.5 | | / | / |
| 27 | 10.080 | 2-ethyl-1,4-dimethyl-benzene | 134 | 1085.2 | | 10.060 | 1084.2 |
| 28 | 10.182 | 4-ethyl-1,2-dimethyl-benzene | 134 | 1091.0 | | 10.188 | 1091.4 |
| 29 | 10.290 | 2-ethyl-1,3-dimethyl-benzene | 134 | 1097.1 | | 10.300 | 1097.7 |
| 30 | 10.528 | 1-ethyl-2,3-dimethyl-benzene | 134 | 1113.1 | | 10.530 | 1113.2 |
| 31 | 10.676 | 1,2,4,5-tetramethyl-benzene | 134 | 1123.2 | | 10.687 | 1124.0 |
| 32 | 10.745 | 1,2,3,5-tetramethyl-benzene | 134 | 1127.9 | | 10.725 | 1126.6 |
| 33 | 11.250 | 1,2,3,4-tetramethyl-benzene | 134 | 1161.4 | | / | / |
| | | C5-Benzene | | | | | |
| 34 | 10.430 | C5-Benzene | 148 | 1106.3 | | | |
| 35 | 10.481 | C5-Benzene | 148 | 1109.8 | | | |
| 36 | 10.530 | C5-Benzene | 148 | 1114.6 | | | |

(*Continued on p. 332*)

Table 2 (*continued*)

| Peak no. | $t_R$ (min) | Compound identified | $M_r$ | Cal. *I* | Lit. *I* | Std. $t_R$ (min) | Std. *I* |
|---|---|---|---|---|---|---|---|
| 37 | 10.992 | C5-Benzene | 148 | 1144.5 | | | |
| 38 | 11.080 | C5-Benzene | 148 | 1150.3 | | | |
| 39 | 11.108 | C5-Benzene | 148 | 1154.1 | | | |
| 40 | 11.230 | C5-Benzene | 148 | 1160.1 | | | |
| 41 | 11.304 | amylbenzene | 148 | 1164.9 | 11.306 | 1165.0 | |
| 42 | 11.360 | C5-Benzene | 148 | 1168.5 | | | |
| 43 | 11.424 | C5-Benzene | 148 | 1172.6 | | | |
| 44 | 11.458 | C5-Benzene | 148 | 1174.8 | | | |
| 45 | 11.575 | C5-Benzene | 148 | 1182.2 | | | |
| 46 | 11.922 | C5-Benzene | 148 | 1204.5 | | | |
| 47 | 12.101 | C5-Benzene | 148 | 1217.6 | | | |
| 48 | 12.236 | C5-Benzene | 148 | 1227.5 | | | |
| 49 | 13.138 | pentamethyl-benzene | 148 | 1290.4 | 13.133 | 1290.0 | |
| | | C6-Benzene | | | | | |
| 50 | 12.334 | C6-Benzene | 162 | 1234.5 | | | |
| 51 | 12.481 | C6-Benzene | 162 | 1245.0 | | | |
| 52 | 12.579 | C6-Benzene | 162 | 1251.9 | | | |
| 53 | 12.798 | *n*-hexyl-benzene | 162 | 1267.2 | 12.800 | 1267.3 | |
| 54 | 12.906 | C6-Benzene | 162 | 1274.6 | | | |
| 55 | 13.004 | C6-Benzene | 162 | 1281.3 | | | |
| 56 | 13.053 | C6-Benzene | 162 | 1284.6 | | | |
| | | C7-Benzene | | | | | |
| 57 | 14.722 | C7-Benzene | 176 | 1408.8 | | | |
| | | C8-Benzene | | | | | |
| 58 | 15.522 | C8-Benzene | 190 | 1473.0 | | | |

The literature *I*-values listed here are the values after correction of the temperature effect on *I* according to the temperature coefficient given in Ref. [25].

(2) Tightly-capped oil samples were put into a refrigerator to precipitate asphaltenes to the bottom of the vials in order to avoid performance deterioration of the capillary GC column due to the introduction of asphaltenes into the column;
(3) $C_3$-benzenes in oil were quantitated using the RRFs directly obtained from the respective individual $C_3$-benzene standards instead of using the RRFs obtained from benzene or $C_1/C_2$-substituted benzenes.

Individual BTEX compounds and eight $C_3$-benzene compounds in over 200 oils have been quantified by using the procedures described above. The contents of BTEX and BTEX + $C_3$-benzenes vary from oil to oil. They can range from 0% up to 6% for BTEX and from 0% up to 7% for BTEX + $C_3$-benzenes, respectively, depending on the nature and origin of the oil sample. In general, however, the dominance of BTEX and $C_3$-benzenes in the alkyl-substituted benzene category is obvious.

The loss of BTEX and alkyl benzenes is immediate and significant after an oil spill. It was found that the major changes in alkyl benzene composition on increase of the weathering percentage can be summarized as follows: (1) the rate of loss is significantly correlated to the molecular mass and boiling points of the alkyl benzene compounds. Relative to $C_3$-benzenes, the low-molecular-mass- and the most volatile BTEX compounds are lost more quickly upon weathering (approximately at weathering percentages of 10–15%, BTEX were nearly com-

pletely lost); (2) the homologous group shows a clear evaporation trend: $C_0 > C_1 > C_2 > C_3 > C_4$; (3) when oil was weathered to approximately 20–25%, the BTEX and $C_3$-benzenes were completely lost.

### 3.3. PAHs and their alkylated homologues

PAHs are relatively stable constituents of petroleum and, as from the environmental aspect, they are probably the most important analytes in an oil-spill natural resource damage assessment. As shown in Table 1, the target PAHs and their alkylated homologues include naphthalene, phenanthrene, dibenzothiophene, fluorene, and chrysene homologous series. Unlike the sixteen EPA-defined priority PAH compounds, these homologous series are very useful in oil-spill assessment, in addition to being essential in evaluating the biological effects. This is because: (1) These alkylated PAH homologues are the most abundant PAH compounds in oil, and they persist for relatively longer periods of time than their parent compounds. Other 4- and 5-ring PAHs are very minor constituents of most crude oils, or are not even detected in many oil samples. (2) Different oils have different distribution profiles of alkylated PAH homologues. They are more valuable than the parent PAHs in fingerprinting the weathered oil, distinguishing between sources of hydrocarbons in the environment, and providing information on the extent and degree of oil weathering and degradation. (3) Reporting values of alkylated PAH homologues more truly reflects the composition of PAHs in oil than using data on parent PAH compounds. The changes in PAH composition caused by weathering and degradation can be more easily detected and traced as well.

Some studies have been performed using distribution of the alkylated PAH homologues as environmental fate indicators and source-specific markers of oil in sediments [12,18,19] and tissue samples [20,21]. Recently, a method using double-ratio plots of alkyl PAH homologues for petroleum source identification has been proposed [12]. This method has been successfully used to correlate the 1989 EXXON VALDEZ spilled-oil sediment samples to the source oil.

Fig. 5A shows the alkylated PAH-homologue distributions in ASMB oil and NOBE oil (Newfoundland Offshore Oil Burn Experiment oil, a type of Alberta oil used specifically for this experiment). For comparison, the abundances of the alkylated PAH homologues were normalized relative to C2-P. These two oils come from very similar origins, but exhibit different PAH signatures, especially the abundances and relative ratios of alkyl dibenzothiophenes. Fig. 5B shows the distribution of alkylated PAH homologues for Bunker C crude. The unusual high abundances of the alkyl phenanthrene series in Bunker C are pronounced. The distinctive

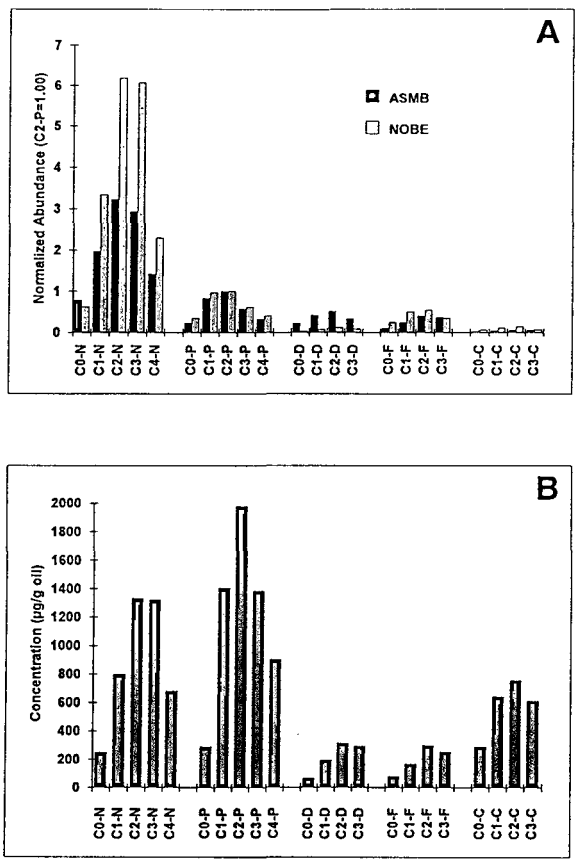


Fig. 5. Alkylated PAH homologous distribution for ASMB oil and NOBE oil (normalized abundance: C2-P = 1.00, A), and for Bunker oil (B).

character of each oil, as evidenced by the alkylated PAH-homologue distributions, is apparent. If only the 16 priority PAH compounds were the target analytes, such differences of composition between two oils would not be evident.

Fig. 6A–C shows the GC–SIM-MS chromatograms of the aromatic compounds of ASMB oil

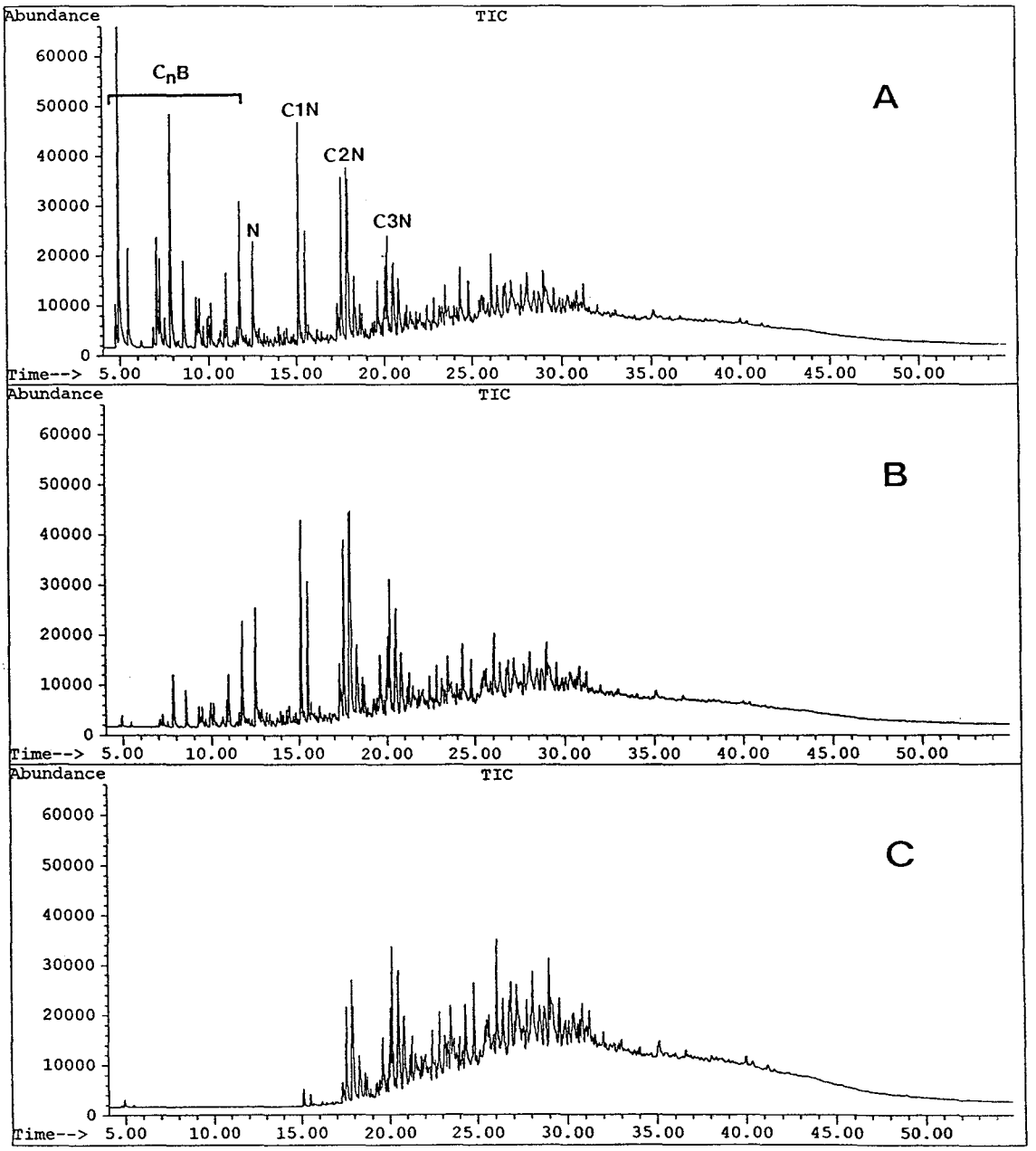


Fig. 6. GC–MS chromatograms of aromatic compounds of ASMB oil at weathering percentages 0% (A), 29.8% (B), and 44.5% (C). CnB, N, C1N, C2N, and C3N represent alkyl benzenes, naphthalene, and alkylated naphthalenes, respectively.

samples at 0%, 29.8%, and 45% artificially weathered (by evaporation). The loss of low-boiling alkyl benzenes and alkylated naphthalene homologues is very apparent as weathering increase. Fig. 7 shows the alkylated-PAH fingerprints of weathered Arrow oil, and three 22-year-old spilled Arrow oil samples S-6, S-A and S-9, showing the preferential loss of certain alkylated PAH homologues in highly-weathered Arrow oil samples and illustrating the effect of field weathering on PAH composition [in order to clearly show the changes in the distribution patterns within the different PAH families, different scales for $y$-axis were applied to Fig. 7A (0–3200 $\mu$g/g TSEM), 7B (0–800 $\mu$g/g TSEM), 7C and 7D (0–400 $\mu$g/g TSEM), respectively]. Conducting such analyses over time and at different locations with different exposures will provide essential information on the long-term impact of spilled oil on the environment.

It has been demonstrated [6] that the ratios for PAH compounds within an isomer group are relatively consistent even after evaporation. However, if any biodegradation occurs, the ratios of the isomers change within the same isomeric group [15,16]. Fig. 8A–E shows GC–

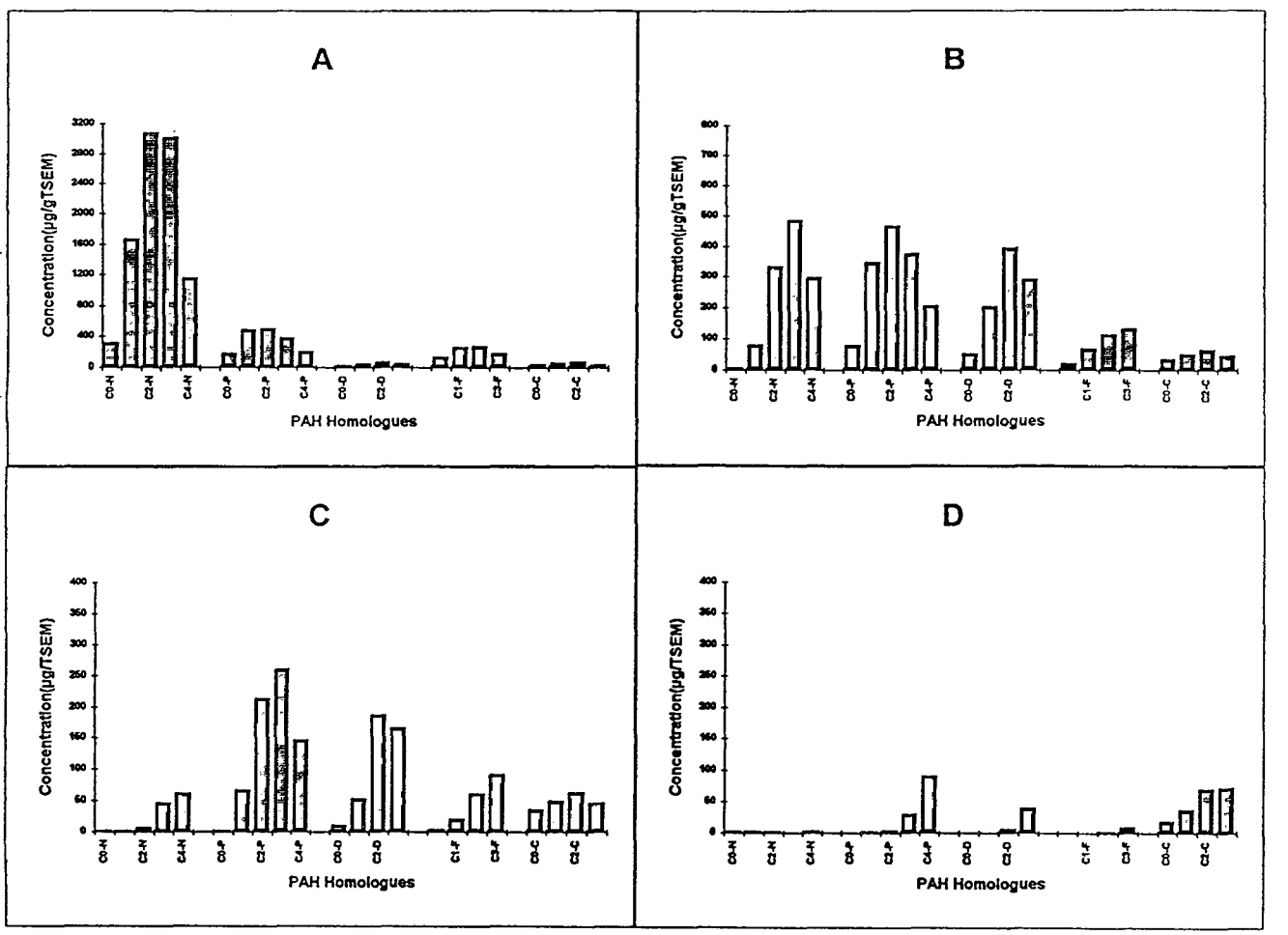


Fig. 7. Alkylated PAH fingerprints of the weathered source oil (A), samples S-6 (B), S-A (C), and S-9 (D) illustrating the effects of weathering on PAH compositions. N, P, D, F, and C represent naphthalene, phenanthrene, dibenzothiophene, fluorene, and chrysene, respectively; 0, 1, 2, 3, and 4 represent carbon numbers of alkyl groups in alkylated PAH homologoues.

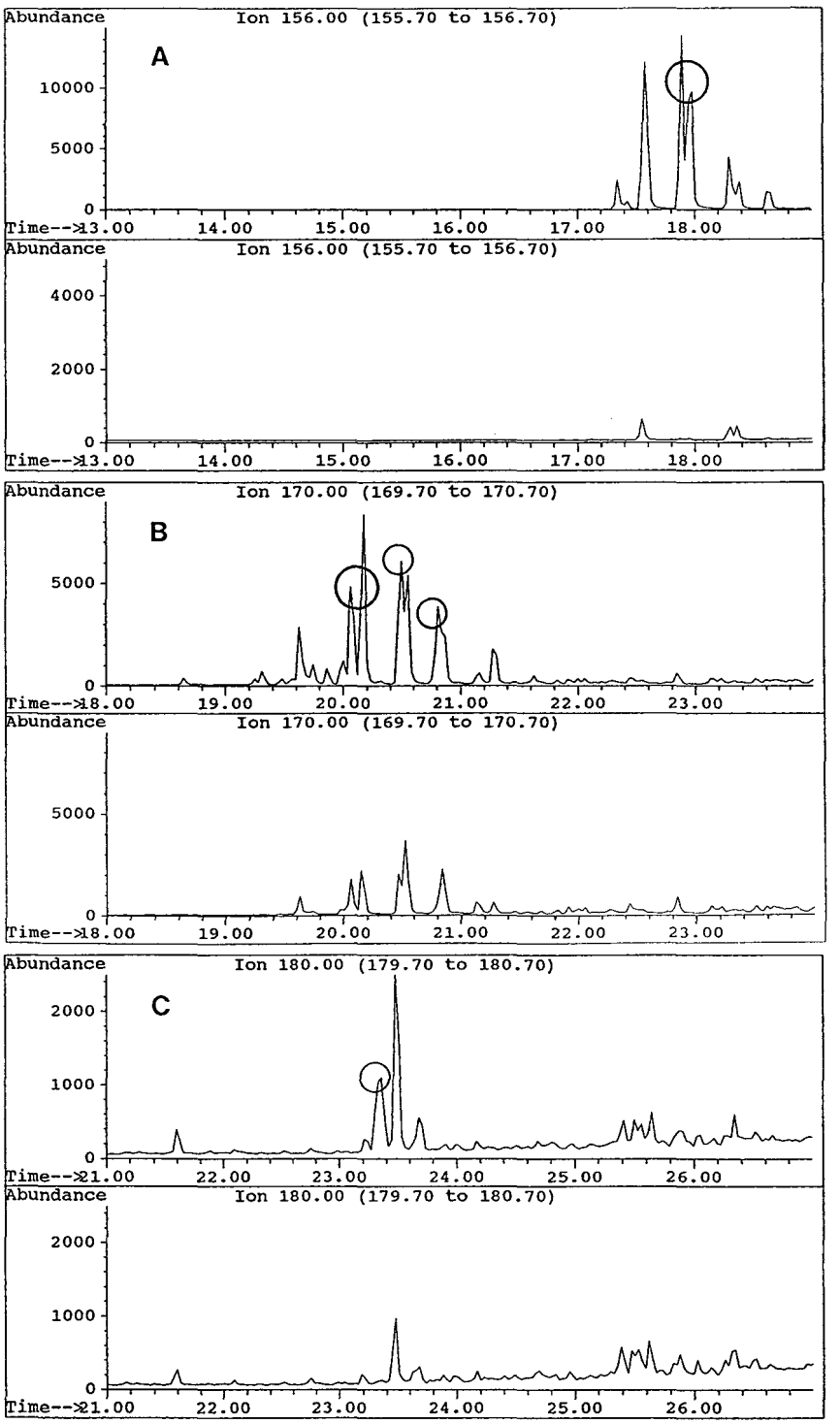


Fig. 8. Extracted ion chromatograms for $C_2$-naphthalenes (*m/z* 156, A), $C_3$-naphtalenes (*m/z* 170, B), $C_1$-fluorenes (*m/z* 180, C), $C_1$-phenanthrenes (*m/z* 192, D), and $C_1$-dibenzothiophenes (*m/z* 198, E) in the source ASMB oil and corresponding biodegradation ASMB oil samples. The circled regions show the changes in distribution among isomers that were preferentially degraded by bacteria.

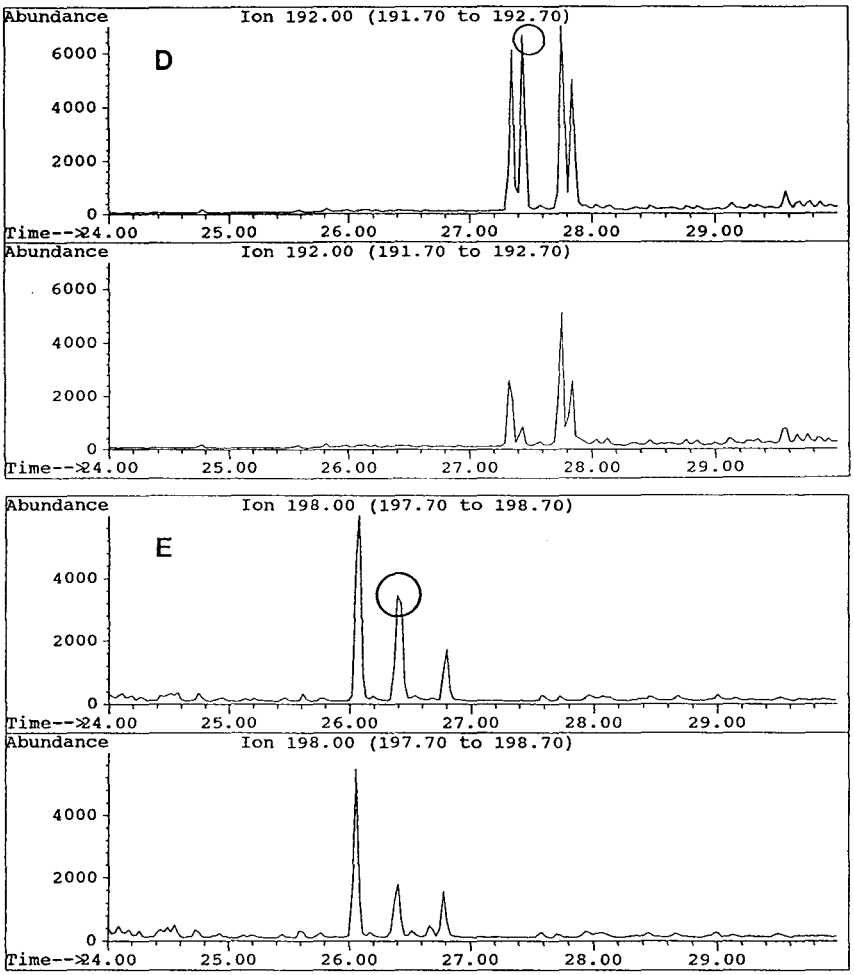


Fig. 8 (*continued*).

MS fragmentograms of $C_2$-naphthalenes (*m/z* 156), $C_3$-naphthalenes (*m/z* 170), $C_1$-fluorenes (*m/z* 180), $C_1$-phenanthrenes (*m/z* 192), and $C_1$-dibenzothiophenes (*m/z* 198) in the source ASMB oil and the biodegradated oil samples incubated for 28 days at 4°C with cold marine standard inoculum. The circled regions in Fig. 8 show the changes in distribution among isomers that were selectively altered by biodegradation. It can be seen from Fig. 8 that among six identified $C_2$-naphthalenes (Fig. 8A: ethyl-, 2,6-, 1,3-, 1,6-, 2,3-, and 1,2-dimethyl-naphthalene), eight identified $C_3$-naphthalenes (Fig. 8B: $\beta\beta$-ethylmethyl-, $\alpha\beta$-ethylmethyl-, 1,3,7-, 1,3,6-, 1,3,5-, 2,3,6-, 2,3,5-, 1,2,7-, 1,2,5-trimethyl-naphthalene), three identified $C_1$-methyl-fluorenes (Fig. 8C: methyl-, 2-, and 1-methyl-fluorene), four identified $C_1$-phenanthrenes (Fig. 8D: 3-, 2-, 4-/9-, and 1-methyl-phenanthrene), and three identified $C_1$-dibenzothiophenes (Fig. 8E: 4-, 2-/3-, and 1-methyl-dibenzothiophene), bacteria most preferentially degraded 1,3- and 1,6-dimethyl-naphthalene, 1,3,7-, 1,3,6-, 1,3,5-, and 2,3,5-trimethyl-naphthalene, methyl-fluorene, 2-methyl-phenanthrene, and 2-/3-methyl-dibenzothiophene. This finding has great importance because the ratios within the isomeric PAH groups can be used as markers of biodegradation. The concentrations and relative distributions among and between isomers of

alkyl homologue groups from hundreds of biodegradation samples have been calculated. Evaluation of the data results in a qualitative determination of the extent and progress of biodegradation in the samples. These qualitative data, when used in conjunction with quantitative data on the changes in distribution of the entire PAH homologous groups, may be used to evaluate the effects of bioremediation products on oil degradation.

### 3.4. Biomarker compounds

For decades triterpanes and steranes have been used as biomarker compounds for the identification of petroleum deposits by petroleum geochemists [22–29]. These biomarkers were later used for oil fingerprinting by environmental chemists to study the fate and to trace the source of spilled oil [30–35]. Analysis of biomarker compounds offers several distinct advantages: (1) triterpanes and steranes are unique for each oil. The distribution patterns of biomarker compounds, in general, are different from oil to oil. Therefore they are useful in identification of the oil source; (2) they are highly degradation-resistant compounds in comparison to the aliphatic and aromatic compounds. As an oil becomes more degraded the concentration of biomarker compounds should increase relative to the more easily degraded constituents; (3) calculation based on hopane analysis to estimate percent of oil depletion can provide a more accurate representation of the degree of oil degradation than the traditional aliphatic/isoprenoid hydrocarbon ratio, and can greatly improve the ability to resolve biodegradation differences between sites.

Fig. 9A–F shows hopane and sterane distribution chromatograms of three crude oils (ASMB oil, NOBE oil, and California oil). ASMB oil and NOBE oil are of similar origins and both are light oils. California oil is much heavier than ASMB oil and NOBE oil (the API gravity for California oil and ASMB oil is 15 and 37, respectively). Even by visual comparison, these three oils can be readily distinguished by the distribution profiles and the relative amount of hopanes and steranes. Analysis of several hundreds of different oils and spilled-oil samples demonstrates that triterpane compounds in oils are distributed in a wide range from $C_{19}$ to $C_{35}$ with various pentacyclic hopanes (such as $C_{29}$-$\alpha\beta$- and $C_{30}$-$\alpha\beta$-hopane, peaks 17 and 19 in Fig. 9A) being prominent. In the distribution of steranes, the dominance of $C_{27}$, $C_{28}$, and $C_{29}$ steranes (peaks 42 through 53 in Fig. 9B) is apparent for most oils. A significant contribution from the diasteranes is also observed for some oils.

A lightly degraded oil is usually indicated by partial depletion of *n*-alkanes; a moderately-degraded one is often indicated by heavy loss of *n*-alkanes and partial loss of lighter PAH compounds. However, from extensively degraded oil samples [such as 22-year-old Arrow oil samples and heavily-weathered Baffin Island Oil Spill (BIOS) samples], the *n*-alkanes and branched alkanes might have been completely lost, and PAHs and their alkyl homologues could be highly degraded. In such cases, identification through recognition of *n*-alkanes and/or PAH distribution pattern would be rather difficult, and analysis of biomarker compounds would be not only necessary but also particularly important and valuable, because only these highly degradation-resistant compounds remain in the samples after long-term weathering and can give chemical "fingerprinting" information of the source, degree of weathering, characteristics and fate of the spilled oil.

Two criteria are used for matching the long-term weathered oil with the source oil: (1) whether the distribution profile and pattern of the *m/z* 191 and 217 fragments are the same; (2) whether the computed ratios of some target pairs of terpane and sterane compounds are near identical. Table 3 lists and compares some diagnostic ratios from two groups of highly-weathered and degraded oil samples (Arrow and BIOS). Due to the extensive weathering, the Arrow oil samples were characterized by the total loss of *n*-alkanes and isoprenoids and heavy loss of PAH compounds, resulting in the traditional *n*-alkane/isoprenoid ratios being non-calculable. The double ratios of some remaining

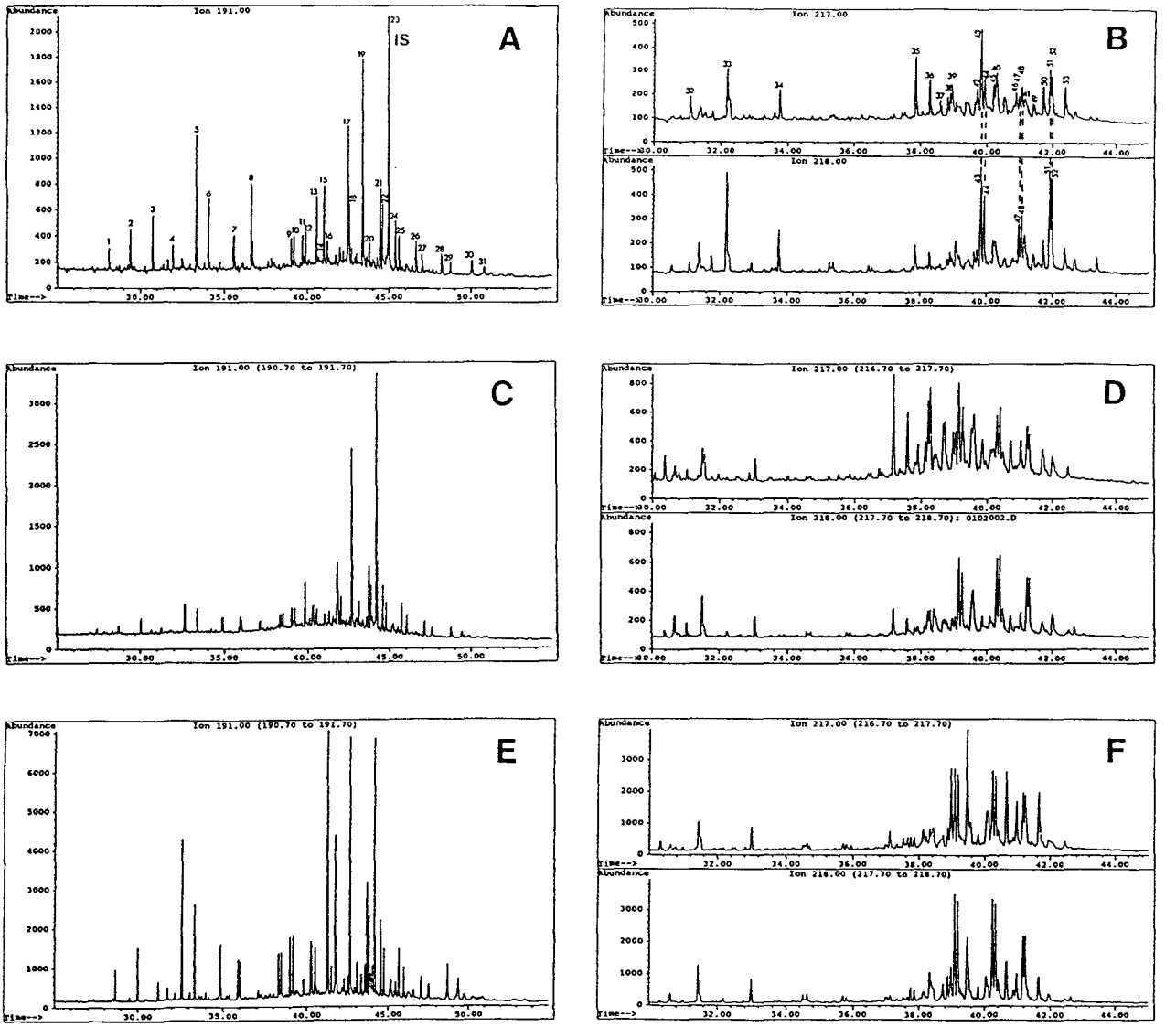


Fig. 9. Distribution of hopanes ($m/z$ 191) and steranes ($m/z$ 217 and 218) in ASMB oil (A and B), NOBE oil (C and D), and California oil (E and F).

PAH homologues ($C_2D/C_2P$ and $C_3D/C_3P$) did not show any clear correlation between samples either. Less weathered BIOS samples showed similar results except that $n$-alkanes and isoprenoids were only partially lost and the ratios of pristane/phytane showed some correlation between samples. Fortunately, however, the GC–MS measurements demonstrate that the profiles and patterns of the $m/z$ 191 and 217 ion chromatograms of the Arrow oil and BIOS samples are nearly identical, except that a few samples (such as S-1 and S-10) showed the similar distribution patterns but with some peaks being less abundant and even undetectable. More importantly, the computed ratios of target hopane compounds ($C_{29}/C_{30}$) appear to be consistent for all samples (0.86 and 0.95 for Arrow and BIOS series, respectively) and, therefore, can be

Table 3
Comparison of diagnostic ratios for Arrow and BIOS samples

| Sample | Weathered source oil | Arrow oil samples | | | | | | | | | | |
|---|---|---|---|---|---|---|---|---|---|---|---|---|
| | | S-1 | S-2 | S-3 | S-4 | S-5 | S-6 | S-7 | S-8 | S-9 | S-10 | S-A |
| C17/pristane | 1.66 | non-calculable | | | | | 1.37 | non-calculable | | | | |
| C18/phytane | 1.47 | non-calculable | | | | | 1.00 | non-calculable | | | | |
| pristane/phytane | 0.87 | non-calculable | | | | | 0.75 | non-calculable | | | | |
| C2D/C2P | 0.85 | 0.22 | 1.80 | 0.85 | 0.98 | 1.20 | 0.85 | 0.79 | 2.40 | 1.90 | 0.65 | 0.88 |
| C3D/C3P | 0.78 | 0.60 | 1.40 | 0.67 | 0.83 | 1.10 | 0.77 | 0.95 | 0.96 | 1.30 | 0.65 | 0.64 |
| C23/C24 | 2.07 | 0.62 | 2.05 | 2.06 | 2.07 | 2.10 | 2.06 | 2.09 | 2.07 | 1.98 | 1.00 | 2.05 |
| Ts/Tm | 0.26 | 0.31 | 0.28 | 0.26 | 0.27 | 0.27 | 0.26 | 0.27 | 0.28 | 0.29 | 0.36 | 0.27 |
| C29/C30 | 0.86 | 0.87 | 0.84 | 0.86 | 0.86 | 0.87 | 0.86 | 0.87 | 0.86 | 0.86 | 0.89 | 0.86 |
| | | BIOS oil samples | | | | | | | | | | |
| | | BIOS-1 | BIOS-2 | BIOS-3 | BIOS-4 | BIOS-5 | BIOS-6 | BIOS-7 | BIOS-8 | BIOS-9 | BIOS-10 | BIOS-11 |
| C17/pristane | 3.44 | 2.20 | 0.00 | 0.90 | 1.16 | 0.76 | 0.90 | 0.16 | 2.25 | 2.42 | 2.29 | 0.19 |
| C18/phytane | 1.47 | 1.05 | 0.00 | 0.77 | 0.51 | 0.31 | 0.42 | 0.13 | 1.03 | 1.01 | 1.04 | 0.14 |
| pristane/phytane | 0.53 | 0.55 | 0.32 | 1.09 | 0.54 | 0.41 | 0.40 | 0.26 | 0.54 | 0.55 | 0.51 | 0.54 |
| C2D/C2P | 1.10 | 1.78 | 1.33 | 0.71 | 1.06 | 1.11 | 0.87 | 1.20 | 2.24 | 0.13 | 1.87 | 1.52 |
| C3D/C3P | 0.91 | 1.15 | 1.03 | 0.74 | 0.95 | 1.09 | 0.84 | 1.05 | 1.08 | 0.24 | 1.29 | 1.02 |
| C23/C24 | 2.17 | 2.18 | 2.15 | 1.53 | 2.14 | 1.94 | 1.61 | 2.02 | 2.12 | 2.14 | 2.16 | 2.16 |
| Ts/Tm | 0.22 | 0.24 | 0.23 | 0.22 | 0.24 | 0.28 | 0.33 | 0.27 | 0.23 | 0.24 | 0.24 | 0.23 |
| C29/C30 | 0.95 | 0.95 | 0.93 | 0.94 | 0.95 | 0.95 | 0.94 | 0.95 | 0.95 | 0.95 | 0.96 | 0.94 |

used as a good indicator for oil identification. Besides that, the relatively lower abundant, but well-resolved, paired $C_{32}$ and $C_{33}$ 22*S*/22*R* hopane isomers (peaks 24 through 27 in Fig. 9A) also show very good consistency in the values of $22S/(22S + 22R)$ ratios for each series of samples.

It is noticed that for most of the Arrow and BIOS samples the ratios of paired terpanes Ts/Tm (Ts: 18$\alpha$(H),21$\beta$(H)-22,29,30-trisnorhopane; Tm: 17$\alpha$(H),21$\beta$(H)-22,29,30-trisnorhopane; peak 13 and 15 in Fig. 9A) and $C_{23}/C_{24}$ (peaks 5 and 6 in Fig. 9A) are also quite consistent, but for samples S-1 and S-10, BIOS no. 5, no. 6, and no. 7, much lower $C_{23}/C_{24}$ values and higher Ts/Tm values were observed. The ratio of the $C_{27}$ pentacyclic terpanes Ts and Tm has been used as a geochemical parameter to characterize both source input and maturity of a crude [36] and as an indicator for oil matching [8,37]. In most cases, Ts and Tm were apparently independent of weathering effect and therefore can be useful in matching of oils. However, this does not hold for those residual oils in sediments which have undergone long-term extensive weathering and biodegradation, as in the case of samples S-1 and S-10, and nos. 5, 6 and 7. As shown in Table 3, the ratios of Ts/Tm increased from a value around 0.27 for most Arrow samples and 0.23 for most BIOS samples to 0.31, 0.36, 0.28, 0.33 and 0.27 for these five samples, respectively. It has been reported [37] that as maturation takes place either in the kerogen matrix or in the reservoir on a geological time scale, Tm shows a relatively faster rate of depletion than Ts. This study also demonstrated that Tm has a relatively faster rate of biodegradation than Ts (even though Ts chromatographically elutes earlier than Tm), resulting in higher Ts/Tm ratios for those very

Table 4
Quantitation of TSEM. TPH. *n*-alkanes. PAHs. and selected paired hopane isomers. and estimation of weathering percentages of oil in BIOS samples

| Sample | Quantitation of hydrocarbons | | | | Target hopanes ($\mu$g/g TSEM) | | | | Weathering perentages (%) | | |
|---|---|---|---|---|---|---|---|---|---|---|---|
| | TSEM (mg/g of sample) | TPH by GC (mg/g of sample) | Total *n*-alkanes (mg/g TSEM) | Alkylated PAHs (mg/g TSEM) | C23 ($\mu$g/g TSEM) | C24 ($\mu$g/g TSEM) | C29 a$\beta$ ($\mu$g/g TSEM) | C30 a$\beta$ ($\mu$g/g TSEM) | Based on C29 hopane | Based on C30 hopane | Average |
| BIOS-1 | 36.3 | 17.9 | 44.3 | 3.0 | 163 | 75 | 129 | 136 | 10.1 | 10.3 | 10 |
| BIOS-2 | 9.3 | 3.4 | 1.40 | 3.9 | 174 | 81 | 145 | 157 | 20.0 | 22.3 | 21 |
| BIOS-3 | 0.0115 | 0.0014 | 7.17 | 0.41 | 109 | 72 | 131 | 139 | 11.5 | 12.2 | 12 |
| BIOS-4 | 29.9 | 13.4 | 27.9 | 4.1 | 179 | 84 | 145 | 153 | 20.0 | 20.3 | 20 |
| BIOS-5 | 0.169 | 0.042 | 4.97 | 0.49 | 267 | 138 | 287 | 303 | 60.0 | 60.0 | 60 |
| BIOS-6 | 0.0807 | 0.0164 | 4.36 | 0.22 | 185 | 116 | 289 | 308 | 60.0 | 60.4 | 60 |
| BIOS-7 | 0.55 | 0.15 | 7.11 | 0.47 | 222 | 109 | 221 | 231 | 47.5 | 47.2 | 47 |
| BIOS-8 | 4.0 | 2.1 | 44.4 | 3.5 | 166 | 78 | 136 | 143 | 14.7 | 14.7 | 15 |
| BIOS-9 | 19.3 | 10.4 | 41.2 | 2.4 | 158 | 74 | 126 | 132 | 8.0 | 7.6 | 8 |
| BIOS-10 | 33.3 | 15.1 | 39.7 | 1.8 | 166 | 77 | 132 | 138 | 12.1 | 11.6 | 12 |
| BIOS-11 | 15.1 | 7.4 | 13.3 | 4.5 | 180 | 83 | 150 | 160 | 22.7 | 23.8 | 23 |
| Weathered source oil | 868 | 530 | 56.0 | 8.0 | 156 | 72 | 125 | 131 | 7.2 | 6.9 | 7 |
| "Fresh" source oil | | | | | 142 | 65 | 116 | 122 | | | |

heavily biodegraded samples. The same hold for $C_{23}/C_{24}$. Both of these two relatively small terpanes are biodegradable, but with the degradation rate of $C_{23}$ being faster than that of $C_{24}$, resulting in lower $C_{23}/C_{24}$ ratios.

As shown in Table 3, the combined ratios of the selected pairs of terpanes, especially the ratio of $C_{29}/C_{30}$ hopane, are apparently independent of weathering effects and can be useful in identification of oil source and in oil matching. It should be understood, however, that there is no single ratio which can be used to positively identify the source of an unknown spilled oil by itself without matching it to known oils. Other diagnostic ratios (such as those obtained from *n*-alkanes and alkylated PAH homologues) remain necessary and useful for oil source identification and characterization.

A method based on biomarker compounds (using $C_{29}$-$\alpha\beta$- and $C_{30}$-$\alpha\beta$-hopane as internal oil references) to estimate oil weathering percentages in environmental samples has been developed and successfully used for determination of weathering percentages of oil in BIOS samples using the following equation [6,9,32]:

$$P(\%) = (1 - C_s/C_w) \times 100(\%)$$

where $P$ is the weathering percentage of the weathered samples; $C_s$ is the concentration of $C_{29}$-$\alpha\beta$- and $C_{30}$-$\alpha\beta$-hopane in the source BIOS oil; $C_w$ is the concentration of $C_{29}$-$\alpha\beta$- and $C_{30}$-$\alpha\beta$-hopane in the weathered BIOS samples.

The results in Table 4 show that the BIOS samples nos. 1, 4, 8, 9, and 10 were less weathered with weathering percentages in the range 8–20%, while the weathering percentages for the highly weathered samples nos. 5, 6, and 7 were determined to be as high as 50–60%. These results show excellent correlation to the TSEM (total solvent extractable materials), TPH (total petroleum hydrocarbons by GC), aliphatic, PAH, and biomarker compound analysis results. For example, the samples nos. 5, 6, and 7 with the highest weathering percentages showed the lowest TSEM and TPH values, the lowest concentrations of *n*-alkanes and alkylated PAH homologues, the highest concentrations of hopanes (Table 4), while the samples with the lowest weathering percentages, nos. 1, 4, 8, 9, and 10, demonstrated the reverse trends.

## 4. Conclusions

This paper described a high-performance capillary gas chromatographic–mass spectrometric technique for the determination of individual petroleum hydrocarbon compounds and specific compound types and classes including $C_8$ through $C_{40}$ normal alkanes, the isoprenoids pristane and phytane, BTEX and alkyl benzenes, target polycyclic aromatic hydrocarbons and their alkylated homologues, and biomarker triterpanes and steranes. The analytical methods described for the determination of target hydrocarbons in crude oil, weathered oil, spilled oil and oil-spill-related environmental samples are more selective and more representative of the true composition of oil, and hence more defensible than some other traditional methods which were originally designed for industrial waste and hazardous waste. The analytical data and results obtained by using these methods are important and essential in differentiating individual crude oils, monitoring the changes in oil composition during weathering, understanding the fate and behaviour of the spilled oil in the environment, and assessing the damage of spilled oil to the natural resources. In addition, the present work also demonstrated that the efficient oil source identification and estimation of weathering percentages for very heavily weathered oil samples can be accomplished by the selective use of biomarker parameters.

It should be noted that although the GC–MS techniques described provide an increase in hydrocarbon fingerprint resolution, other analytical approaches remain necessary, and are complementary to the GC–MS techniques.

## References

[1] M.F. Fingas, W.S. Duval and G.B. Stevenson, The Basics of Oil Spill Cleanup, Environment Canada, Hull, Que., Canada, 1979.

[2] J.R. Bragg, R.C. Prince, E.J. Harner and R.M. Atlas, Nature, 368 (1994) 413–418.
[3] J.R. Bragg, R.C. Prince, J.B. Wilkinson and R. M Atlas, Bioremediation for Shoreline Cleanup Following the 1989 Alaskan Oil Spill, published by EXXON Company, Houston, TX, 1992.
[4] Z.D. Wang, M. Fingas and K. Li, J. Chromatogr. Sci., 32 (1994) 361–366.
[5] E. Lundances and T. Greibrokk, J. High. Res. Chromatogr., 17 (1994) 197–202.
[6] Z.D. Wang, M. Fingas, Proceeding of The 17th Arctic and Marine Oil Spill Program (AMOP) Technical Seminar, June 8–10, 1994, Vancouver, Canada; Environment Canada, Ottawa, 1994, pp. 133–172.
[7] Z.D. Wang, M. Fingas and K. Li, J. Chromatogr. Sci., 32 (1994) 367–382.
[8] Z.D. Wang, M. Fingas and G. Sergy, Environ. Sci. Technol., 28 (1994) 1733–1746.
[9] Z.D. Wang, M. Fingas and G. Sergy, Proceedings of The 18th Arctic and Marine Oil Spill Program (AMOP) Technical Seminar, June 14–16, 1995, Edmonton, Alb., Canada, Environment Canada, Ottawa, 1995.
[10] S. Blenkinsopp, G. Sergy, Z.D. Wang, M. Fingas, J. Foght and D.W.S. Westlake, Proceedings of the 1995 International Oil Spill Conference, American Petroleum Institute, Washington, DC, 1995, ID No. 111.
[11] Z.D. Wang, M. Fingas, M. Landriault, L. Sigouin and N. Xu, Proceedings of The 18th Arctic and Marine Oil Spill Program (AMOP) Technical Seminar, June 14–16, 1995, Edmonton, Alb., Canada, Environment Canada, Ottawa, 1995.
[12] D.S. Page, P.D. Boehm, G.S. Douglas, A.E. Bence, in Third ASTM Symposium on Environmental Toxicology and Risk Assessment: Aquatic, Plant and Terrestrial, April 25–28, 1993, Atlanta, GA, American Society for Testing and Materials, Philadelphia, PA, 1993.
[13] T. Sauer and P. Boehm, Proceedings of the 1991 Oil Spill Conference, American Petroleum Institute, Washington, DC, 1991, pp. 363–369.
[14] National Academy of Science, Oil in The Sea: Inputs, Fates and Effects, National Academy Press, Washington, 1985.
[15] Z.D. Wang, M. Fingas, S. Blenkinsopp, Study of the Effects of Biodegradation on Chemical Composition of Crude Oil, in preparation, 1995.
[16] M.C. Kennicutt II, Oil Chem. Pollut., 4 (1989) 89–112.
[17] A.J. Lubeck, D.L. Sutton, J. High Res. Chromatogr. Chromatogr. Commun., 6 (1983) 328–332.
[18] J.M. Teal, J.W. Farrington, K.A. Burst, J.J. Stegeman, B.W. Tripp, B. Woodin and C. Phinney, Mar. Pollut. Bull., 24 (1992) 607.
[19] A. Farran, J. Grimelt, J. Albaiges, A.V. Botello and S.A. Macko, Mar. Pollut. Bull., 18 (1987) 284.
[20] S. Sinkkonen, in J. Albaiges, R.W. Frei and E. Merian (Editors), Chemistry and Analysis of Hydrocarbons in The Environment, Gordon and Breach Science Publishers, New York, NY, 1983, pp. 207–215.
[21] A.E. Bence and W.A. Burns, in Third ASTM Symposium on Environmental Toxicology and Risk Assessment: Aquatic, Plant and Terrestrial, April 25–28, 1993, Atlanta, GA, American Society for Testing and Materials, Philadelphia, PA, 1993.
[22] W.K. Seifert and J.W. Moldowan, Geochim. Cosmochim Acta, 43 (1979) 111–126.
[23] W.K. Seifert and J.W. Moldowan, Geochim. Cosmochim Acta, 45 (1979) 785–794.
[24] W.K. Seifert and J.W. Moldowan, in R.B. Johns (Editor), Biological Markers in the Sedimentary Record, Elsevier, Amsterdam, 1986, pp. 261–290.
[25] K.E. Peter and J.W. Moldowan, Org. Geochem., 17 (1991) 47–61.
[26] J.K. Valkman, R. Alexander and R.I. Kagi, Geochim. Cosmochim. Acta, 47 (1983) 1033–1040.
[27] J.K. Valkman, R. Alexander, R.I. Kagi and G.W. Woodhouse, Geochim. Cosmochim. Acta, 47 (1983) 785–794.
[28] K.E. Peter and J.W. Moldowan, The Biomarker Guide: Interpreting Molecular Fossils in Petroleum and Ancient Sediments, Prentice Hall, New Jersey, 1993.
[29] S.D. Killops and V.J. Howell, Chem. Geol., 91 (1991) 65.
[30] O. Grahl-Nielsen and T. Lygre, Mar. Pollut. Bull., 21 (1991) 176–183.
[31] D.S. Page, J.C. Foster, P.M. Fickeett and E.S. Gilfillan, Mar. Pollut. Bull., 19 (1988) 107–115.
[32] E.L. Bulter, G.S. Douglas, W.G. Steinhauter, in R.E. Hinchee and R.F. Olfenbuttel (Editors), On-site Bioreclamation, Butterworth–Heinemann, Stoneham, MA, 1991, pp. 515–521.
[33] F. Brakstad and O. Grahl-Nielsen, Mar. Pollut. Bull., 19 (1988) 319–324.
[34] G.S. Douglas, in P.T. Kostecki and E.J. Calabrese (Editors), Contaminated oils, Diesel Fuel Contamination, Lewis Publishers, Ann Arbor, MI, 1992, Ch. 1.
[35] K.A. Kvenvolden, F.D. Hostettler, J.B. Rapp and P.R. Carlson, Mar. Pollut. Bull., 26 (1993) 24.
[36] W.K. Seifert and J.W. Moldowan, Geochim. Cosmochim. Acta, 42 (1978) 77.
[37] J. Shen, Anal. Chem., 56 (1984) 214.

ELSEVIER

Journal of Chromatography A, 712 (1995) 345–354

JOURNAL OF CHROMATOGRAPHY A

# General method for determining ethylene oxide and related $N^7$-guanine DNA adducts by gas chromatography–electron capture mass spectrometry

Manasi Saha, Amir Abushamaa, Roger W. Giese*

*Department of Pharmaceutical Sciences in the Bouve College of Pharmacy and Health Professions, Barnett Institute of Chemical Analysis and Chemistry Department, Northeastern University, Boston, MA 02115, USA*

First received 23 February 1995; revised manuscript received 3 May 1995; accepted 8 May 1995

**Abstract**

A 112-$\mu$g sample of DNA was spiked with 103 pg of $N^7$-(2′-hydroxyethyl)guanine and 100 pg of $N^7$-(2′-hydroxyethyl-d4)guanine, the internal standard. The sample was subjected to the following sequence of steps: heating at 100°C, precipitation of the DNA with HCl, reaction with nitrous acid to form the corresponding xanthines, reaction twice with pentafluorobenzyl bromide (first to derivatize NH, then OH), solid-phase extraction on silica and detection by gas chromatography–electron capture mass spectrometry. The absolute, overall yield of final product for both the analyte and internal standard was 9.7%. Conveniently, the three chemical reactions are conducted sequentially in the same vial and, aside from a washing step, are separated only by evaporations. Corresponding $N^7$-guanine methyl, phenyl and styrene oxide adducts were detected at about the 50-ng level by the procedure, to indicate the generality of the method.

## 1. Introduction

The $N^7$-position of guanine (G) is a prominent site of attack on DNA both in vitro and in vivo by a variety of alkylating agents, as has been reviewed [1]. Ethylene oxide, styrene, methylnitrosourea, vinyl chloride and aflatoxin (or their metabolites) are examples of such agents. For the "olefins" in this group, metabolic activation leads to a corresponding epoxide, which may then react with DNA. Certainly the exposure of the $N^7$-G site in the minor groove of DNA ($N^7$-G is not involved directly in Watson–Crick base pairing) is important for the propensity of this site to alkylate. It is therefore not surprising, perhaps, that at least some of these adducts are repaired enzymatically in vivo [1].

Humans are exposed occupationally, chemotherapeutically or otherwise (e.g., smokers) to alkylating agents [2]. For example, ca. $2.5 \cdot 10^6$ tons of ethylene oxide are produced annually in the USA, where 150 000 workers deal with it daily in various industrial processes [3] (1986 figures). Ethylene oxide is carcinogenic, mutagenic and teratogenic in animals, such as the rat, and is considered a probable carcinogen in humans [1]. The measurement of $N^7$-G adducts may be helpful as a biomonitor of such exposure,

* Corresponding author.

0021-9673/95/$09.50 
*SSDI* 0021-9673(95)00545-5

e.g., to facilitate epidemiological studies relating chemical exposure to health risks.

$N^7$-G adducts potentially are a favorable class of DNA adducts for measurement since they can be isolated conveniently from the DNA. Simply heating the DNA in water releases such adducts as free nucleobases [4]. Several procedures, even automated (e.g., from Applied Biosystems or Integrated Separation Systems) are available to purify DNA from biological samples.

The $N^7$-G adduct of ethylene oxide has been measured in biological samples by HPLC with fluorescence [5] and electrochemical detection [6] and GC–electron impact (EI) mass spectrometry [7]. Background adduct levels, per $10^6$ nucleotides, of 2–6 (mice and rats), 0.15 (salmon sperm DNA) and 2 (rats), respectively, were reported. However, where the data were shown, the peak seen was at or near the detection limit of the method in a complex chromatogram, so the true background level remains to be confirmed. Walker et al. [5] pointed out the need for a more sensitive method for this adduct, since they were unable to measure the adduct in rats and mice exposed to 3 ppm of ethylene oxide.

We are developing a general method for the detection of "small" $N^7$-G DNA adducts by gas chromatography–electron capture mass spectrometry (GC–EC-MS). Our initial focus is the detection of $N^7$-(2′-hydroxyethyl)guanine, an ethylene oxide adduct, as a representative analyte of this type. Previously we reported the preparation of an electrophoric derivative of this compound at the milligram level [8]. We also compared its purification (as an electrophoric derivative) at the trace level by solid-phase extraction vs. HPLC [9], and determined that carryover of this compound in an HPLC system was largely due to the injector [10]. In additional work involving this analyte, a new electrophoric derivatizing agent was introduced [11].

Here we report further advances towards our long-term goal of measuring this class of adducts at trace levels in biological samples. We have succeeded in measuring 100 pg of $N^7$-(2′-hydroxyethyl)guanine spiked into about 100 $\mu$g of DNA, and demonstrate that the method also detects corresponding methyl, benzene and styrene DNA adducts (tested as standards at the nanogram level), which similarly are of toxicological interest [1,2,12].

## 2. Experimental

### 2.1. Materials

$N^7$-(2′-Hydroxyethyl)guanine was purchased from Chemsyn Science Laboratories (Lenaxa, KS, USA). *tert.*-Butyl nitrite (handle with caution [13]), pentafluorobenzyl bromide (PFBzBr), potassium carbonate, trifluoroacetic acid (TFA), potassium hydroxide and tetrabutylammonium hydrogensulphate were obtained from Aldrich (Milkwaukee, WI, USA). Organic solvents (HPLC grade) were purchased from Doe & Ingalls (Medford, MA, USA). Calf thymus DNA, $N^7$-methylguanine and guanosine were purchased from Sigma (St. Louis, MO, USA). Ethylene oxide-d4 gas was obtained from Cambridge Isotope Laboratories (Woburn, MA, USA). Racemic $N^7$-(2′-hydroxy-1′-phenylethyl)-guanine was prepared from the crude ribonucleoside preparation by heating 1.3 mg in 1.3 ml of 1 *M* HCl at 50°C for 53 h. The UV spectrum became constant after 18 h, matching that of 7-benzylguanine prepared similarly by others (see below). The starting ribonucleoside was prepared originally by Dipple and co-workers as described [14], and given to us by A. Dipple, who suggested the hydrolysis procedure [15]. He also gave us the UV spectrum of 7-benzylguanine. $N^7$-Phenylguanine was provided by K. Norpoth, who prepared it as described [16]. Shaking of reactions was done with a Mistral Multi-Mixer from Lab-Line Instruments (Melrose Park, Il, USA) at a setting of 0.3 full speed.

### 2.2. Internal standard

Racemic $N^7$-(2′-hydroxyethyl-d4)guanine was prepared by a procedure adopted from Brookes and Lawley [17]. Ethylene oxide-d4 gas was bubbled for 5 min through a mixture of 1.4 g of guanosine and 20 ml of acetic acid at 0°C (ice-

bath). After an additional 10 min, the mixture was heated for 1 h at 100°C with stirring under a reflux condenser. Evaporation (rotary evaporator) was followed by the addition of 10 ml of 1 *M* HCl and then similar heating for 1.5 h. The cooled (0°C) reaction mixture was neutralized with 1 *M* KOH and centrifuged at 3000 rpm for 10 min. The supernatant liquid was decanted twice, water was added to the residue and the centrifugation was repeated (until the supernatant liquid was colorless). Rotary evaporation of the residue gave a fluffy brown solid that was treated with 10 ml of 0.1% TFA–$H_2O$ and centrifuged. The supernatant liquid was taken, and this process was repeated with 5 ml twice more. The pooled supernatant liquid was purified by HPLC (0.2-ml injections) using a Rainin Microsorb $C_{18}$-silica column (25 cm × 10 mm I.D.), 0.1% TFA–water as eluent at 5 ml/min and detection at 250 nm. The product eluted at 10.8 min. Some of this product was converted into a corresponding tris(pentafluorobenzyl) derivative, analogous to **3**, as described [8].

### 2.3. Methods

Solid-phase extraction (SPE) columns were prepared using disposable 5.25-in. borosilicate pasteur pipets firmly plugged with silanized glass-wool (J.T. Baker). Silica gel (60 Å pore, 40 μm irregular particles; J.T. Baker) was the packing material (200 mg per column). Each column was freshly washed with 1 ml of ethyl acetate and 1.5 ml of hexane prior to sample application. All washing and elution solvents were pushed to the upper bed surface with pressure from a rubber bulb.

All standard solutions were prepared in toluene for GC–EC-MS. Quantitative values were based on the masses of the free bases unless noted otherwise.

GC–EC-MS was carried out on a Hewlett-Packard Model 5988A mass spectrometer equipped with an HP5977 MS Chem-Station data system. Methane (2 Torr) and helium (20 p.s.i.) were used as the reagent and carrier gases, respectively. Injections were made in the on-column mode and the oven was programmed from 120 to 290°C at 70°C/min. A Hewlett-Packard Ultra-1 capillary column (25 m × 0.2 mm I.D., 0.11 μm film thickness) was used.

*Step 1: neutral thermal hydrolysis*

Based on mass, stock solutions of $N^7$-(2′-hydroxyethyl)guanine and $N^7$-(2′-hydroxyethyl-d4)guanine (the internal standard) were prepared in 0.1 *M* HCl, and a combined solution was prepared and diluted with this solvent to give a final solution containing 1.03 and 1.00 pg/μl, respectively. This latter solution was stored at 4°C in the dark and used for as long as 6 months. An aliquot (100 μl) of this latter solution was evaporated in a 2-ml conical vial in a Speed Vac, and then 100 μl of water containing 112 μg of dissolved DNA were added. The vial was heated at 100°C for 15 min and then placed in an ice-bath. Cold, 1 *M* HCl (150 μl) was added to precipitate the DNA. After 1 h, the cold solution was centrifuged (3100 rpm) at 0°C for 15 min, then the separated supernatant liquid was combined with a 100-μl wash (1 *M* cold HCl) of the pellet (with a second centrifugation) and evaporated in a Speed Vac.

*Step 2: nitrous acid oxidation*

The vial was placed in an ice-bath and 50 μl of 6 *M* HCl (degassed for 5 min with $N_2$) and 20 μl of *tert.*-butylnitrite were added. After shaking at 0°C for 4 h, the sample was evaporated under vacuum. The residue was subjected to liquid–liquid extraction using 150 μl of ethyl acetate and 50 μl of water. The separated aqueous layer was evaporated under vacuum.

*Step 3: derivatization and detection*

To the residue were added 5 mg of $K_2CO_3$ (stored as a powder at 60°C), followed by 100 μl of a freshly prepared solution of 10 μl of PFBzBr in 1 ml of acetonitrile. The sample was shaken for 20 h at room temperature and evaporated under nitrogen. The residue was treated with 50 μl of 1 *M* KOH containing 125 μg of $Bu_4NHSO_4$, 150 μl of $CH_2Cl_2$ and 5 μl of PFBzBr. After shaking for 20 h at room temperature, the $CH_2Cl_2$ was slowly evaporated under nitrogen and 3 × 200-μl ethyl acetate

extractions were combined and evaporated under nitrogen. The residue was dissolved in 25 μl of ethyl acetate and 25 μl of hexane were added. This solution was transferred to the silica SPE column, followed by washing (4.5 ml of hexane, then 6 ml of 10% ethyl acetate in hexane) and elution (2 ml of ethyl acetate). The ethyl acetate eluate was evaporated under nitrogen and the residue dissolved in 50 μl of toluene for injection of 1 μl into the GC–EC-MS system.

*Detection of styrene oxide, methyl and phenyl $N_7$-guanine adducts*

A vial was charged with 5 μl of 1 *M* HCl containing 50 ng of $N^7$-(2′-hydroxy-1′-phenylethyl)guanine. After evaporation in a Speed-Vac, 100 μl of water (not containing DNA) were added followed by heating, etc., as above. Similarly, 67 ng of $N^7$-methylguanine and 52 ng of $N^7$-phenylguanine were reacted, except that the latter was dissolved at the outset in 2 *M* HCl owing to its slow rate of dissolution in 1 *M* HCl. For the $N^7$-G methyl and phenyl adducts, step 5 was omitted: the evaporated residue after step 4 was dissolved in 50 μl of water and extracted with ethyl acetate as usual (step 6), etc. The final, evaporated samples (at the end of the procedure), were dissolved in 50 μl of toluene and 1 μl was injected into the GC–EC-MS.

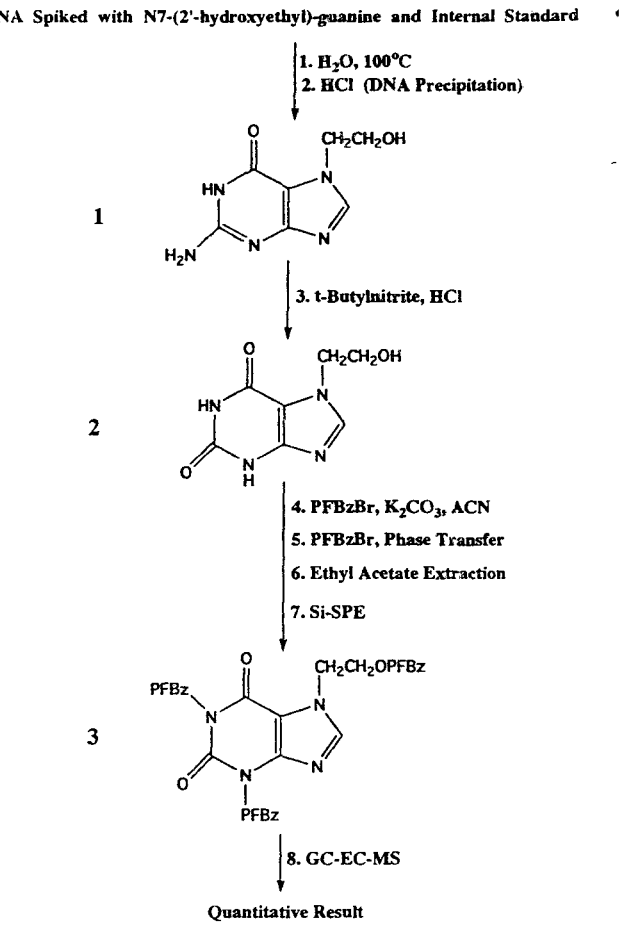


Fig. 1. Scheme for the detection of $N^7$-(2′-hydroxyethyl)guanine.

## 3. Results and discussion

The scheme that we have developed to detect $N^7$-(2′-hydroxyethyl)guanine spiked into DNA at the 100-pg level is summarized in Fig. 1. This scheme evolved from our earlier work in which we converted a standard of compound **1** to derivative **3** at the milligram level [8], and demonstrated that **3** as a standard could be detected at the low attomole level by GC–EC-MS [18]. In our earlier work, we also found that a derivatization precursor of **3**, in which the hydroxyethyl group was left underivatized, gave a good response by GC–EC-MS. However, peak tailing was more noticeable for the latter compound, suggesting that its performance would worsen more rapidly with column aging. We therefore elected to continue working only with **3**.

In step 1 of the analytical scheme, the spiked (analyte plus internal standard) DNA sample is heated in water at 100°C since adducts of DNA are well known to undergo depurination under such conditions, usually referred to as "neutral thermal hydrolysis" [4]. Although the step is unnecessary for a spiked DNA sample, it was incorporated here in anticipation of the future application of this method to biological samples containing DNA-bound $N^7$-G adducts. The simplicity and specificity of this step contribute significantly to the attraction of the overall

method. For example, the $N^7$-methyl-G adduct is reported to undergo release 30 000 times faster than normal guanine under typical such conditions [19].

Next (step 2), the DNA is precipitated with HCl. This step is carried out in the cold mainly to minimize additional depurination of the DNA. After evaporation of the supernatant liquid containing the analyte, nitrous acid is used to form the corresponding xanthine. Initially we formed the nitrous acid for this reaction from sodium nitrite and hydrochloric acid, and purified the intermediate product **2** by HPLC prior to conducting the two pentafluorobenzylation reactions (steps 4 and 5). Although this was successful, it was inconvenient. No final product **3** was detected, however, when xanthine **2** was not purified prior to steps 4–7. This was studied (data not shown) and found to arise from inhibition of the phase-transfer reaction (step 5) by sodium chloride derived from the nitrous acid reaction. Changing from sodium nitrite to *tert.*-butyl nitrite overcame this interference, allowing us to subject xanthine **2** without purification to the subsequent steps in the procedure.

Xanthine **2** can be converted into the final derivative **3** by omitting the first pentafluorobenzylation reaction (step 4, which utilizes potassium carbonate as a base). However, the overall yield is about 1.5-fold higher when step **4** is included. In this step the two NH sites on **2** are pentafluorobenzylated. We speculate that the product from step **4**, since it is less polar than **3**, more readily transfers into the organic phase of the phase-transfer reaction. As shown in Fig. 1, post-derivatization clean-up (steps 6 and 7) prior to detection by GC–EC-MS is accomplished by extraction with ethyl acetate (step 6) followed by solid-phase extraction on a silica packing (step 7).

The measurement of a sample in quadruplicate of 112 $\mu$g of DNA spiked with $N^7$-(2′-hydroxyethyl) guanine and internal standard (103 and 100 pg, respectively) gave absolute yields of $9.7 \pm 3.0\%$ and $9.7 \pm 3.3\%$ (mean ± S.D.), respectively, of final products. These yields were calculated by external calibration with standards of the final products (synthesized at the milligram level for both **1** and the internal standard). The ratio of analyte to internal standard (peak areas) in the four samples was 1.00, 0.96, 0.99 and 1.04. Representative GC–EC-MS traces for a sample and blank (only DNA) are shown in Fig. 2A and B, respectively. In Fig. 2C is presented the similar measurement of this analyte and internal standard (same yield) in the absence of DNA. As seen, the latter sample gives a cleaner chromatogram. The peaks for the analyte and internal standard in Fig. 2C elute later and are narrower than those in Fig. 2A and B because a longer, newer column was used, and because these peaks are plotted more compressed in Fig. 2A in order to reveal fully the other peaks in the chromatogram. (Compressing the display of a given peak makes it easier to see its asymmetry, as illustrated by the inset in Fig. 2C.)

The method was developed with the intent that it could be used, with little or no modification, to determine a variety of "simple" $N^7$-G adducts. To test this, we applied it to corresponding styrene oxide, methyl and phenyl adducts. When the procedure shown in Fig. 1 was applied to the styrene oxide adduct, step 5 (phase-transfer reaction) was omitted for the methyl and phenyl adducts, since it was not needed. Amounts near 50 ng of each were measured so that we could employ scanning conditions in the mass spectrometer to locate the desired products in the GC–EC-MS traces. The criterion selected initially for a peak to be the intended product was that the peak should be prominent, have a reasonable retention time and have a mass spectrum comprising a single ion at M − 181 (loss of pentafluorobenzyl from the parent anion radical), just like that of **3**. This was the case for the $N^7$-G methyl and phenyl adducts, which gave peaks at 4.1 min ($m/z$ 345) and 5.1 min ($m/z$ 407), respectively. Reconstructed selected ion mass chromatograms for these two products are shown in Fig. 3A and B, respectively. Interestingly, the apparent GC peak for the styrene oxide adduct gave an electron-capture mass spectrum in which two ions were prominent: $m/z$ 603 and 631, in a ratio of about 2:1. The latter is the expected mass at

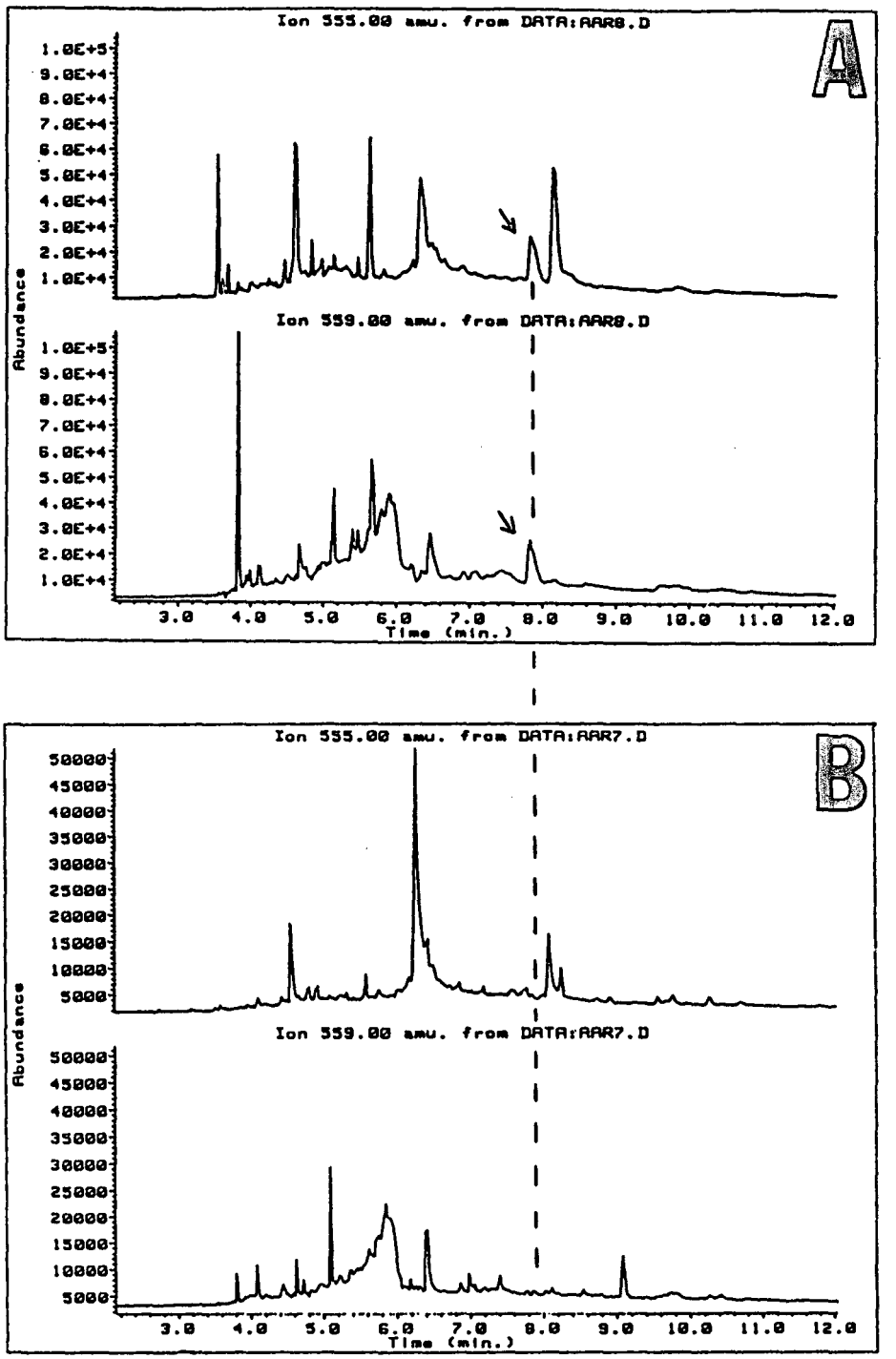


Fig. 2. GC–EC-MS traces obtained from the following samples using the scheme shown in Fig. 1: (A) 103 pg of **1** ($m/z$ 555; upper chromatogram) and 100 pg of internal standard ($m/z$ 559; lower chromatogram) spiked into 112 $\mu$g of DNA; (B) 112 $\mu$g of DNA; and (C) same as (A) except no DNA. In each case, 1 $\mu$l of a final sample volume (in toluene) of 50 $\mu$l was injected. Inset in C: same peak of a standard of **3** plotted at different heights.

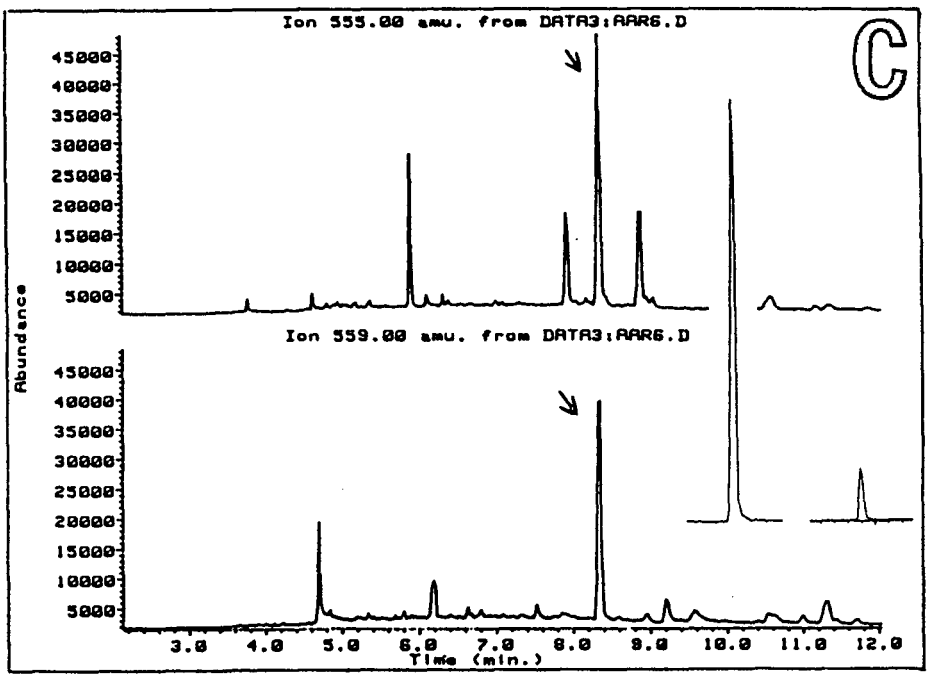


Fig. 2c. (*Continued*)

M − 181. A reconstructed selected ion chromatogram for this ion is shown in Fig. 3C. The ion at *m/z* 603 (data not shown) corresponds to an additional loss of 28 u. We speculate that the *m/z* 603 ion derives from *m/z* 631 starting with transfer of the PFBz group to $O^6$. This in turn changes the conjugation of the fused pyrimidine ring to which $O^6$ is attached, leading to loss of CO to form a final ion which might be the one shown here.

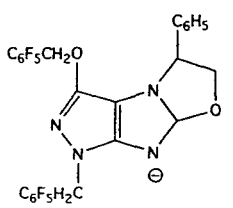


m/z=603

## 4. Conclusion and future

A procedure has been developed that detects an $N^7$-G ethylene oxide adduct spiked into about 100 μg of DNA at a level corresponding to one adduct in $10^6$ normal nucleotides. Detection of corresponding $N^7$-G methyl, phenyl and styrene oxide adducts at the 50-ng level in the same way (except that one step was not needed for the first two compounds) implies the generality of the procedure. While the method involves multiple steps, this is the nature of definitive trace organic analysis. At least the steps are simple; for example, the three reactions are conducted sequentially in the same vial and, aside from a washing step, only evaporation is done between them.

Our original method, applied to 20 mg of a pure sample of the $N^7$-G ethylene oxide adduct, gave a 17% overall yield preparatively of the final product **3** [8]. Now, starting with about $10^8$ times less analyte, and spiked into DNA, the absolute, analytical yield is 9.7%. We plan to focus next on finding out where the losses are taking place in the procedure, so that we might be able to raise the current yield. The current method has been transferred to another labora-

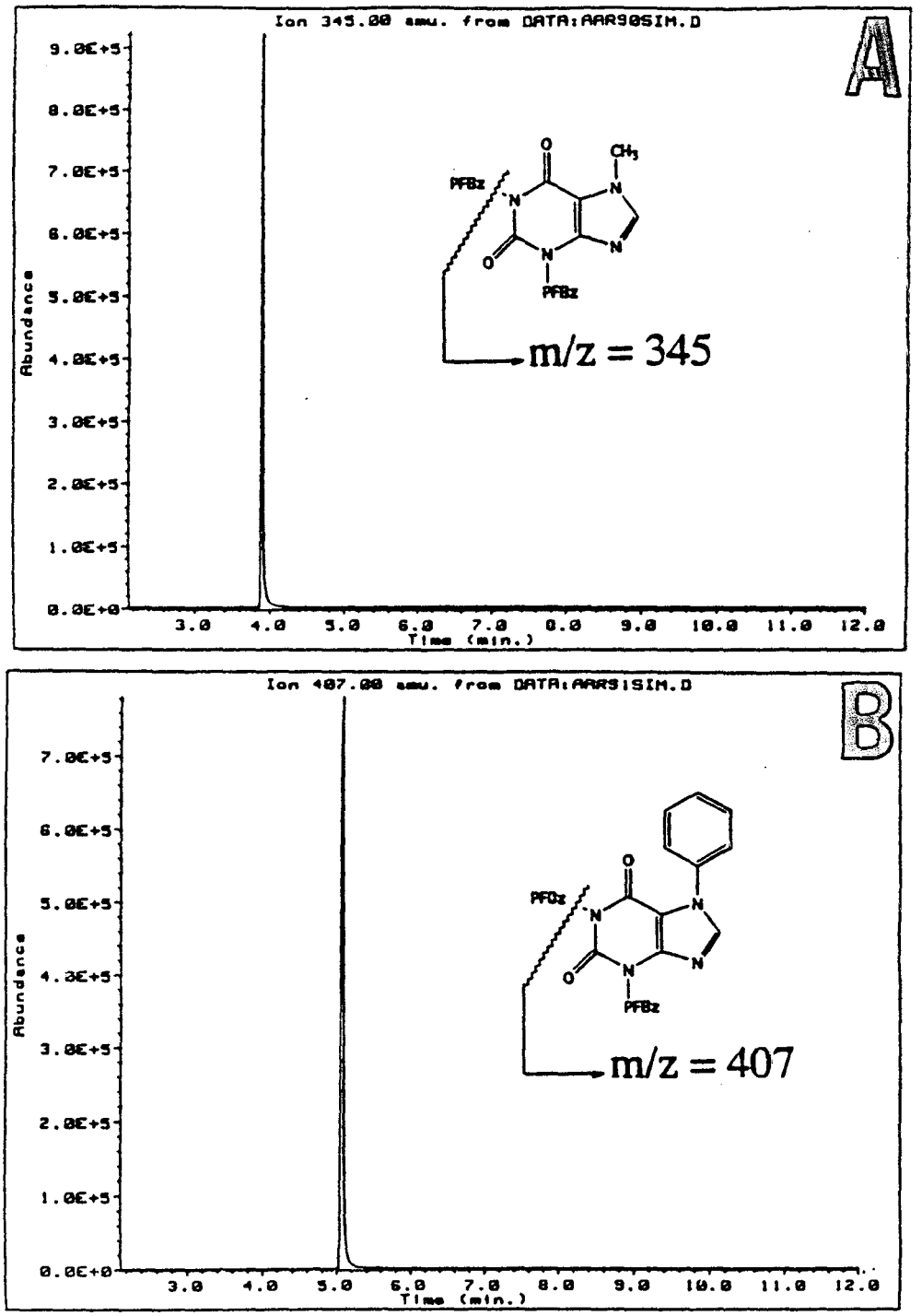


Fig. 3. Detection by GC–EC-MS (reconstructed selected-ion chromatograms) using the scheme shown in Fig. 1 (or this scheme without step 5; see text), of (A) 67 ng of $N^7$-methylguanine ($m/z$ 345); (B) 52 ng of $N^7$-phenylguanine ($m/z$ 407); and (C) 50 ng of $N^7$-(2′-hydroxy-1′-phenylethyl)guanine ($m/z$ 631). In each case, 1 $\mu$l of a final sample volume (in toluene) of 50 $\mu$l was injected.

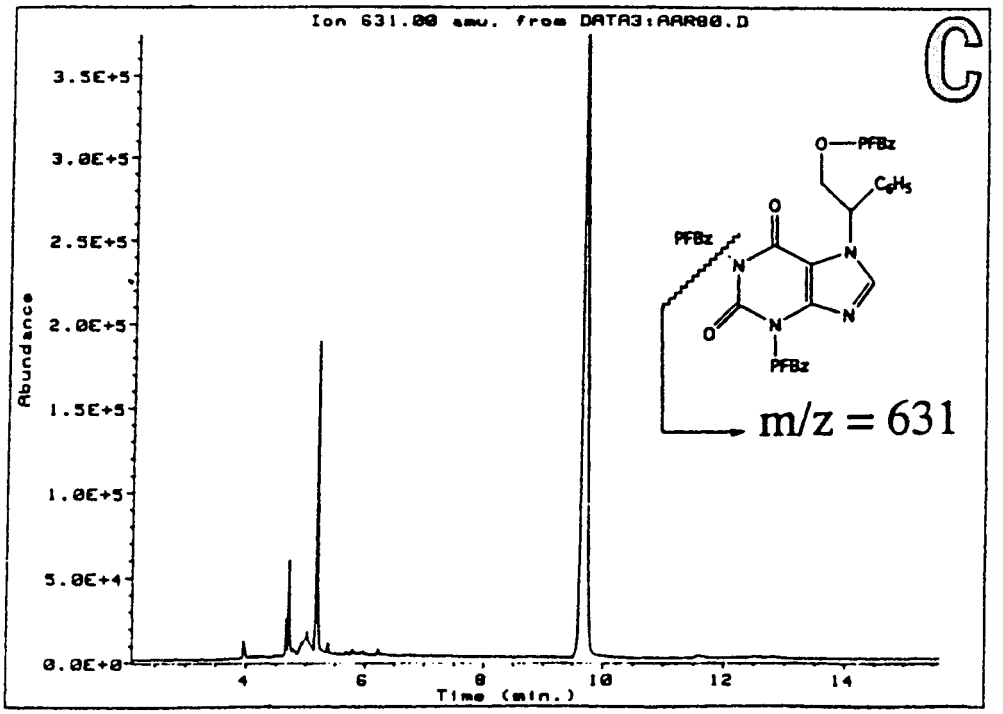


Fig. 3c. (*Continued*)

tory where it is being used successfully to measure this adduct in animal samples [20] and also in human liver samples [21].

## Acknowledgements

This work was supported by Grant OH02792 from the National Institute for Occupational Safety and Health (NIOSH), Centers for Disease Control, and also Order No. 88-80536 from NIOSH, Robert A. Taft Labs. Contribution No. 656 from the Barnett Institute of Chemical Analysis.

## References

[1] M. Uziel, N.B. Munro, D.S. Katz, T. Vo-Dinh, E.A. Zeighami, M.D. Waters and J.D. Griffith, Mutat. Res., 277 (1992) 35.

[2] C.P. Wild and R. Montesano, in J.D. Groopman and P.L. Skipper (Editors), Molecular Dosimetry and Human Cancer: Analytical, Epidemiological, and Social Considerations, CRC Press, Boca Raton, FL, 1991, p. 263.

[3] A. Kolman, M. Naslund and C.J. Calleman, Carcinogenesis, 7 (1986) 1245.

[4] P. Vodicka and K. Hemminki, Carcinogenesis, 9 (1988) 1657.

[5] V.E. Walker, T.R. Fennell, P.B. Upton, T.R. Skopek, V. Prevost, D.E.G. Shuker and J.A. Swenberg, Cancer Res., 52 (1992) 4328.

[6] J.H.M. van Delft, E.J.M. van Weert, M.J.M. van Winden and R.A. Baan, Chem.-Biol. Interact., 80 (1991) 281.

[7] U. Fost, B. Marczynski, R. Kasemann and H. Peter, Arch. Toxicol., Suppl., 13 (1989) 250.

[8] K. Allam, M. Saha and R.W. Giese, J. Chromatogr., 499 (1990) 571.

[9] M. Saha and R.W. Giese, J. Chromatogr., 629 (1993) 35.

[10] M. Saha and R.W. Giese, J. Chromatogr., 631 (1993) 161.

[11] M. Saha, J. Saha and R.W. Giese, J. Chromatogr., 641 (1993) 400.

[12] C. Schell, C. Verkoyen, E. Krewet, G. Müller and K. Norpoth, J. Cancer Res. Clin. Oncol., 119 (1993) 221.

[13] F. Lopez, Chem. Eng. News, December 29 (1992) 2.
[14] F. Latif, R.C. Moschel, M. Hemminki and A. Dipple, Chem. Res. Toxicol., 1 (1988) 364.
[15] P. Brookes, A. Dipple and P.D. Lawley, J. Chem. Soc., (1968) 2026.
[16] C. Verkoyen, E. Golovinski, G. Muller, M. Kolbel and K. Norpoth, Liebigs Ann. Chem., (1987) 957.
[17] P. Brookes and P.D. Lawley, J. Chem. Soc., (1961) 3923.
[18] S. Abdel-Baky and R.W. Giese, Anal. Chem., 63 (1991) 2986.
[19] D.N. Mhaskar, J.M. Raber and S.M. D'Ambrosio, Anal. Biochem., 125 (1982) 74.
[20] K.Y. Wu, N. Scheller, M. Cho, A. Ranasinghe, P. Upton, V.E. Walker and J.A. Swenberg, Poster 839, presented at the 86th Annual Meeting of the American Association for Cancer Research, March 18–22, 1995, Toronto, Ont., Canada.
[21] J. Swenberg, personal communication.

ELSEVIER

Journal of Chromatography A, 712 (1995) 355–364

JOURNAL OF CHROMATOGRAPHY A

# Steam distillation–solvent extraction, a selective sample enrichment technique for the gas chromatographic–electron-capture detection of organochlorine compounds in milk powder and other milk products☆

Gerda Filek, Marcello Bergamini, Wolfgang Lindner*

*Institut für Pharmazeutische Chemie, Karl-Franzens-Universität Graz, A-8010 Graz, Austria*

First received 21 February 1995; revised manuscript received 2 May 1995; accepted 8 May 1995

**Abstract**

The application of a simultaneous water steam distillation–organic solvent extraction (SDE) method for the GC–electron-capture detection of hexachlorobenzene, α-hexachlorocyclohexane (α-HCH), γ-HCH, *cis*-heptachlorepoxide, 2,4′-DDE, 4,4′-DDE, dieldrin, 2,4′-DDT and 4,4′DDT in milk powder and other milk products is described. The SDE apparatus was a newly designed modification of the apparatus of Likens and Nickerson and Godefroot and co-workers and light petroleum was used as the extraction solvent. The method extracted the organochlorine pesticides selectively and with high recovery from interfering matrix compounds. Extraction and clean-up were performed in one step, followed by a simple concentration step. Quantification was performed using pentachlorobenzene and Mirex as internal standards. The limit of determination was between 0.5 and 2 ng/g, depending on the analyte.

## 1. Introduction

Several organochlorine pesticides (OCPs) have been widely used in Europe and are still used by some countries for agricultural and sanitary purposes. Because of their stability towards biodegradation and their lipophilic character, they can accumulate in fatty tissues of human, animal or plant origin. In this context a number of studies have been carried out on the OCP content of human milk [1–6]. In three studies, carried out in France [1], Yugoslavia [4] and Norway [3], hexachlorobenzene (HCB), α-hexachlorocyclohexane (α-HCH), β-HCH, γ-HCH, DDE, DDT and polychlorinated biphenyls (PCBs) were detected in human milk samples. The DDE levels in French human milk were above the EEC Directive level of 10 ppb in milk products. Jensen [5] calculated the maximum tolerable concentrations for these compounds in human milk from acceptable daily intakes of these compounds. The PCB levels of breast milk samples in some Yugoslavian areas exceed the proposed tolerable values [4].

With respect to the trace determination of organochlorine compounds in milk and particu-

☆ Dedicated to Professor Karl Winsauer on the occasion of his 70th birthday.

* Corresponding author.

0021-9673/95/$09.50 
*SSDI* 0021-9673(95)00544-7

larly in milk powder, these matrices are regarded as difficult to handle. The main problem is the separation of OCPs, highly fat-soluble compounds, from milk fat. The membrane of the milk fat globules has to be disrupted in order to obtain sufficient recoveries of the OCPs. Milk powder, however, contains denatured milk proteins and clusters thereof, which have to be broken up because they enclose or entrap the OCPs.

Conventional methods for the determination of OCPs in milk or milk powder involve the extraction of OCPs from matrix components by liquid–liquid partitioning with organic solvents [7] or solid-phase extraction [8], mostly followed by the isolation of the OCPs from interfering co-eluted lipophilic compounds by column chromatographic separation. Clean-up by means of alumina [9], Florisil [7,8], $C_{18}$-modified silica gel cartridges [10], gel permeation [11], HPLC [12] and in some cases with the use of sulphuric acid [13,14] or potassium hydroxide [15] as efficient chemical emulsifiers has been described. A straightforward on-line extraction and clean-up procedure for OCPs using "normal" solid-phase extraction was described by Steinwandter [16] and a "reversed" solid-phase extraction method by Mañes et al. [17].

In this paper, and as an alternative to conventional methods, the application of simultaneous steam distillation–solvent extraction (SDE) as a sample preparation technique for the enrichment and determination of OCPs in a variety of sample matrices including milk and milk products is described. The SDE technique was employed by Likens and Nickerson [18] in 1964 for the determination of essential oil contents in flowers. In the meantime, the original apparatus [18] has been modified by incorporating a vacuum jacket in the arm which conducts the solvent vapour to the extractor body [19] and by introducing more efficient cooling surfaces [20]. Godefroot and co-workers [21,22] modified the apparatus by scaling down the original device. In this work, the application of a newly designed SDE apparatus [23] for the GC-ECD determination of OCPs in milk and milk powder is described. The apparatus is constructed in such a way that permits more complete mixing of steam vapour, e.g., of water and of an organic solvent such as light petroleum, and condensing the gas phase on a greater surface, which allows the use of tap water as coolant (10–12°C). Moreover, it permits the use of a larger amount of sample, thus enhancing the overall sensitivity of the method.

## 2. Experimental

### 2.1. Capillary gas chromatography

A Hewlett-Packard HP 5890 A gas chromatograph equipped with a $^{63}Ni$ electron-capture detector was used. Sample volumes of 1 and 2 $\mu$l were injected using an HP 7673 A autosampler equipped with a 10-$\mu$l Hamilton syringe into a capillary inlet with a glass liner in the splitless mode. The column was a fused-silica capillary column (30 m × 0.25 mm I.D.), coated with 0.25-$\mu$m cross-linked 65% dimethyl–35% diphenylpolysiloxane (RTX-35; Restec). The injector was heated at 290°C and the detector at 325°C. As carrier and make-up gas, nitrogen of 5.5 grade at 18 p.s.i. (125 kPa) column head pressure (corresponding to a flow-rate of 55 ml/min at split vent) was used. The temperature programme was as follows: initial temperature, 100°C for 1 min, then increased at 12°C/min to 220°C, followed by (A) 1.5°C/min to 240°C and (B) 6°C/min to 290°C, the final temperature of 290°C being held for 5 min.

GC control and data processing were performed with an HP 5895 A ChemStation.

### 2.2. Chemicals and sample materials

*Standards*

All pesticide standards (HCB, $\alpha$-HCH, $\gamma$-HCH, *cis*-heptachlorepoxide, 2,4′-DDE, 4,4′-DDE, dieldrin, endrin, 2,4′-DDT, 4,4′-DDT) were obtained from Dr. Ehrenstorfer (Augsburg, Germany), each in the form of a stock solution in isooctane or cyclohexane (10 ng/$\mu$l). For the spiking procedure two different mixtures and

dilutions of these pesticide stock solutions were prepared, one with a concentration of 1 ng per 10 μl and the other 1 ng/μl of each pesticide. As internal standards pentachlorobenzene (PCBz) and Mirex in the form of a stock solution (10 ng/μl) in cyclohexane were used. To obtain a concentration of 1 ng/μl for the spiking procedure a dilution of this stock solution was prepared.

*Reagents*

Light petroleum (b.p. 40–60°C) for residue analysis was obtained from Merck (Darmstadt, Germany) and ethanol for UV spectroscopy from Fluka (Buchs, Switzerland). As antifoam agent Simethicon (polydimethylsiloxane) from Aldrich was used; a stock solution containing 800 mg of Simethicon in 10 ml of light petroleum was prepared.

*Milk powder*

Milk powder was purchased in a supermarket and characterized as containing 1% (w/w) fat, 3.3% (w/w) protein and 4.7% (w/w) lactose.

Two certified milk powder reference samples (natural milk powder CRM 187 and spiked milk powder CRM 188) were supplied by the EEC Community Bureau of Reference (BCR) (Brussels, Belgium).

## 2.3. Steam distillation–solvent extraction apparatus

The SDE apparatus used in this work (Fig. 1) was designed as a modification of the original apparatus of Likens and Nickerson [18] and Godefroot and co-workers [21,22]. The extraction head chamber was constructed in such a way as to provide more complete mixing of solvent and steam vapours, and the condensing surface area was increased to about 500 $cm^2$, which allows the use of tap water (10–12°C) as coolant. More details with respect to the design and function of the SDE apparatus can be found in a paper by Seidel and Lindner [23].

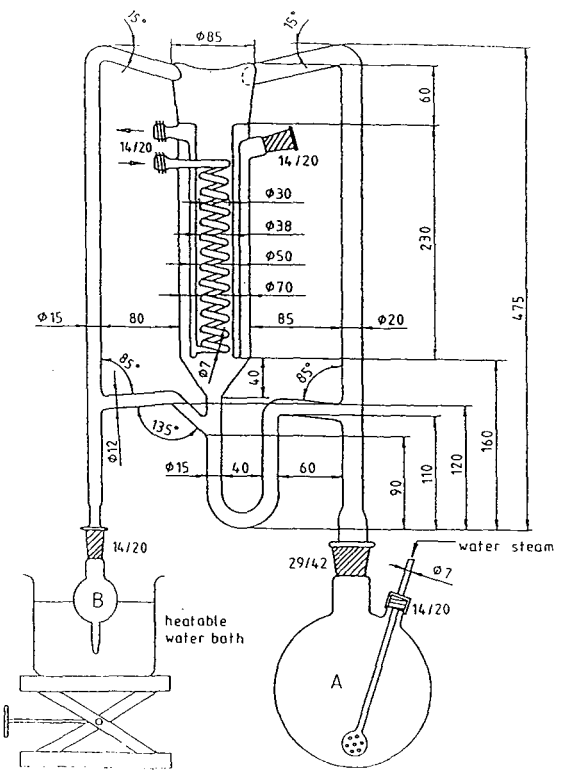


Fig. 1. Scale drawing (dimensions in millimetres) of the continuous steam distillation–solvent extraction (SDE) apparatus. Vessel A, sample in water, total volume 700 ml; vessel B, organic solvent, e.g., light petroleum, total volume 30 ml.

The small exit opposite the condenser inlet serves as a pressure-regulating vent and should have a minimum aperture of 7 mm. Water steam was generated from tap water by a Büchi (Flawil, Switzerland) DG 1500 steam generator and the steam flow was controlled by hydrostatic pressure regulation. The SDE apparatus was constructed for the use of organic solvents with density lower than that of water (in contrast to the apparatus developed by Godefroot and co-workers). To avoid contamination of the apparatus with interfering organochlorine compounds stemming from external components, all tubing was made of PTFE or glass and for the sealing of glass connections PTFE sleeves were used.

### 2.4. Steam distillation solvent extraction procedure

A 5-g amount of milk powder was weighed into the water steam extraction chamber (round-bottomed flask A), wetted with 80 ml of 2 M sulfuric acid, spiked with internal standard solution (PCBz and Mirex in cyclohexane) and ultrasonicated for 1 min. Subsequently, 1 ml of UV-grade ethanol and 0.5 ml of Simethicon solution (corresponding to 40 mg) were added before the water steam flow was switched on and the SDE process was carried out. After filling the U-shaped separation chamber with tap water and the small conical-tapered vessel (B, 50 ml) with the extraction solvent (e.g., light petroleum, b.p. 40–60°C), the apparatus was first filled with organic vapour by heating vessel B in a water-bath at 70°C. Subsequently, the water steam, generated and flow controlled by a separate steam generator, was blown through the milk sample to extract the volatile OCPs. After an efficient gas-phase nebulization-type extraction by spiral (helical) vapour flows in the extraction head chamber (Fig. 1), the vapours were condensed by a cooling device and the light petroleum flowed back to flask B and the water back to flask A. After about 1.5 h, the sample flask A (1000 ml) was filled with about 800 ml of condensed water and at this volume the steam distillation was stopped. In this way all the lipophilic, volatile and water steam-distillable compounds were extracted and collected in the final, ca. 20-ml, light petroleum extract (vessel B), which was concentrated to 1 ml by means of a Kuderna–Danish concentrator [23]. This sample solution was then ready for GC analysis without any further purification steps.

### 2.5. Determination of OCPs

The determination of the OCPs was performed via calibration graphs obtained with spiked milk powder samples [or alternatively with spiked whole milk samples (see below)], whereby the area of each identified peak was referred to the peak area of the internal standard (PCBz and Mirex). "Blank" milk powder (5 g) was spiked with 25, 50, 100, and 250 $\mu$l of the 1 ng per 10 $\mu$l pesticide mixture, corresponding to concentrations of 0.5, 1, 2 and 5 ng/g. To obtain concentrations of 10, 20 and 50 ng/g, 5 g of "Blank" milk powder were spiked with 50, 100 and 250 $\mu$l of the 1 ng/$\mu$l pesticide mixture. Each of these calibration samples was spiked with 3 ng/g of PCBz and 5 ng/g of Mirex. Because of the injection volume of 2 $\mu$l, in the low ng/g range (0.5–10 ng/g) the detector response was not linear, and did not become so until the higher range (20–50 ng/g). For this reason, an injection volume of only 1 $\mu$l for the 20 and 50 ng/g calibration samples was chosen.

In addition, a calibration graph for whole milk (cow milk, 3.6% fat content) was obtained. A 5-g amount of whole milk was spiked with the OCP standard solution in the same way as for the milk powder calibration samples. The concentration range was between 0.5 and 50 ng/g, and 3 ng/g of PCBz and 5 ng/g of Mirex were added as internal standards.

## 3. Results and discussion

### 3.1. Determination of OCPs

The determination of the OCPs was performed via internal standard calibration, whereby each peak area value was referred to that of the internal standard (PCBz and Mirex). For the low-boiling compounds HCB, $\alpha$-HCH, $\gamma$-HCH and *cis*-heptachlorepoxide, PCBz was chosen as the internal standard, whereas the high-boiling compounds 2,4′-DDE, 4,4′-DDE, dieldrin, 2,4′-DDT and 4,4′-DDT were calibrated with Mirex; for calibration data, see Table 1. The recoveries of the analytes and analyte groups are comparable to those of the internal standard (see also Table 3). In order to increase the determination sensitivity in the low ng/g range (0.5–10 ng/g), an injection volume of 2 $\mu$l was chosen, otherwise 1 $\mu$l was injected.

### 3.2. Performance and ruggedness of the method

A 5-g amount of milk powder was spiked with 10 ng/g of nine OCPs and distilled with the SDE apparatus. In the first attempts the samples were

Table 1
Calibration data for the determination of OCPs in milk powder and whole milk

| Compound | Milk powder (0.5–50 ng/g) | | | Whole milk (0.5–50 ng/g) | | |
|---|---|---|---|---|---|---|
| | Correlation coefficient | Slope | Intercept | Correlation coefficient | Slope | Intercept |
| HCB | 0.999 | 0.388 | 0.213 | 0.999 | 0.383 | 0.223 |
| α-HCH | 0.999 | 0.331 | −0.335 | 0.999 | 0.343 | −0.789 |
| γ-HCH | 0.998 | 0.226 | −0.039 | 0.998 | 0.228 | −0.134 |
| HEPO[a] | 0.999 | 0.236 | −0.153 | 0.999 | 0.241 | −0.364 |
| 2,4'-DDE | 0.999 | 0.191 | 0.077 | 0.999 | 0.190 | 0.103 |
| 4,4'-DDE | 0.996 | 0.249 | −0.302 | 0.999 | 0.233 | −0.168 |
| Dieldrin | 0.998 | 0.226 | 0.032 | 0.998 | 0.227 | −0.027 |
| 2,4'-DDT | 0.999 | 0.184 | 0.197 | 0.998 | 0.182 | 0.267 |
| 4,4'-DDT | 0.998 | 0.077 | 0.096 | 0.999 | 0.073 | 0.223 |

[a] *cis*-Heptachlorepoxide.

distilled without the addition of 2 M sulfuric acid; later they were distilled with the addition of 2 M sulfuric acid (see also Experimental). The recoveries from spiked milk powder obtained without sulfuric acid treatment were compared with those obtained with sulfuric acid treatment (Table 2). Without sulfuric acid treatment the recoveries were relatively low, but with the addition of sulfuric acid the recovery increased significantly and the results were satisfactory. The limit of determination was determined for the nine OCPs and the data are included in Table 2. The recoveries from 5 g of spiked whole milk (3.6% fat) obtained with sulfuric acid treatment were also determined and compared with the results for spiked milk powder (1% fat). The results are given in Table 3. For high-boiling OCPs and Mirex the recovery was lower.

The day-to-day reproducibility for an 8-day period was determined by analysing milk powder samples that had been spiked with OCPs corresponding to a concentration of 10 ng/g each. The reproducibility is expressed as the relative standard deviation of these eight values and the data are given in Table 2.

The method was cross-validated with certified milk powder reference samples (natural milk powder CRM 187 and spiked milk powder CRM 188) from the EEC BCR [24–27]. The results obtained with these reference samples are given in Table 4. The techniques for the determination of OCPs in the certified milk powder samples

Table 2
Day-to-day reproducibility, recoveries and limits of determination of the SDE technique for milk powder samples

| Compound | R.S.D. (%) ($n = 8$) | Recovery without acid (%) | Recovery with acid (%) | Limit of determination (ng/g) |
|---|---|---|---|---|
| HCB | 8 | 87 | 97 | 0.5 |
| α-HCH | 8 | 85 | 79 | 1 |
| γ-HCH | 11 | 61 | 96 | 1 |
| HEPO[a] | 7 | n.d.[b] | 93 | 1 |
| 2,4'-DDE | 7 | 73 | 94 | 1 |
| 4,4'-DDE | 9 | 71 | 83 | 1 |
| Dieldrin | 9 | 82 | 121 | 1 |
| 2,4'-DDT | 10 | 57 | 87 | 2 |
| 4,4'-DDT | 13 | 42 | 78 | 2 |

[a] *cis*-Heptachlorepoxide.
[b] Not determined.

Table 3
Recoveries for milk powder samples (1% fat content) compared with recoveries for whole milk samples (3.6% fat content)

| Compound | Recovery for milk powder (%) | Recovery for whole milk (%) |
|---|---|---|
| PCBz | 90 | 88 |
| HCB[a] | 97 | 97 |
| α-HCH[a] | 79 | 88 |
| γ-HCH[a] | 96 | 91 |
| HEPO[a,b] | 93 | 85 |
| 2,4′-DDE | 94 | 67 |
| 4,4′-DDE | 83 | 65 |
| Dieldrin | 121 | 57 |
| 2,4′-DDT | 87 | 47 |
| 4,4′-DDT | 78 | 46 |
| Mirex | 75 | 51 |

[a] To calibrate these OCPs PCBz was used as internal standard; for the others Mirex was used.
[b] *cis*-Heptachlorepoxide.

can be summarized as follows: the pesticides were extracted commonly with milk fat and other interfering compounds from reconstituted milk with various solvents. For the clean-up of the sample extracts, aluminium oxide (ten laboratories), Florisil (seven laboratories) and silica gel (one laboratory) were used, and gel permeation chromatography was also employed by four laboratories [24].

The problem with the BCR reference samples was that they were 2–3 years old. In order to obtain sufficient recoveries, we had to break up the sample matrix by a combined sulfuric acid treatment, ultrasonication and heat. Nevertheless, the result for 4,4′-DDE in CRM 187 (natural milk powder) was not in agreement with the certified levels (see Table 4). The samples were analysed in triplicate, but for 4,4′-DDE the analysis value remained low. We assume that the milk powder sample and its composition may have changed as an effect of aging.

### 3.3. Extraction

The SDE technique has proved to be a powerful method to extract OCPs from complex matrices such as low-fat milk powder. The advantage of steam distillation is that the OCPs, as volatile compounds, can be separated selectively from interfering matrix compounds. However, milk powder, rich in proteins, lecithins, carbohydrates, etc., sometimes several years old, is a very difficult to handle matrix, because the OCPs can become entrapped by denatured milk proteins. Matrices rich in fat components need emulsifiers to make possible a "homogeneous" aqueous matrix; in order to optimize this process, we added lecithin as emulsifier to extraction flask A, but the recoveries of the OCPs were not significantly improved. We assume that the lipo-

Table 4
Cross-validation of the SDE technique with BCR certified milk powder reference samples (natural milk powder CRM 187 and spiked milk powder CRM 188)

| Compound | Concentration (μg/kg)[a] | | | |
|---|---|---|---|---|
| | CRM 187, certified value | CRM 187, SDE method | CRM 188, certified value | CRM 188, SDE method |
| HCB | 1.5 ± 0.20 | 1.1 | 37.4 ± 2.7 | 47.2 |
| α-HCH | 1.8 ± 0.14 | 1.3 | 20.0 ± 0.9 | 16.5 |
| γ-HCH | 5.7 ± 0.70 | 6.3 | 45.4 ± 2.9 | 47.0 |
| HEPO[b] | n.d.[c] | n.d. | 32.0 ± 1.8 | 36.0 |
| 4,4′-DDE | 6.6 ± 0.60 | 2.5 | 51.3 ± 3.5 | 48.3 |
| Dieldrin | n.d. | n.d. | 36.1 ± 2.4 | 35.8 |
| 4,4′-DDT | n.d. | n.d. | 69.0 ± 4.6 | 62.6 |

[a] Contents in dry mass.
[b] *cis*-Heptachlorepoxide.
[c] n.d. = Not determined.

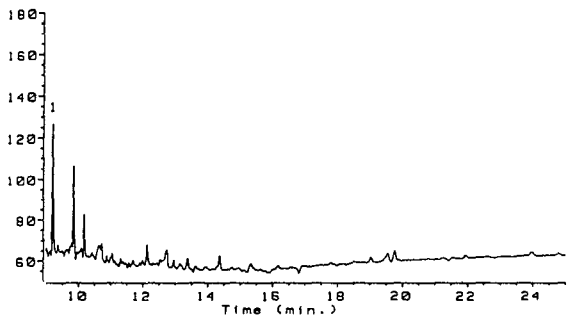


Fig. 2. GC–ECD of milk powder "blank". The milk powder was distilled with the SDE apparatus after it had been spiked with pentachlorobenzene (1) and wetted with 80 ml of 2M sulfuric acid (see also Experimental).

philic OCPs become "attached" to the lipophilic parts of the lecithins, which act like surfactants forming, e.g., micelles. In order to obtain sufficient recoveries, milk proteins have to be broken up, which can be stimulated by ultrasonication, sulfuric acid treatment and heat: the SDE technique allows the simultaneous treatment of the sample in the above-described way.

Milk and milk powder are matrices which cause numerous negative peaks in the GC–ECD trace, which interfere seriously with the peaks of some OCP analytes (see Fig. 3A). The sulfuric acid treatment, however, was very helpful in suppressing the negative peaks in the chromatograms to a large extent (see Figs. 2 and 3B). As shown earlier and instead of cleaning up the sample extract on an Extrelut column charged with concentrated sulfuric acid [13,14,28], we wetted the milk powder sample with 80 ml of 2 M sulfuric acid prior to the steam distillation procedure. With concentrated sulfuric acid the fat and the triglycerides are destroyed by this harsh chemical treatment, and the addition of only dilute sulfuric acid helps mainly to break up denatured milk proteins. In this way we achieved sufficient recoveries for all OCPs except endrin; the gas chromatograms had good baselines (see Fig. 3B). Endrin is unstable to acid treatment; according to published data [13,29] it is converted into the ketone. Dieldrin, DDE and DDT, however, showed good recoveries (between 80 and 95%; see Table 2), indicating that these compounds are not degraded by means of this relatively mild sulfuric acid treatment. It should be mentioned that the 2 M sulfuric acid is diluted to 0.2 M during the steam distillation process and buffered by sample matrix components.

With the object of achieving optimum extraction of the OCPs in a suitable time, it was necessary to add a co-distillation solvent to the extraction flask A. Polar solvents such as ethanol, 2-propanol and acetonitrile were tested. The addition of 10–15% of ethanol (referred to the volume in the extraction flask A prior to the distillation; see Experimental) under the SDE

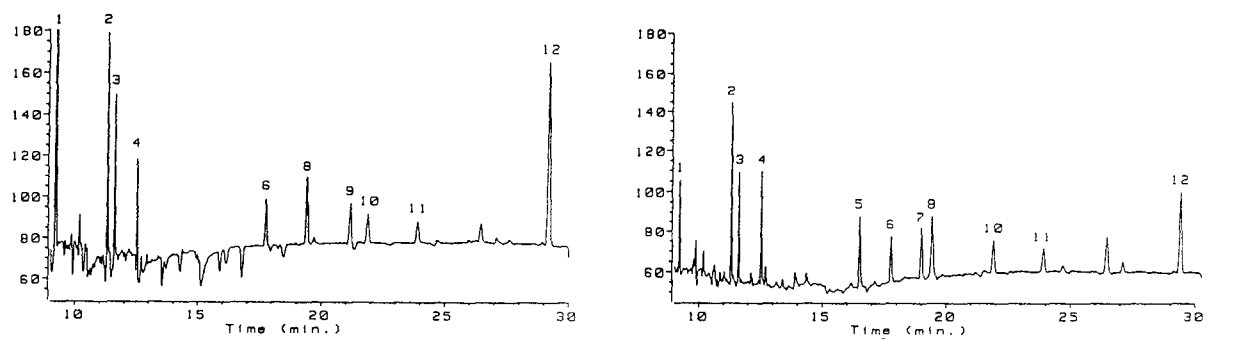


Fig. 3. GC–ECD of spiked milk powder (5 ng/g of each OCP) after sample pretreatment with the SDE technique. The distillation process was carried out (A) without and (B) with the addition of 2 M sulfuric acid to the sample. Pentachlorobenzene and Mirex were added as internal standards. Peaks: 1 = pentachlorobenzene; 2 = hexachlorobenzene; 3 = α-HCH; 4 = γ-HCH; 5 = *cis*-heptachlorepoxide; 6 = 2,4′-DDE; 7 = 4,4′-DDE; 8 = dieldrin; 9 = endrin; 10 = 2,4′-DDT; 11 = 4,4′-DDT; 12 = Mirex. For GC conditions, see Experimental.

starting conditions was sufficient, although it should be noted that a steady dilution of the ethanol content in vessel A occurred.

The milk powder samples showed severe foam formation during the distillation process, so we tested various substances to reduce the foaming. Celite, Kieselguhr (diatomaceous earth), NaCl and Simethicon (a polysiloxane) were examined for their antifoaming properties. With the addition of 25% (w/w) of Celite to the milk powder the foam was suppressed well, but the recoveries for the OCPs were very low. The addition of 20, 30 or 50 g of NaCl to 10 g of milk powder did not suppress the foam formation. However, the addition of 40 mg of Simethicon to 5 g of milk powder reduced the foaming without influencing the recoveries of the OCPs.

If the fat content of the milk product sample is not higher than 5%, a selective and adequate isolation of the OCPs from such samples can be achieved by the SDE method. The recovery, however, is dependent on the fat content, but also on the volatility of the analyte. If the fat content is about 1%, the recoveries of all the OCP analytes examined (low and high boiling) ranged between 78 and 95%. For whole milk (3.6% fat), the recoveries of PCBz, HCB, $\alpha$-HCH, $\gamma$-HCH and *cis*-heptachlorepoxide were hardly influenced, whereas the recoveries of 2,4'DDE, 4,4'-DDE, dieldrin, 2,4'DDT, 4,4'-DDT and Mirex decreased in the specified sequence (see also Table 3). When analysing milk samples with a 3.6% fat content, the calibration should be carried out with whole milk. With a higher fat content of the samples the recoveries of certain OCPs drop significantly, but even if the fat content exceeds 10% this method is applicable, provided that one calibrates with spiked samples of the same fat content. If the distillation process could be extended for a longer period of time, a further increase in the recovery would result. In the present case the water steam is not generated by a separate steam generator, but by heating the sample flask A with an external heat source. The water steam formation in flask A could be extended for a long period of time (a condensation volume of 800 ml was not final), giving much higher recoveries.

The sensitivity of the overall method could easily be further increased by, e.g., concentrating the organic sample solution to 100 $\mu$l instead of 1 ml (see Experimental). Many volatile and ECD-sensitive compounds such as chlorophenols, PCBs and dioxanes could possibly interfere in the course of the GC determination of OCPs. On the other hand, the SDE method could also be extended to preconcentrate a wide variety of analytes from a complex matrix followed by additional chromatographic work-up and analysis techniques. Ramos et al. [30] described the application of the SDE technique to the determination of PCBs, polychlorinated dibenzo-*p*-dioxins and polychlorinated dibenzofurans in water samples.

### *3.4. OCP content found in various milk samples*

Various whole milk and breast milk samples were analysed for their OCP content with the SDE method described above. The fat content of some of these samples and the OCP values determined are summarized in Table 5.

## 4. Conclusion

The simultaneous water steam distillation–organic solvent extraction (SDE) method represents a selective sample enrichment technique for the determination of organochlorine pesticides in milk, milk powder and other milk products. This technique is reasonably fast; the distillation process for the extraction and clean-up method takes 1–1.5 h per sample and the following concentration of the organic extract takes 15–30 min. Owing to the unique SDE set-up, several selective sample pretreatment steps, e.g. ultrasonication, chemical treatment and heating, can be integrated. The resulting sample extracts are very suitable for direct GC analysis, resulting in long term stability of the GC columns and the injector liners. Another noticeable advantage is that one needs only small amounts of organic solvents for extraction. However, compounds that are unstable to heat, acid

Table 5
OCP content of various milk samples

| Sample | Fat content | Concentration (ng/g) | | | | | |
|---|---|---|---|---|---|---|---|
| | (%) | HCB (d.l.[a] 0.5) | α-HCH (d.l. 1) | γ-HCH (d.l. 1) | 4,4′-DDE (d.l. 1) | Dieldrin (d.l. 1) | 4,4′-DDT (d.l. 2) |
| Milk | 3.6 | 2 | <d.l. | 2 | <d.l. | <d.l. | <d.l. |
| Breast milk sample 1 | 4 | 5 | <d.l. | 5 | 8 | <d.l. | 3 |
| Breast milk sample 2 | 4 | 10 | <d.l. | 5 | 4 | <d.l. | 2 |

[a] d.l. = Determination limit (ng/g).

and oxidation (e.g., endrin) cannot be determined with the SDE method.

The separation and enrichment principles of this method are based on simultaneous steam distillation–solvent extraction, which are controlled by liquid–liquid extraction equilibria influenced by the type and volume of extraction media (equal to the amount of steam generated) and to a certain extent the matrix component and composition. Thus, the extraction recoveries of the highly lipophilic OCPs are influenced by the fat content of the matrix and by the volatility of the analyte. A high fat content ($>5\%$) and low volatility lead to a decrease in recovery, although the value is reproducible owing to the equilibria to be controlled. The decisive step for obtaining reliable results is calibration with an internal standard of a similar volatility to the analyte and calibration with a matrix of similar fat content.

In the analysis of complex matrices other than milk powder, the addition of dilute sulfuric acid prior to the distillation process might not be required.

## References


[1] F. Bordet, J. Mallet, L. Maurice, S. Borrel and A. Venant, Bull. Environ. Contam. Toxicol., 50 (1993) 425–432.

[2] Y.K. Matuo, J.N.C. Lopes, I.C. Casanova, T. Matuo and J.L.C. Lopes, Arch. Environ. Contam. Toxicol,, 22 (1992) 167–175.

[3] J.U. Skaare and A. Polder, Arch. Environ. Contam. Toxicol., 19 (1990) 640–645.

[4] B. Krauthacker, Bull. Environ. Contam. Toxicol., 46 (1991) 797–802.

[5] A.A. Jensen, Residue Riv., 89 (1983) 1–128.

[6] M.A. Alawi, N. Ammari and Y.Al-Shuraiki, Arch. Environ. Contam. Toxicol., 23 (1992) 235–239.

[7] T. Suzuki, K. Ishikawa, N. Sato and K.I. Sakai, J. Assoc. Off. Anal. Chem., 62 (1979) 681.

[8] A. Di Muccio, M. Rizzica, A. Ausili, I. Camoni, R. Dommarco and F. Vergori, J. Chromatogr., 456 (1988) 143–148.

[9] A.M. Gillespie and S.M. Walters, J. Assoc. Off. Anal. Chem., 67 (1984) 290.

[10] T. Prapamontol and D. Stevenson, J. Chromatogr., 552 (1991) 249–257.

[11] D.P. Goodspeed and L.I. Chesnut, J. Assoc. Off. Anal. Chem., 74 (1991) 388.

[12] E.A. Hogendoorn, G.R. van der Hoff and P. van Zoonen, J. High Resolut. Chromatogr., 12 (1989) 784.

[13] A. Di Muccio, A. Santilio, R. Dommarco, M. Rizzica, L. Gambetti, A. Ausili and F. Vergori, J. Chromatogr., 513 (1990) 333–337.

[14] A. Di Muccio, A. Ausili, R. Dommarco, D. Attard Barbini, A. Santilio, F. Vergori, G. De Merulis and L. Sernicola, J. Chromatogr., 552 (1991) 241–247.

[15] R. Frank, H.E. Braun, G.H. Sirons, J. Rasper and G.G. Ward, J. Food Protect., 48 (1985) 499.

[16] H. Steinwandter, Fresenius' J. Anal. Chem., 312 (1982) 342–345.

[17] J. Mañes, G. Font and Y. Picò, J. Chromatogr., 642 (1993) 195–204.

[18] S.T. Likens and G.B. Nickerson, Am. Soc. Brew. Chem. Proc., (1964) 5.

[19] H. Maarse and R.E. Kepner, J. Agric. Food Chem., 18 (1970) 1095.

[20] R.A. Flath and R.R. Forrey, J. Agric. Food Chem., 25 (1977) 103.

[21] M. Godefroot, P. Sandra and M. Verzele, J. Chromatogr., 203 (1981) 325–335.

[22] M. Godefroot, M. Stechele, P. Sandra and M. Verzele, J. High Resolut. Chromatogr. Commun., 5 (1982) 75–79.

[23] V. Seidel and W. Lindner, Anal. Chem., 65 (1993) 3677–3683.

[24] B. Griepink, E.J. Mulders, C.G. van der Paauw and J.K. Quirijns, BCR Information Reference Materials, Report EUR 12319 EN, 1989.

[25] C.G. van der Paauw, E.J. Mulders, J.K. Quirijns and B. Griepink, Fresenius' Z. Anal. Chem., 322 (1988) 698–700.
[26] J.K. Quirijns, C.G. van der Paauw, E.J. Mulders and B. Griepink, J. Assoc. Off. Anal. Chem., 73 (1990) 773–776.
[27] B. Griepink, J.K. Quirijns, C.G. van der Paauw and E.J. Mulders, J. Assoc. Off. Anal. Chem., 73 (1990) 777–782.
[28] V. Seidel, I. Tschernuter-Meixner and W. Lindner, J. Chromatogr., 642 (1993) 253–262.
[29] A.S.Y. Chau, Bull. Environ. Contam. Toxicol., 8 (1972) 169.
[30] L. Ramos, G.P. Blanch, L. Hernández and M.J. González, J. Chromatogr. A, 690 (1995) 243–249.

ELSEVIER

Journal of Chromatography A, 712 (1995) 365–371

JOURNAL OF CHROMATOGRAPHY A

# Synthesis and use of novel chiral surfactants in micellar electrokinetic capillary chromatography☆

Desmond D. Dalton[a,*], David R. Taylor[a], David G. Waters[b]

[a]*Chemistry Department, UMIST, Sackville Street, P.O. Box 88, Manchester M60 1QD, UK*

[b]*SmithKline Beecham Pharmaceuticals, Old Powder Mills, Tonbridge, nr Leigh, Kent TN11 9AN, UK*

First received 25 August 1994; revised manuscript received 29 March 1995; accepted 7 April 1995

**Abstract**

This paper presents the synthesis of some novel chiral surfactants based on (*R,R*)-tartaric acid and long-chain aliphatic amines. Evidence for their ability to form micelles based on surface tension measurements will be given. Several chiral separations have been achieved and these will be presented for one of the surfactants. A discussion of the chiral selectivity data will show a preference for resolving certain compounds of a similar structure. Ideas for further work with these surfactants will be outlined.

## 1. Introduction

In 1981 Jorgenson and Lukacs [1] described the use of small-diameter capillaries in the electrophoretic separations of derivatised amino acids and amines. The small diameters of the capillaries enabled efficient heat dissipation and consequently resulted in highly efficient separations. The technique was named capillary electrophoresis (CE) and proved useful for the simultaneous separation of positively and negatively charged species. For the separation of neutral species this technique was modified by Terabe et al. [2], who added surfactants to the background electrolyte (BGE). The surfactants act as a pseudo-stationary phase and the resulting separation has characteristics of both an electrophoretic and chromatographic nature. Terabe et al. named their modified technique micellar electrokinetic capillary chromatography (MEKC or often abbreviated as MECC). The most common additive used in MECC to date is sodium dodecyl sulfate (SDS), but since it is achiral it cannot differentiate between enantiomers.

To achieve chiral discrimination either a chiral surfactant is required or some chirality must be imparted into the micelle. This second option has been achieved by the formation of mixed micelles, i.e., a chiral compound has been added to an SDS solution and is included into the SDS micelle, thus forming a so-called mixed micelle which will have some chiral selectivity.

Compounds that have been successfully added in this manner include digitonin [3], and sodium N-dodecanoyl-L-valinate [3,4]. Digitonin is a

* Corresponding author.

☆ Presented at the *3rd International Symposium on Capillary Electrophoresis, York, 24–26 August 1994.*

0021-9673/95/$09.50 
*SSDI* 0021-9673(95)00449-1

non-ionic compound which incorporates into the SDS micelle; this effectively results in a chiral ionic micelle. Sodium N-dodecanoyl-L-valinate has been used in a mixed micelle system containing SDS. These approaches resulted in good separation of phenylthiohydantoin-derivatised amino acids [3].

Relatively few chiral surfactants have so far been used in the absence of SDS in MECC. By far the most widely used chiral surfactants are the bile salts [5,6] which have a steroidal backbone and form helical rather than spherical micelles. Sodium N-dodecanoyl-L-valinate has also been used on its own as a chiral micellar agent. [3] The synthesis of novel chiral surfactants would widen the number and scope of applications for this technique.

The work presented describes the preparation and use of two novel chiral surfactants based on (*R*,*R*)-tartaric acid and long-chain amines. Details of the synthetic methods used will be given, as will evidence of micelle formation. Their use in chiral discrimination will be demonstrated by showing the enantiomeric separation of a number of compounds. Some ideas as to structures likely to be best separated will be proposed. Further work with these and other surfactants will also be outlined.

## 2. Experimental

### 2.1. Synthesis of surfactants

*Chemicals*

(*R*,*R*)-Tartaric acid (99+%), $C_{10}H_{21}NH_2$ (97%) and $C_{12}H_{25}NH_2$ (98%) were purchased from Janssen Chimica (Cheshire, UK), acetic anhydride (99%) was supplied by Aldrich (Milwaukee, WI, USA); dichloromethane was of GLR grade, and ethyl acetate (99%) was obtained from Fisons Laboratory Supplies (Loughborough, UK). Sodium bicarbonate (99.5%) and magnesium sulfate were purchased from Vickers (Watford, UK). Aqueous solutions were prepared using glass-distilled water.

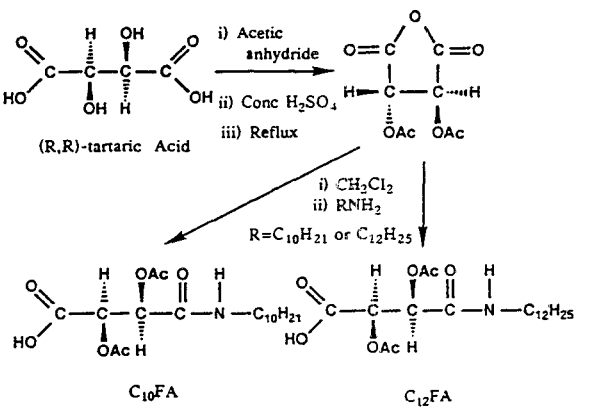


Fig. 1. Reaction scheme 1.

*Procedure*

*Reaction scheme 1* (Fig. 1). (*R*,*R*)-Tartaric acid was refluxed with acetic anhydride in the presence of sulfuric acid for 40 min. On cooling the acetylated anhydride precipitated out. This was filtered and washed with portions of toluene followed by ether, giving a white crystalline material with a melting point of 129–131°C (Ref. [7] gives a value of 130–132°C). This material was dissolved in dichloromethane and a slight excess of amine was added slowly while stirring. After two hours the dichloromethane was removed under vacuum and the residue was dissolved in ethyl acetate and washed with aliquots of a saturated sodium bicarbonate solution until effervescence ceased; the organic layer was then discarded. The aqueous/bicarbonate layer was then acidified to pH 1 and the precipitated material was re-extracted back into ethyl acetate, dried with magnesium sulfate, filtered and the solvent removed under vacuum, leaving the pure free acid, in most cases as a very sticky/hard gum. Typical elemental analysis results are given below. $C_{18}H_{31}NO_7$ ($C_{10}FA$); calculated: C, 57.9; H, 8.3; N, 3.8%; found: C, 57.8; H, 8.0; N, 3.9%. $C_{20}H_{35}NO_7$ ($C_{12}FA$); calculated: C, 59.9; H, 8.7; N, 3.5%; found: C, 59.9; H, 8.8; N, 3.5%.

*Reaction scheme 2* (Fig. 2). The carboxylic acid was dissolved in methanol and a slight molar deficiency of sodium methoxide was added: the mixture was left stirring overnight. The methanol

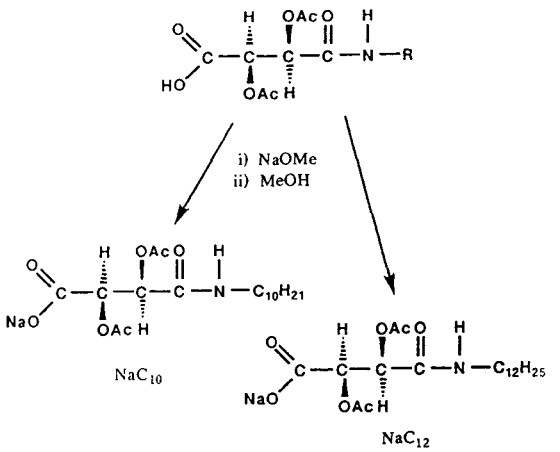


Fig. 2. Reaction scheme 2.

was removed under vacuum, leaving a sticky white residue, which was dissolved in ethyl acetate. After allowing this solution to stand overnight the salt precipitated. It was filtered off and dried under vacuum. Typical elemental analysis results for the salts are given below. $C_{18}H_{30}NO_7Na$ ($NaC_{10}$); calculated: C, 54.7; H, 7.6; N, 3.5; Na, 5.8%; found: C, 54.4; H, 7.9; N, 3.7; Na, 5.6%. $C_{20}H_{34}NO_7Na$ ($NaC_{12}$); calculated: C, 56.7; H, 8.0; N, 3.3; Na, 5.4%; found: C, 56.8; H, 8.2; N, 3.3; Na, 5.4%.

### 2.2. Determination of critical micelle concentration (cmc) by surface tension measurements

Measurements were carried out on a Cruss Model K12 processor tensiometer (Hamburg, Germany) using a Wilhelmy plate. All solutions were thermostatically maintained at 25°C prior to and during analysis. Between each solution the plate was rinsed with deionised water, flame dried and then allowed to cool to room temperature.

A series of solutions of known concentration were prepared in deionised water. A plot of surface tension versus surfactant concentration enabled interpolation of the critical micelle concentration.

### 2.3. Electrophoresis

A Beckman P/ACE 2050 instrument (Fullerton, CA, USA) was used with UV detection at 254 nm. An uncoated fused-silica capillary with dimensions of 57 cm × 50 μm I.D. was used throughout; the detection window was located 50 cm from the inlet end. Injection was achieved by the use of an overpressure of nitrogen (0.13 MPa) for 1 s in all cases. The electrophoretic medium consisted of 20 m*M* di-sodium hydrogen phosphate at pH 8.2 and 5 m*M* $NaC_{12}$, and the applied voltage was 20 kV.

## 3. Results and discussion

### 3.1. Critical micelle concentrations

Many methods for determining the critical micelle concentration (cmc) of a surfactant are available, such as laser light scattering, conductivity and surface tension [8]. Surface tension is one of the oldest and most widely used techniques and was used in this work, leading to the plots of surface tension versus surfactant concentration shown for $NaC_{10}$ in Fig. 3 and for $NaC_{12}$ in Fig. 4.

By the interpolation shown on the graph in Fig. 3 the cmc of the surfactant $NaC_{10}$ was determined to be 2.6 m*M*, whereas from Fig. 4 the cmc of the surfactant $NaC_{12}$ was determined as 2.4 m*M*.

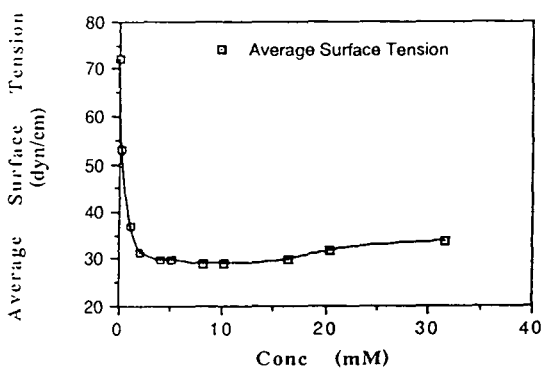


Fig. 3. Surface tension versus $NaC_{10}$ concentration.

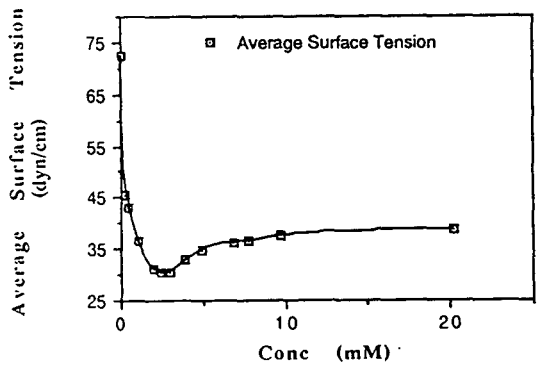


Fig. 4. Surface tension versus $NaC_{12}$ concentration.

In this case the minimum of the plot in Fig. 4 was used due to the fact that interpolation was difficult with this shape of curve. It must be borne in mind that these determinations are only approximate. The shape of the graph in Fig. 4 is indicative of impurities in the surfactant [9], which further complicates the determination. The cmc's of the two salts are very close, which is a little surprising as a change in alkyl chain length usually has an appreciable effect on the cmc. For example, the cmc of SDS is 8.1 m*M* while that of sodium decyl sulfate is 38.8 m*M* [8].

When making up the solutions for analysis the salts were assumed to have 100% purity. Even if this is not the case the value obtained could be used to obtain micelles provided the concentration is maintained above the cmc. Both graphs clearly indicate that the synthesised salts are surfactants that are capable of forming micelles at concentrations of over 3 m*M*.

### 3.2. Electrophoresis

The percentage separation factor was calculated as $100 \times (p/h)$ (Fig. 5). Baseline separations are obtained as the separation factor approaches 100. (Note: recent guidelines [10] indicate that the term separation factor should be restricted to $\alpha$, where $\alpha = k_2'/k_1'$, with $k'$ the capacity factor.)

The percentage separation factors quoted in Table 1 were achieved using near-identical conditions (different batches of capillary were used)

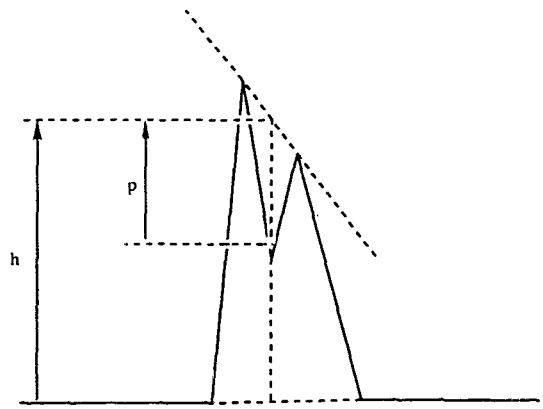


Fig. 5. The calculation of percentage separation factors.

for each of the analytes. The different sample concentrations reflect differences in the UV absorbance characteristics.

It is well established that compounds include into micelles to different extents depending upon their hydrophobicity. In the present work compounds with fused polyaromatic rings appear to separate more easily (Figs. 6–9) than those with only a single aryl group (see compounds 1, 4 and 5 compared with compounds 3 and 6, Figs. 10). A possible reason for this is that separation arises as a result of stronger inclusion within the micelle, promoted by the fused polyaromatic nucleus of the analyte. However, interactions at other points of the molecule are equally important, as demonstrated by compounds 5 and 7 (Fig. 10). Separation is achieved due to very slight differences in stability of the complex

Table 1
Calculated percentage separation factors for compounds 1–8 (Fig. 10)

| Compound number | Concentration (mg $ml^{-1}$) | Percentage separation factor |
|---|---|---|
| 1 | 0.20 | 86 |
| 2 | 0.06 | 34 |
| 3 | 0.50 | 12 |
| 4 | 0.25 | 90 |
| 5 | 0.06 | 72 |
| 6 | all concentrations | 0 |
| 7 | all concentrations | 0 |
| 8 | all concentrations | 0 |

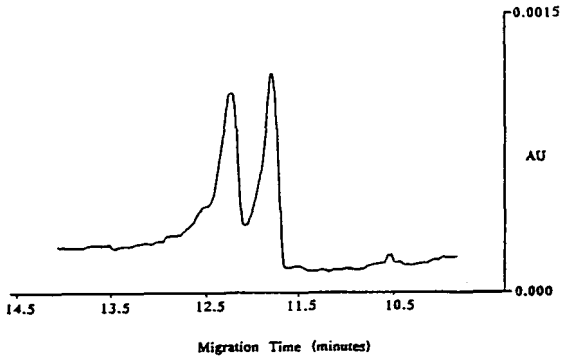


Fig. 6. Enantiomeric separation achieved for compound 1.

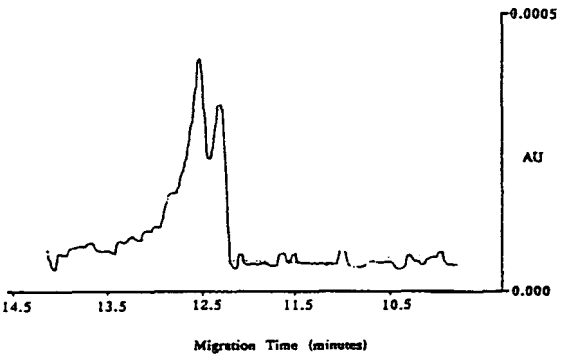


Fig. 8. Enantiomeric separation achieved for compound 4.

formed between each enantiomer and the chiral medium.

## 4. Conclusions

Some novel chiral surfactants have been shown to be applicable to enantiomeric separations in MECC. As yet the mechanisms involved in the separation process are unclear and further work will be carried out to elucidate them. Measurements of change in surface tension with surfactant concentration have proved to be a convenient method for the determination of critical micelle concentrations. The position of the chiral centre within the micelle may have an important effect on separations, and to investi-

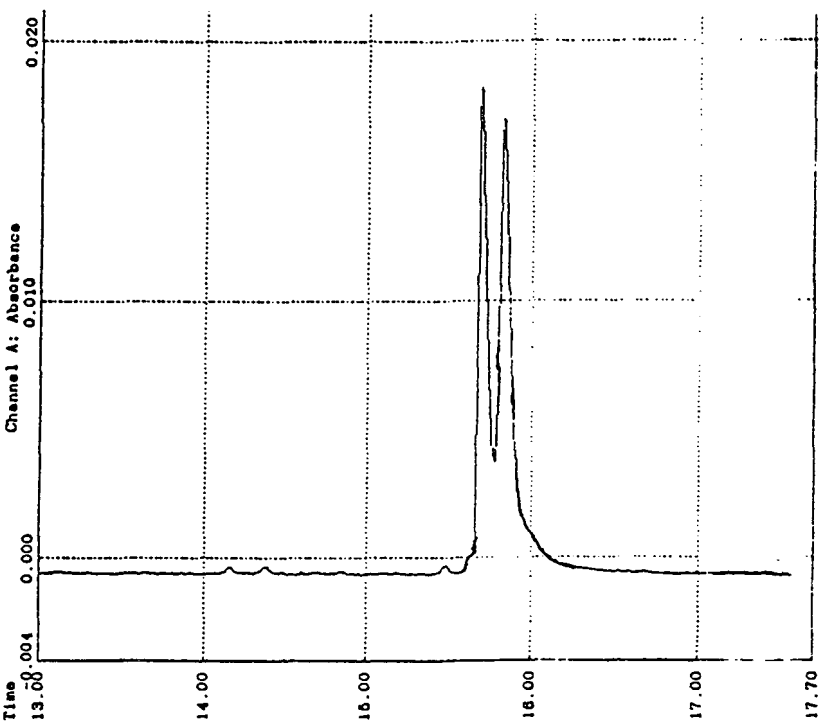


Fig. 7. Enantiomeric separation achieved for compound 2.

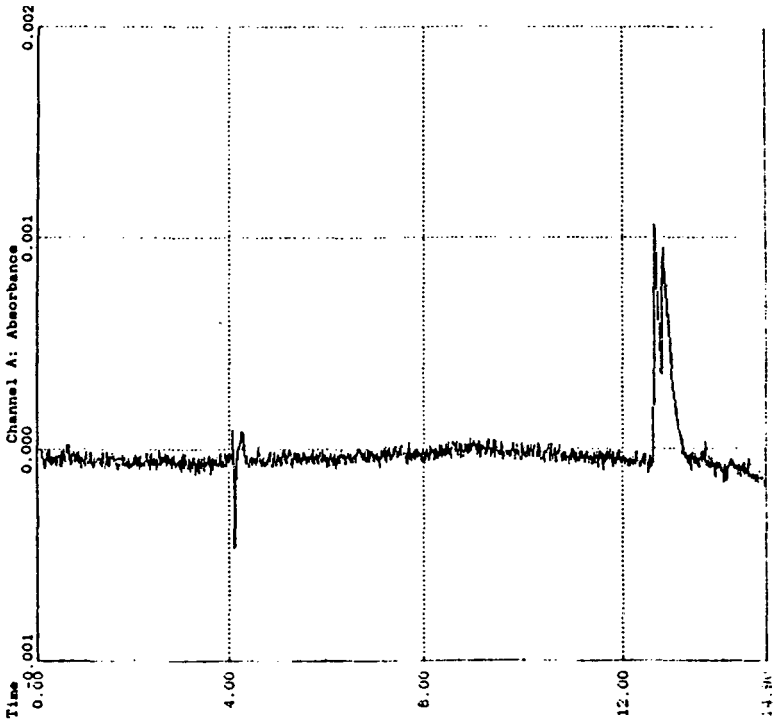


Fig. 9. Enantiomeric separation achieved for compound 5.

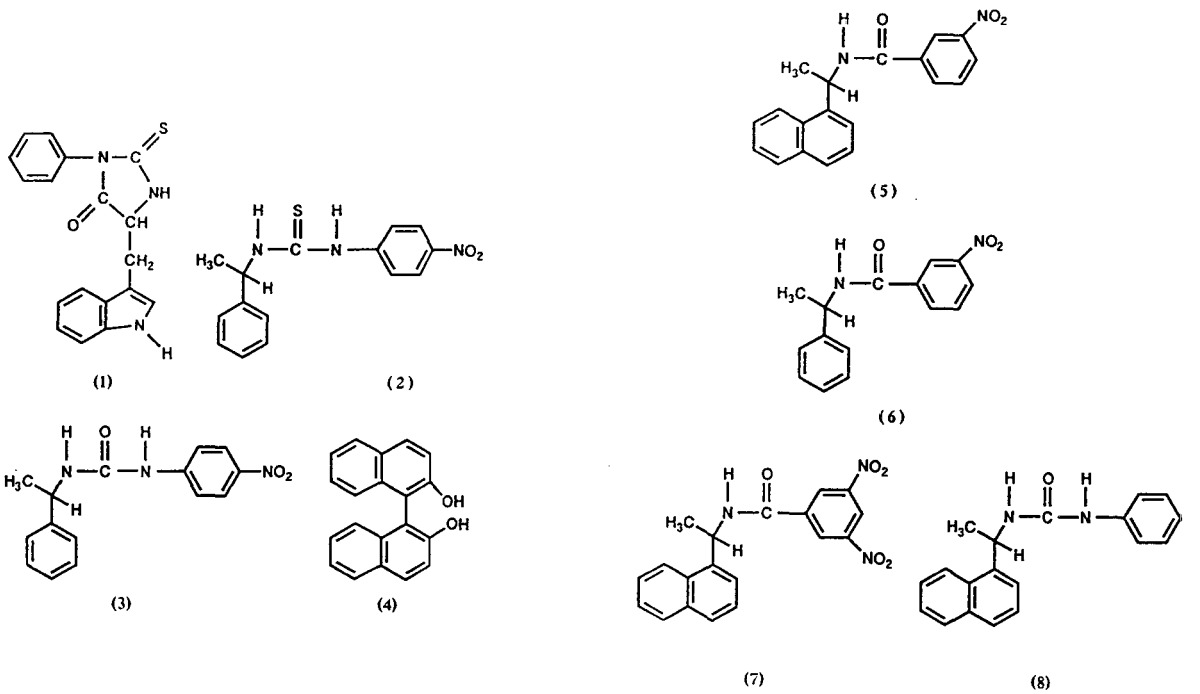


Fig. 10. Some analyte structures examined.

gate this some more novel chiral surfactants are currently being designed and synthesised.

## Acknowledgements

This work was supported by EPSRC and SmithKline Beecham Pharmaceuticals under a Total Technology initiative. The surface tension apparatus was available by courtesy of the Chemical Engineering department at UMIST.

## References

[1] J. Jorgenson and K.D. Lukacs, Anal. Chem., 53 (1981) 1928–1302.
[2] S. Terabe, K. Otsuka, K. Ichiwara, A. Tsuchiya and T. Ando, Anal. Chem., 56 (1984) 111–113.
[3] K. Otsuka and S. Terabe, J. Chromatogr., 515 (1990) 212–226.
[4] A. Dobashi, T. Ono, S. Hara and J. Yamaguchi, Anal. Chem., 61 (1989) 1984–1986.
[5] S. Terabe, M. Shibata and Y. Miyashita., J. Chromatogr., 480 (1989) 403–411.
[6] H. Nishi, T. Fukuyama and M. Matsuo, J. Chromatogr., 515 (1990) 233–243.
[7] N. Rabjohn (Editor), Organic Synthesis Coll., Vol. IV, John Wiley, New York, 1963, p. 242.
[8] P. Mukerjee and M.J. Mysels, Critical Micelle Concentration of Aqueous Surfactant Systems, NSROS-NBS 36, U.S. Department of Commerce, Washington, DC, 1971.
[9] K.J. Mysels, Introduction to Colloid Chemistry, Interscience Publishers, New York, 1967, p. 186.
[10] L.S. Ettre, Pure Appl. Chem., 65 (1993) 819–872.

ELSEVIER

Journal of Chromatography A, 712 (1995) 372–377

JOURNAL OF CHROMATOGRAPHY A

Short communication

# Determination of 9,10-dihydroxyanthracene and anthraquinone in Kraft pulping liquors by high-performance liquid chromatography

J. Revenga, F. Rodríguez*, J. Tijero

*Departamento Ingeniería Química, Facultad Ciencias Químicas, Universidad Complutense de Madrid, 28040 Madrid, Spain*

First received 12 December 1994; revised manuscript received 2 May 1995; accepted 15 May 1995

**Abstract**

A simple chromatographic method was developed to determine the amount of anthraquinone (AQ) and its reduced form, the disodium salt of 9,10-dihydroxyanthracene ($Na_2AQ$), in white pulping liquors. The method is based on the different solubilities of AQ (insoluble) and $Na_2AQ$ (soluble) in aqueous medium. Prior to analysis, samples (containing AQ + $Na_2AQ$) are filtered to remove the insoluble quinone (AQ) and oxidized with hydrogen peroxide. The resulting oxidized material, which corresponds to the initial amount of $Na_2AQ$ present in the sample, is dissolved in N,N-dimethylformamide (DMF) and this final solution is analysed for AQ by high-performance liquid chromatography. The basic operating conditions are as follows: detection wavelength, 254 nm; flow-rate, 1.5 ml $min^{-1}$; temperature, 40°C; eluent, methanol–water (82:18, v/v); and volume of sample injected, 10 $\mu$l. The method is suitable for the determination of quinonoid compounds in the 5–2500 $\mu g\ ml^{-1}$ range in Kraft pulping liquor and the limit of detection is 0.5 $\mu g\ ml^{-1}$.

## 1. Introduction

Anthraquinone (AQ) is used in the pulping industry because it increases the cellulose yield and lowers the energy consumption during the alkaline pulping of wood [1]. AQ is reduced to the disodium salt of 9,10-dihydroxyanthracene ($Na_2AQ$) by the sodium sulfide present in the pulping liquor according to the following equation:

$$NaHS + 9\ NaOH + 4\ AQ \rightleftharpoons Na_2SO_4 + 4\ Na_2AQ + 5\ H_2O \quad (1)$$

However, the determination of $Na_2AQ$ is difficult as it is present at very low levels and it is extremely susceptible to air oxidation [2]. Therefore, the concentration of reduced quinone must be determined in an indirect way. Several methods have been applied to solve this problem, including high-performance liquid chromatography (HPLC) [2–8], gas chromatography (GC) [9], GC–mass spectrometry [10], differential pulse polarography [11] and spectrophotometry [12]. These methods require extensive sample extraction and solvent concentration and their operating costs are high. In this paper, a simple, rapid and isocratic HPLC method is proposed for the measurement of the concentration of AQ and its reduced form, which is soluble in the

* Corresponding author.

0021-9673/95/$09.50 
*SSDI* 0021-9673(95)00574-9

pulping liquor. A minimum of sample preparation is necessary without solvent extractions where incomplete recoveries could occur. The method is based on the different solubilities of AQ and $Na_2AQ$ in aqueous medium. The detection limits are in the low ppm range and the method is therefore a satisfactory alternative to previously reported techniques.

## 2. Experimental

### 2.1. Apparatus and conditions

A Perkin-Elmer (Norwalk, CT, USA) Series 2 liquid chromatograph, equipped with a Rheodyne Model 7105 injection valve (175-$\mu$l loop), an LC-75 UV detector and an LC-100 column oven, was used. The stainless-steel column (25 cm × 4.6 mm I.D.) was packed with 10-$\mu$m reversed-phase $C_{18}$ Spherisorb ODS 2 (Supelco, Bellefonte, PA, USA). Chromatograms were obtained with a Varian (Sunnyvale, CA, USA) Model 4290 integrator. The operating conditions were as follows: detection wavelength, 254 nm; flow-rate, 1.5 ml $min^{-1}$; temperature, 40°C; and chart speed, 1 cm $min^{-1}$. The eluent was methanol–water (82:18, v/v).

### 2.2. Reagents

Anthraquinone was obtained from Aldrich (Steinheim, Germany). Prior to use, the mobile phase was filtered through a 0.45-$\mu$m pore-size HA membrane filter (Millipore, Bedford, MA, USA) and degassed for 50 min using an ultrasonic bath. The water used was prepared by glass distillation and filtration with a Milli-Q water-purification system (Millipore). Methanol and DMF were purchased form Merck (Darmstadt, Germany). All reagents were of analytical-reagent grade.

### 2.3. Procedure

To obtain artificial samples of white pulping liquor, containing 0.7–1.7 mol $l^{-1}$ of sodium hydroxide, 0.1–0.3 mol $l^{-1}$ of sodium sulfide and 0.005–2500 $\mu$g $ml^{-1}$ of AQ, a set of experiments were carried out in a 1000-ml pressure vessel (Autoclave Engineers Group, Erie, PA, USA) at different temperatures. The reduction reaction was allowed to proceed under the different experimental conditions for 1 h to ensure that the maximum conversion of AQ to $Na_2AQ$ was attained. Then, quinone compounds (AQ and $Na_2AQ$) were recovered from the pulping liquors by the procedure described below.

For the determination of $Na_2AQ$ (see Fig. 1), since some of the initial quinone is reduced by the sodium sulfide present in pulping liquor to $Na_2AQ$ according to Eq. 1, samples (10 ml) must be filtered to remove the unreacted AQ, which is insoluble in this medium. The filtered samples are oxidized with hydrogen peroxide (10 ml) and the resulting material (AQ suspension,

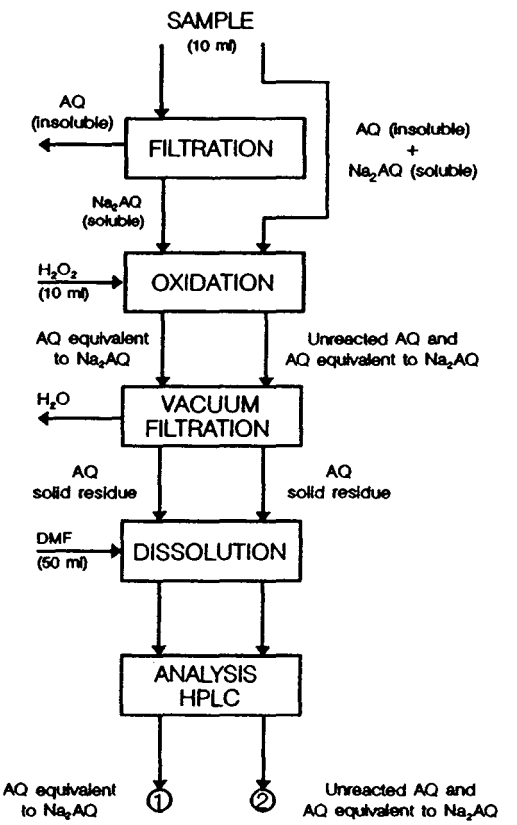


Fig. 1. Analytical procedure for AQ and $Na_2AQ$ analysis in white pulping liquors.

which corresponds to the amount of $Na_2AQ$ present in the sample) is separated by vacuum filtration as shown in Fig. 1, path 1. The solid residue is dissolved in 50 ml of DMF by shaking for 10 min, then an aliquot of this organic solution is analysed by HPLC.

For the determination of the total quinone ($Na_2AQ$ soluble + AQ insoluble), the procedure is similar to that for $Na_2AQ$, but the samples are not filtered to remove the insoluble AQ (as shown in Fig. 1, path 2).

Standards of AQ in DMF in the concentration range 1–500 $\mu$g ml$^{-1}$ were prepared in DMF by serial dilution.

## 3. Results and discussion

DMF does not interfere in the determination of AQ because its retention time is 1.7 min, whereas that of AQ is 4.2 min with a standard deviation of 0.09 min under the chromatographic conditions used. A typical HPLC trace is shown in Fig. 2. The AQ peak is sharp and well separed from the matrix (DMF).

### 3.1. Range

Analysis of standard solutions of AQ in DMF showed that the absorbance of AQ is essentially a linear function of concentration between 1 and 500 $\mu$g ml$^{-1}$, but deviated slightly above this range.

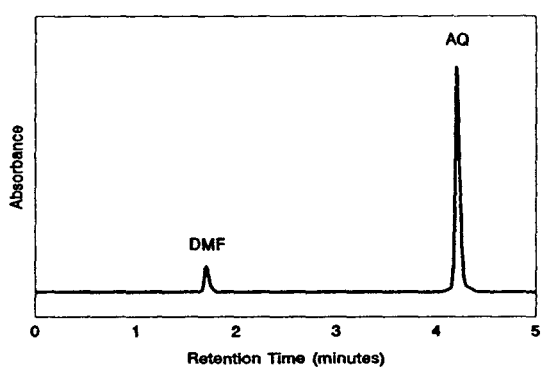


Fig. 2. Chromatogram of 50 $\mu$g ml$^{-1}$ of AQ concentration in DMF. Operating conditions: detection wavelength, 254 nm; flow-rate, 1.5 ml min$^{-1}$; temperature, 40°C; eluent, methanol-water (82:18 v/v); and volume of sample injected, 10 $\mu$l.

### 3.2. Calibration

A calibration graph of peak area versus the concentration of AQ in the injected aliquot of DMF (10 $\mu$l) covering the range 1–500 $\mu$g ml$^{-1}$ was plotted. There is a very strong relationship between the two variables. In order to quantify this relationship, the data were fitted by a least-squares regression equation of the form $y = a + bx$:

$$y = 0.0185 + 0.03511x \qquad r^2 = 0.998 \qquad (2)$$

where $y$ is the peak area in cm$^2$ and $x$ is the AQ concentration in DMF solution in $\mu$g ml$^{-1}$. The standard deviations of the slope and intercept are $s_b = 9.2 \cdot 10^{-5}$ and $s_a = 0.0217$, respectively. The standard error is 0.0511 and the number of data points $n = 10$. The 95% confidence interval for the true slope is $b \pm ts_b$:

$$0.03511 \pm (2.306 \cdot 9.2 \cdot 10^{-5}) = 0.03511 \pm 0.00021$$

(i.e. 0.03490–0.03532 cm$^2$ ml $\mu$g$^{-1}$)

The 95% confidence interval for the true intercept is $a \pm ts_a$:

$$0.01849 \pm (2.306 \cdot 0.02170) = 0.01849 \pm 0.05004$$

(i.e. 0.06853 to −0.03156 cm$^2$)

The confidence interval for the true intercept extends from −0.03156 to 0.06853 cm$^2$ ml $\mu$g$^{-1}$, which includes zero. Therefore, it would be reasonable to fit a line which passed through the origin of the form $y = bx$. The equation of the best line through the original is

$$y = 0.03516x \qquad r^2 = 0.999 \qquad (3)$$

This equation is not very different from the best line through the origin ($y = 0.01848 + 0.03511x$) over the range of concentrations used in the calibration. The standard deviation of the slope is $s_b = 6.8 \cdot 10^{-5}$, the standard error is 0.0503 and $n = 10$. The 95% confidence interval for the true slope is $b \pm ts_b$:

$0.03516 \pm (2.306 \cdot 6.8 \cdot 10^{-5}) = 0.03516 \pm 0.0015$

(i.e. 0.03501–0.03531 $cm^2$ ml $\mu g^{-1}$)

However, the confidence interval for the true slope extends from 0.03490 to 0.03501 $cm^2$ ml $\mu g^{-1}$ for the line through the origin, whereas the confidence interval for the true slope of the other line was much wider (0.0349–0.03532 $cm^2$ ml $\mu g^{-1}$). By assuming that the true line passes throught the origin, one obtains a better estimate of the true slope, provided that the assumption is justified.

### 3.3. Confidence intervals for the true concentration

For an unknown sample that gives an peak area $y$, the true concentration and its confidence interval is given by

$$\frac{y}{b} \pm \frac{ts_b}{b}\sqrt{1+\left(\frac{y}{b}\right)^2} \quad (4)$$

For the sample corresponding to a peak area of 1.80 $cm^2$, its concentration in the 95% confidence interval is $51.19 \pm 0.04$ $\mu g$ $ml^{-1}$. That is, the true concentration of the unknown sample lies between 51.15 and 51.23 $\mu g$ $ml^{-1}$. In this way, by substituting several values of $y$ in Eq. 4 different confidence intervals are obtained, which are shown in Table 1. Note that these intervals become wider as $y$ increases.

### 3.4. Limits of detection and quantification

To obtain the limit of detection the following equation must be applied:

$$\text{Limit} = \frac{Ks_{bl}}{b} \quad (5)$$

where $s_{bl}$ is the standard deviation (0.00117) for ten blank readings, $b$ is the slope of the calibration line through the origin (0.03516 $cm^2$ ml $\mu g^{-1}$) and $K$ is equal to 3 for the limit of quantification and $K = 10$ for the limit of detection [13]. Applying Eq. 5, one obtains 0.1 and 0.4 $\mu g$ $ml^{-1}$ for the limits of detection and quantification of AQ in DMF, respectively.

Table 1
95% confidence intervals for ture concentration of AQ in DMF solutions

| Peak area, $y$ ($cm^2$) | 95% Confidence interval (CI) for true concentration $x$ | |
|---|---|---|
| | $x$ ($\mu g\ ml^{-1}$) | CI |
| 0.00 | $0.00 \pm 0.004$ | −0.004 to 0.004 |
| 0.16 | $4.55 \pm 0.01$ | 4.54 to 4.56 |
| 0.37 | $10.52 \pm 0.02$ | 10.50 to 10.54 |
| 1.80 | $51.20 \pm 0.05$ | 51.15 to 51.25 |
| 3.50 | $99.54 \pm 0.22$ | 99.32 to 99.76 |
| 7.07 | $201.08 \pm 0.43$ | 200.51 to 201.51 |
| 10.52 | $299.20 \pm 0.87$ | 298.33 to 300.07 |
| 14.17 | $403.01 \pm 1.30$ | 401.71 to 404.31 |
| 17.50 | $497.72 \pm 1.75$ | 495.97 to 499.47 |

### 3.5. Accuracy and precision

To determine the accuracy of the method, a recovery study was carried out. The recovery of the analyte, $R$, is defined as fraction of analyte added to the sample (fortified sample) prior to analysis, which is measured (recovered) by the method. When the same method is used to analyse both the unfortified and fortified samples $R$ is calculated as follows:

$$R(\%) = \frac{C_F - C_U}{C_A} \cdot 100 \quad (6)$$

where $C_F$ is the concentration of analyte measured in the fortified sample, $C_U$ the concentration of analyte measured in the unfortified sample and $C_A$ the concentration of analyte added to the fortified sample. Note that $C_A$ is a calculated value, not a value measured by the method being used.

Table 2 shows that the recoveries are all near 100%, providing a further example of the excellent accuracy of the analysis by HPLC. The accuracy is excellent at concentrations of AQ between 1 and 500 $\mu g$ $ml^{-1}$, where the recovery of AQ rises 99.24%, but it deteriorates significantly above 500 $\mu g$ $ml^{-1}$. This limit is caused partly by a departure from linearity of the calibration line due to the limited solubility of AQ in DMF at higher AQ concentrations. On other hand, to validate any analytical method,

Table 2
Recovery for AQ in DMF determined by HPLC

| Added ($\mu$g ml$^{-1}$) | Recovery (%) |
|---|---|
| 200 | 100.30, 99.11, 98.63 |
| 250 | 99.61, 99.32, 98.70 |
| 300 | 98.77, 99.15, 99.58 |
| | Average, $A$ 99.24 |
| | Standard deviation, $s$ 0.50 |
| | R.S.D. = $(s/A)\cdot 100$ (%) 0.50 |

the relative standard deviation (R.S.D.) should be no more than 2%. In the present case, the R.S.D. is 0.51%, which indicates good accuracy of the HPLC analysis.

### 3.6. Analysis of white pulping liquor

The concentration of AQ in white pulping liquors may be calculated by using the following equations:

$$C_{AQ\,H_2O} = \frac{V_{DMF} C_{AQ\,DMF}}{V_S}; \quad C_{AQ\,DMF} = \frac{y}{0.03516} \tag{7}$$

where $C_{AQ\,H_2O}$ = concentration of AQ in white pulping liquor ($\mu$g ml$^{-1}$); $C_{AQ\,DMF}$ = concentration of AQ in DMF ($\mu$g ml$^{-1}$); $V_S$ = sample volume of white pulping liquor (10 ml); and $V_{DMF}$ = volume of DMF used in the dissolution stage (50 ml).

The accuracy of the method was evaluated from the percentage recovery of AQ and $Na_2AQ$ from the white pulping liquor samples. As shown in Table 3, the average recovery is 98.80% with a standard deviation of 0.45% and an R.S.D. of 0.45%. These results indicate that the overall analytical procedure has good accuracy.

To test the proposed method, a wide variety of white pulping liquors containing sodium sulfide (0.1–0.3 mol l$^{-1}$) and sodium hydroxide (0.7–1.7 mol l$^{-1}$) at different temperatures (140–160°C) were analysed. This study showed that the proposed method can be used to control the

Table 3
Recovery for determination of AQ in samples of white pulping liquor containing 1.1 mol l$^{-1}$ of sodium hydroxide, 0.184 mol l$^{-1}$ of sodium sulfide and 1–500 $\mu$g ml$^{-1}$ of AQ at 150°C

| Concentration ($\mu$g ml$^{-1}$) | | | | Recovery (%) |
|---|---|---|---|---|
| AQ added | AQ[a] found | $Na_2AQ$[a,b] found | Total found | |
| 5[c] (1)[d] | (n.d.)[e] | 4.91 (0.98) | 4.90 (0.98) | 98.10 |
| 50 (10) | (n.d.) | 49.75 (9.95) | 49.75 (9.95) | 99.50 |
| 250 (50) | 3.30 (0.65) | 242.95 (48.60) | 246.25 (49.25) | 98.50 |
| 500 (100) | 37.10 (7.40) | 454.40 (90.88) | 491.50 (98.30) | 98.30 |
| 1000 (200) | 536.95 (107.40) | 454.05 (90.80) | 991.00 (198.20) | 99.10 |
| 1500 (300) | 1037.85 (207.60) | 448.65 (89.70) | 1486.50 (297.30) | 99.10 |
| 2000 (400) | 1538.00 (307.60) | 444.08 (88.80) | 1982.00 (396.40) | 99.10 |
| 2500 (500) | 2046.25 (409.25) | 421.25 (84.25) | 2467.50 (493.50) | 98.70 |
| | | | Average, $A$ | 98.80 |
| | | | Standard deviation, $s$ | 0.45 |
| | | | R.S.D. = $(s/A)\cdot 100$ (%) | 0.45 |

[a] Average of three injections.
[b] Amount of $Na_2AQ$ expressed as AQ.
[c] Amount of AQ or $Na_2AQ$ in white pulping liquor.
[d] Amount of AQ in DMF solution.
[e] Not detected.

Table 4
Comparison of methods for the determination of AQ in pulping liquors by HPLC

| Ref. | Detection limit ($\mu g\ ml^{-1}$) | Calibration range ($\mu g\ ml^{-1}$) | Recovery (%) | Standard deviation (%) |
|---|---|---|---|---|
| [2] | Low ppm region | 2–120 | 98.0 | 2.30 |
| [3] | 0.1 | 1–200 | 98.4 | 0.70 |
| [4] | Low ppm region | 2–40 | 90.0 | – |
| [5] | | 50–200 | – | 0.24 |
| [6] | – | 1–9 | – | 0.50 |
| [7] | 0.8 | 1–320 | – | – |
| This work | 0.1 | 1–500 | 98.8 | 0.45 |

AQ dosage in the manufacture of pulp. The method offers advantages over other methods with regard to the limit detection, range and accuracy, as shown in Table 4.

## 4. Conclusions

The proposed HPLC method is simple, rapid and precise. It allows the determination of AQ and its reduced form ($Na_2AQ$) in a few minutes. It can be successfully applied to the determination of quinonoid compounds in pulping liquors with a detection limit in the low ppm region.

## Acknowledgement

The authors are grateful to the Comunidad Autónoma de Madrid (Consejería de Educación) for financial support.

## References

[1] T.J. Blain, Tappi J., 76, No. 3 (1993) 137.
[2] D.N. Armentrout, Tappi, 64, No. 9 (1981) 165.
[3] R.D. Mortimer and B.I. Fleming, Tappi, 64, No. 11 (1981) 114.
[4] J.O. Bronsted, B. Dahl and K. Schroder, J. Chromatogr., 206 (1981) 392.
[5] K.H. Nelson and D. Schram, J. Chromatogr. Sci.., 21 (1983) 218.
[6] K.H. Nelson and D.J. Cietek, J. Chromatogr., 281 (1983) 237.
[7] N. Kiba, M. Takamatsu and M. Furusaw, J. Chromatogr., 328 (1985) 309.
[8] M. Schneiderman, A. Sharma and D. Locke, J. Chromatogr., 409 (1987) 343.
[9] G.W. Van Eijk and H.J. Roeijmans, J. Chromatogr., 295 (1984) 497.
[10] L.G. Harruff and M.A. Vazquez, Tappi, 64 (1981) 109.
[11] J.O. Bronsted, K.H. Schroeder, and H.D. Friestad, Anal. Chim. Acta, 119 (1980) 243.
[12] J.E. Doyle and A.F. Wallis, Appita, 36 (1982) 122.
[13] G.L. Long and J.D. Winefordner, Anal. Chem., 55, No. 7 (1983) 712A.

ELSEVIER

Journal of Chromatography A, 712 (1995) 378–381

JOURNAL OF CHROMATOGRAPHY A

Short communication

# Liquid chromatographic determination of the antibiotic fumagillin in fish meat samples

Jenö Fekete*, Zsuzsanna Romvári, Ildikó Szepesi, György Morovján

*Institute of General and Analytical Chemistry, Technical University of Budapest, Gellért tér 4, H-1111 Budapest, Hungary*

First received 22 November 1994; revised manuscript received 2 May 1995; accepted 10 May 1995

**Abstract**

A procedure for the determination of fumagillin, an antibiotic of *Aspergillus fumigatus* in fish meat samples, using reversed-phase high-performance liquid chromatography is described. Liquid chromatography was performed on an octadecylsilane column using acetonitrile–water–phosphoric acid solution as mobile phase, with detection at 350 nm. Two different types of sample preparation were developed, clean-up and enrichment, and the limits of quantification were 100 ng/g and 5 ng/g, respectively, in fish meat. The recovery was 75 ± 3% in the concentration range 100–500 ng/g. To introduce the methodology and demonstrate its usefulness, a practical experiment was performed. Trouts fed with fumagillin were examined for elimination of fumagillin. After 24 h, the concentration was shown to decrease to below 100 ng/g.

## 1. Introduction

Fumagillin (Fig. 1) is a metabolite of *Aspergillus fumigatus* and has a potent amoebicidal property. This activity led to large-scale production and clinical studies of its therapeutic potential. At present, however, because of toxic side-effects encountered in human clinical trials, medical applications of fumagillin are confined to its use by apiarists and to the veterinary profession. Fumagillin may be effective in the treatment of angiogenesis-related diseases [1] and may be effective in suppressing tumor growth, is a potent antibiotic that inhibits *Entamoeba histolytica* [2], may be used in the honey industry to protect bees from *Nosema apis* [3] and has been used against microsporodian in fish [4–6]. Several assay methods have been developed for fumagillin, e.g., thin-layer chromatography [7], microbial assay [8] and spectrophotometric assay [9]. Each of these techniques has its disadvan-

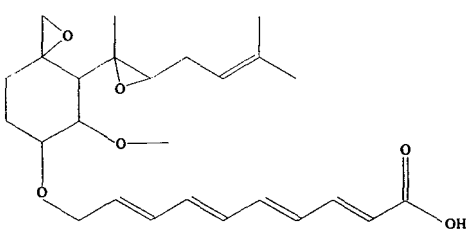


Fig. 1. Structure of fumagillin.

* Corresponding author.

0021-9673/95/$09.50 
*SSDI* 0021-9673(95)00567-6

tages, mainly due to interference caused by degradation products of fumagillin and impurities or poor reproduciblity. High-performance liquid chromatography (HPLC) is rapid and accurate and separates compound from possible impurities and degradation products. Brackett et al. [10] developed an HPLC assay for fumagillin and Assil and Sporns [3] developed a sensitive HPLC method for the determination of fumagillin in honey.

## 2. Experimental

### 2.1. Instrumentation

Solutions obtained from the extraction procedure were injected through a 100-$\mu$l loop (Labor MIM, Budapest, Hungary) for analysis on a reversed-phase silica column ($\mu$Bondapak $C_{18}$ 300 mm × 3.9 mm I.D.) (Waters, Milford, MA, USA) at ambient temperature. The mobile phase was acetonitrile–water–phosphoric acid (600:400:1, v/v/v) pumped by a Waters Model 510 HPLC pump at a flow-rate of 1 ml/min. Detection was carried out using a Bio-Rad (Richmond, CA, USA) Model 1306 variable-wavelength UV monitor at 350 nm. A Waters Model 740 data module integrator was used to record chromatograms and to calculate the peak area of fumagillin.

### 2.2. Chemicals and materials

Acetonitrile for the mobile phase and the extraction procedure was of chromatographic grade (Reanal, Budapest, Hungary). Deionized water was distilled then deionized through a Milli-Q water-purification system. Phosphoric acid was of analytical-reagent grade (Reanal).

Fumagillin DCH (62.1% fumagillin acid content) was supplied by Chinoin Pharmaceutical and Chemical Works (Budapest, Hungary).

For the development of the extraction process, fumagillin-free fish were purchased. Fish fed with fumagillin for the study of fumagillin concentration in muscular tissues were supplied by the University of Veterinary Sciences (Budapest, Hungary). As fumagillin is unstable towards light [9] and heat [11], and to prevent biotic decomposition, samples were stored deep frozen at −20°C packed in aluminium foil.

### 2.3. Procedures

*Standard solution*

To prepare a standard solution, fumagillin was dissolved in acetonitrile–water solution corresponding to the eluent excluded phosphoric acid.

For the recovery study, meat samples were spiked with various amounts of fumagillin in the range 1–1000 ng/g meat.

*Sample preparation*

Two methods of sample preparation were applied according to the fumagillin concentration in the sample. Based on the expected fumagillin concentration in solutions obtained from the extraction process, clean-up was used for the 0.1–5 $\mu$g/ml and enrichment for the 0.01–0.1 $\mu$g/ml range of fumagillin concentration in the extraction solution.

In order to optimize both clean-up and enrichment, we studied the adsorption of fumagillin on a Sep-Pak $C_{18}$ column. Before sample application, the Sep-Pak $C_{18}$ column was washed with acetonitrile.

*Clean-up*

Acetonitrile (4 ml) was added to 1.0 g of meat (pulped by passing through a plastic syringe, measured water content 0.7 ml/g). The suspension was homogenized, then the cells were disrupted with a 10-min treatment in an ultrasonic bath. After centrifugation for 10 min at 10 000 *g*, the supernatant was passed through a Sep-Pak $C_{18}$ column, discarding the first 0.4 ml, then 100 $\mu$l were injected on to the reversed-phase silica column for analysis.

*Enrichment*

Acetonitrile (10 ml) was added to 5.0 g of meat (prepared as above). The suspension was homogenized, then the cells were disrupted with a 10-min treatment in ultrasonic bath. After centrifugation for 10 min at 10 000 *g*, 100 ml of

water were added to the supernatant and the solution was filtered through a Sep-Pak $C_{18}$ column. Fumagillin was eluted with 2 ml of acetonitrile–water eluent (90:10), discarding the first 0.2 ml, then 100 $\mu$l were injected on to the reversed-phase silica column for analysis.

## 3. Results and discussion

No reports on the determination of fumagillin in muscular tissue of fish or on the solid-phase extraction of fumagillin were found. This work involved not only the study of an HPLC assay for fumagillin; our primary aim was to develop a method for the determination of fumagillin in biological samples, including solid-phase extraction, clean-up and enrichment.

Fumagillin is highly sensitive to light and oxidation; however, our studies showed than the ultrasonic bath we utilized for the extraction of fumagillin caused no decomposition of the analyte.

The eluent used for the determination of fumagillin in meat samples is among those not recommended by Brackett et al. [10], as according to their studies fumagillin eluted with its impurities. In the method developed, the use of phosphoric acid instead of acetic acid allowed the separation of fumagillin and its impurities. Moreover, the veterinary fumagillin we used may not contain more than 0.1% of unidentified impurities as prescribed by standards, and the deviation caused by possible impurities fell below the standard margin of the method in the measured concentration range.

Under the chosen conditions (eluent composition, flow-rate), the retention time of fumagillin was about 7.45 min. In the blank sample, no disturbing peaks were detected near the retention time of fumagillin (Fig. 2).

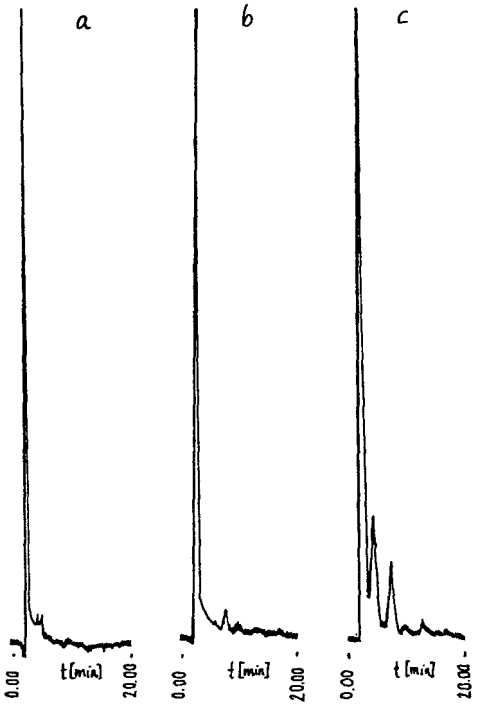


Fig. 2. Chromatograms showing (a) blank muscle sample, (b) limit of detection (muscle spiked with 1 ng/g of fumagillin), (c) sample from muscular tissue of fumagillin-fed trout 9 h after feeding. Loop volume, 100 $\mu$l; column, $\mu$Bondapak $C_{18}$ (300 mm × 3.9 mm I.D.); mobile phase, acetonitrile–water–phosphoric acid (600:400:1, v/v/v); temperature, ambient; flow-rate, 1 ml/min; detection wavelength, 350 nm. $A$ = absorbance ($8 \times 10^{-3}$ AUFS).

### 3.1. Analytical data

*Linearity*

In the examined concentration range (0.01–10 $\mu$g/ml), the detector response was found to be linear for both peak-area and peak-height measurements.

*Limit of detection*

With enrichment, the least possible detectable concentration was found to be 1 ng/g of fumagillin, calculated as three times the standard deviation of the noise.

*Limit of quantitation*

With the clean-up method the limit of quantification was 100 ng/g and for the enrichment method 5 ng/g.

*Recovery*

The recovery was found to be 75 ± 3% in the 100–500 ng/g concentration range for the whole

process. The loss due to the adsorption on the apolar surface of the Sep-Pak $C_{18}$ column was $5 \pm 1\%$. According to our investigations, the 5–10-min ultrasonic treatment caused no degradation of fumagillin.

*Precision*

The intra-day reproducibility was studied. The results showed good agreement, with a relative standard deviation of only 0.67% at a 1 mg/l fumagillin concentration.

### 3.2. Practical application

To illustrate the usefulness of the method, trouts fed with fumagillin were examined. During the feeding experiment, trouts were fed with 20 mg of fumagillin per kilogram body mass. The change in fumagillin concentration was studied in muscular tissue samples obtained from fish bled 3, 9 and 24 h after feeding. The standard deviation was relatively high owing to differences between specimens, such as differences in digestion, metabolism and secretion of drugs. From 3 to 9 h after feeding the fumagillin concentration showed a rapid decrease of more than 70%; 24 h after feeding the fumagillin concentration was less than 100 ng/g. These data indicate that at the beginning the fumagillin concentration is high in muscular tissues and then it is relatively rapidly eliminated.

## 4. Conclusion

The present results demonstrate that HPLC is suitable for the determination of fumagillin in fish meat samples. The method is rapid and accurate and may be used to investigate the pharmacokinetic effects of fumagillin.

## Acknowledgements

The authors thank Chinoin Pharmaceutical and Chemical Works, Budapest, for supplying fumagillin and the University of Veterinary Sciences, Budapest, for performing the feeding experiment. The study was supported by OTKA No. 717. We acknowledge helpful discussions with Dr. Peter Sárközy and Mrs. Zsófia Rózsa during the experimental work.

## References

[1] Takeda Chemical Industries, Eur. Pat. Appl., EP 0 325 199 A2.
[2] M.C. McCowen, M.E. Callender and J.F. Lawlis, Science, 113 (1951) 202.
[3] H.I. Assil and P. Sporns, J. Agric. Food Chem., 39 (1991) 2206.
[4] T. Kano and H. Fukui, Fish Pathol., 16 (1982) 193.
[5] K. Molnár, F. Baska and Cs. Székely, Dis. Aquat. Organisms, 2 (1987) 187.
[6] Cs. Székely, K. Molnár and F. Baska, Acta Vet. Hung., 36 (1988) 239.
[7] H.J. Issaq, E.W. Barr, T. Wei, C. Meyers and A. Aszalos, J. Chromatogr., 131 (1977) 291.
[8] R.L. Girolami, in F. Kavanaugh (Editor), Fumagillin in Analytical Microbiology, Vol. I, Academic Press, New York, 1963, p. 295.
[9] E.R. Garett and T.E. Eble, J. Am. Pharm. Assoc., (1954) 385.
[10] J.M. Brackett, M.D. Arguello and J.C. Schaar, J. Agric. Food Chem., 36 (1988) 762.
[11] E.R. Garett and T.E. Eble, J. Am. Pharm. Assoc., (1954) 539.

ELSEVIER

Journal of Chromatography A, 712 (1995) 382–389

JOURNAL OF CHROMATOGRAPHY A

Short communication

# Quantitative thin-layer chromatography of perbromate

Thi Kieu Xuan Huynh

*Institut de Chimie Minérale et Analytique, Université de Lausanne, Centre Universitaire, CH-1015 Lausanne, Switzerland*

First received 21 February 1995; revised manuscript received 25 April 1995; accepted 12 May 1995

**Abstract**

A thin-layer densitometric micromethod for the determination of perbromate is described using Merck 5577 microcrystalline cellulose thin layers with butanol–10% ammonia as solvent. The spots are evaluated by a starch–iodide reagent in 6 *M* HCl using the Cybertech Gel documentation system WINCAM 2.1. The method was used to determine perbromate in an aged dilute solution and in an impure solid sample.

## 1. Introduction

The perbromate ion was discovered by Appelman in 1968 [1] and although over hundred papers have been written on its properties, only several kilogrammes of it have been synthesized so far. When trying simple methods of synthesis we noted that besides the paper and thin-layer chromatographic separation described by Lederer and Sinibaldi [2] there was no simple test for the presence of perbromate in solution.

Most analytical reactions are based on the liberation of iodine during the reduction of perbromate in the presence of iodide. This can be made more selective by first reducing the bromate; however this reaction seemed to be too unspecific unless preceded by a separation. Besides the reduction reaction, perbromate, like perchlorate, yields a red spot on paper when reacted with methylene blue [2]. While this test would readily distinguish it from bromate and bromide, it is not readily quantitated, because a red spot on a blue background does not give a good contrast in a colorimetric determination.

As shown by Lazarou et al. [3] as well as others, perbromate does not react instantaneously with KI. Thus a scanning technique in which the chromatogram is passed under a photoelectric device would not be satisfactory. A chromatogram sprayed with iodide would liberate further iodide due to its access to air as well as evaporate iodine in addition to a slow formation of the actual colour to be determined.

Recently a CCD camera arrangement was constructed by Cybertech (Berlin) principally for the determination of the intensity of bands obtained by electrophoresis in nucleic acid sequencing. The instrument produces a photographic image of the entire electropherogram or chromatogram, so that in the case of the perbromate reaction with iodide one can obtain a series of standards together with the sample to be analysed exactly at the same moment. Furthermore the data thus obtained can be treated by a computer and directly give the calibration curve and the spot intensities of the sample spots on the same thin layer.

Below we describe the application of this arrangement for the determination of perbromate and the application of the method to the

0021-9673/95/$09.50 
*SSDI* 0021-9673(95)00575-7

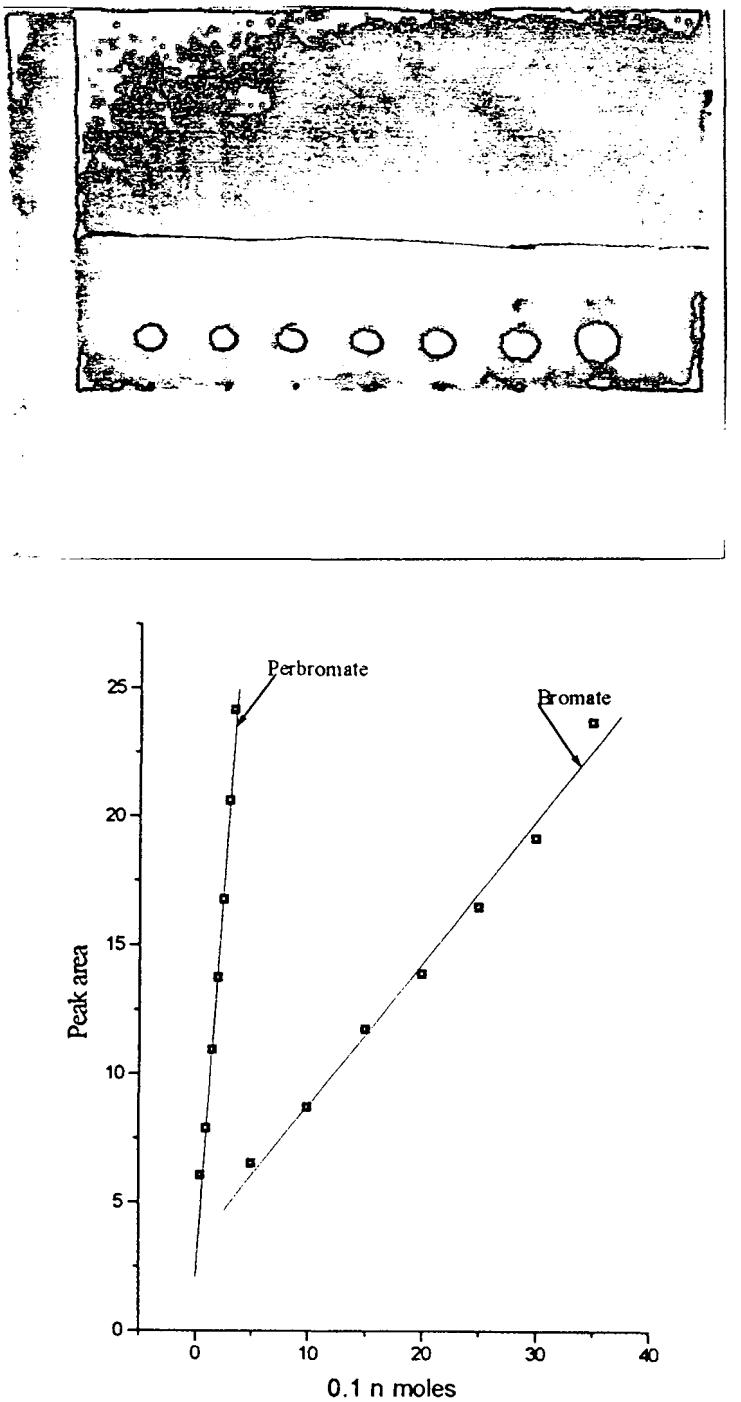


Fig. 1. Calibration curve of mixtures of perbromate and bromate in ratio 1:10. Top: The photo obtained by the CCD camera. Below: The calibration obtained from the densitometric results. Perbromate: $y = (6.10 \pm 0.25)x + 2.09 \pm 0.55$; $r = 0.9960$. Bromate: $y = (0.55 \pm 0.03)x + 3.29 \pm 0.58$; $r = 0.9945$.

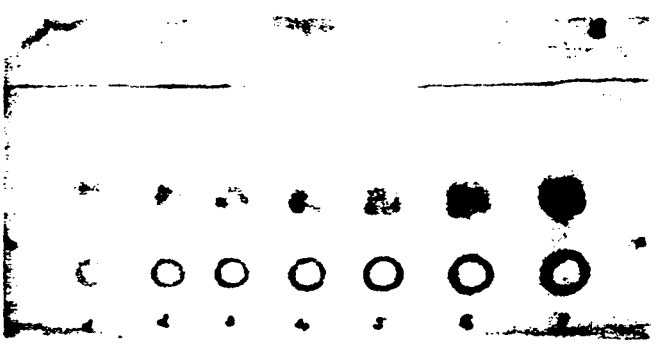

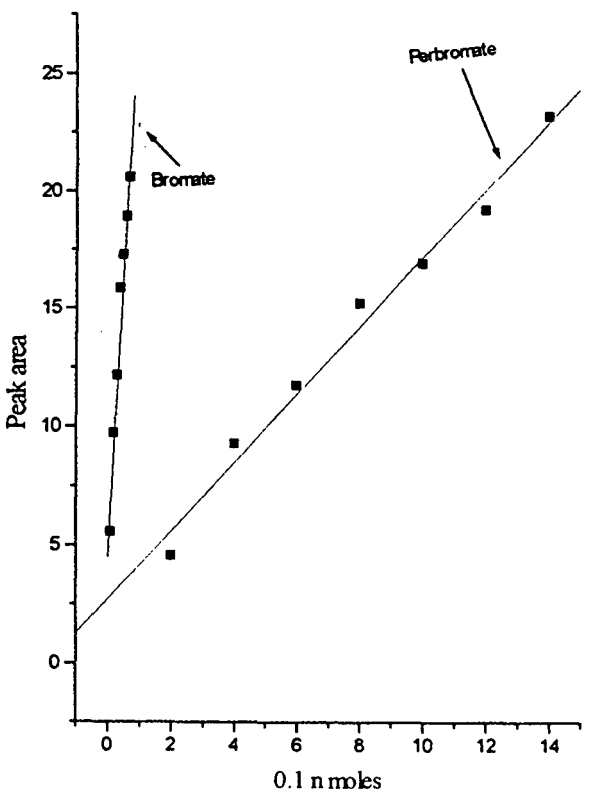


Fig. 2. Calibration curve of mixtures of perbromate and bromate in ratio 20:1. Top: The photo obtained by the CCD camera. Below: The calibration obtained from the densitometric results. Perbromate: $y = (1.44 \pm 0.08)x + 2.72 \pm 0.72$; $r = 0.9924$. Bromate: $y = (24.47 \pm 2.07)x + 4.50 \pm 0.92$; $r = 0.9826$.

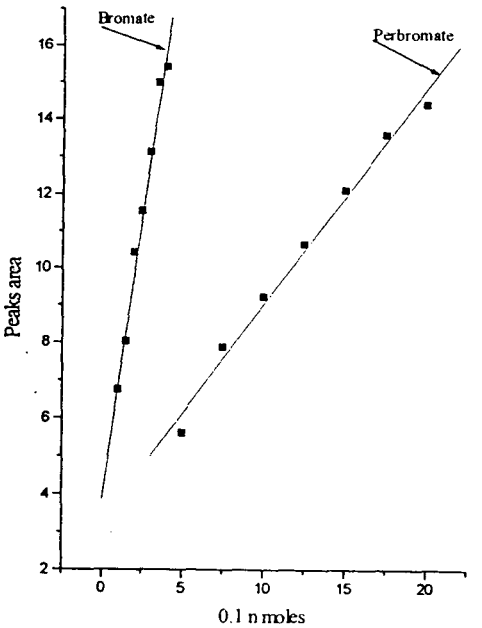


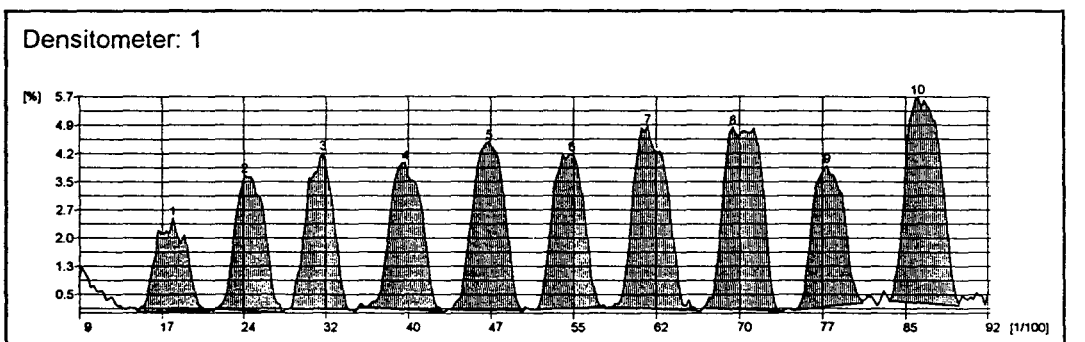


| Peak | Position (1/100) | Height (%) | Area | Area (%) |
|---|---|---|---|---|
| 1 | 17.91 | 2.43 | 0.2929 | 5.60 |
| 2 | 24.60 | 3.54 | 0.4114 | 7.87 |
| 3 | 31.82 | 4.07 | 0.4377 | 8.38 |
| 4 | 39.30 | 3.83 | 0.4816 | 9.22 |
| 5 | 47.06 | 4.40 | 0.5559 | 10.64 |
| 6 | 54.55 | 4.02 | 0.5022 | 9.61 |
| 7 | 61.50 | 4.73 | 0.6317 | 12.09 |
| 8 | 69.25 | 4.73 | 0.7089 | 13.57 |
| 9 | 77.81 | 3.67 | 0.4517 | 8.64 |
| 10 | 86.10 | 5.38 | 0.7514 | 14.38 |

Fig. 3. Analysis of a dilute aged solution of perbromate. Top: Calibration curve. Perbromate: $y = (0.58 \pm 0.03)x + 3.23 \pm 0.38$; $r = 0.9942$. Bromate: $y = (3.04 \pm 0.17)x + 3.85 \pm 0.46$; $r = 0.9921$. Densitometer 1 gives the peaks of perbromate as printed out by the software. Spots 2, 6 and 9 are the spots analysed, the other spots are the solutions used for the calibration curve. Densitometer 2 gives the peaks of bromate. The sequence is that of densitometer 1. The average peak for perbromate is 0.92 nmoles and for bromate 0.11 nmoles. The original solution contained 0.1 mmoles in 100 ml and aged for four years.

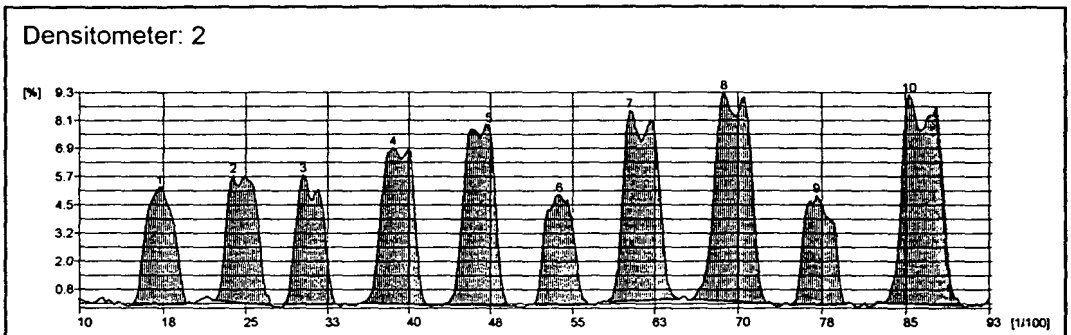


| Peak | Position (1/100) | Height (%) | Area | Area (%) | Quantity |
|---|---|---|---|---|---|
| 1 | 17.65 | 5.11 | 0.5439 | 6.74 | n/a |
| 2 | 24.33 | 5.49 | 0.6471 | 8.02 | n/a |
| 3 | 30.75 | 5.57 | 0.5627 | 6.98 | n/a |
| 4 | 39.04 | 6.75 | 0.8407 | 10.42 | n/a |
| 5 | 47.86 | 7.83 | 0.9299 | 11.53 | n/a |
| 6 | 54.28 | 4.77 | 0.5202 | 6.45 | n/a |
| 7 | 60.70 | 8.23 | 1.0564 | 13.10 | n/a |
| 8 | 69.25 | 9.04 | 1.2072 | 14.97 | n/a |
| 9 | 77.54 | 4.74 | 0.5165 | 6.40 | n/a |
| 10 | 85.83 | 9.06 | 1.2419 | 15.40 | n/a |

Fig. 3 (*continued*).

analysis of an impure sample of potassium perbromate and a dilute solution of potassium perbromate aged for four years at room temperature.

## 2. Experimental

Merck 5577 thin layers consisting of microcrystalline cellulose were used throughout. Solutions were placed on the thin layers using 1-$\mu$l disposable micropipettes (Blaubrand intra End Cat No. 709101).

Volumes of 1$\mu$l were spotted on the layers as round spots. Halmilton microsyringes proved unsatisfactory as the metal tip reduces the perbromate rather quickly even in a neutral solution. The developing solvent was prepared by equilibrating 100 ml of butanol puriss p.a. ACS (from Fluka AG, Buchs, Switzerland) with 100 ml dilute ammonia (5 ml conc. ammonia + 95 ml deionised water). Glass jars (8 × 20 cm, height 17 cm) with glass lids were used. The aqueous phase of the solvent was placed in a small beaker in one corner of the jar. As there is a large difference in $R_F$ between potassium perbromate and potassium bromate a short development was adopted, 1–1.5 h; in this period the solvent moves about 6 cm. The plates are then dried with a hairdryer and dipped into a solution of 1% soluble starch and 2% KI in 6 *M* HCl. After ca. 30–60 s the plate is placed under the CCD camera of the Cybertech Gel documentation system WINCAM 2.1 and after focusing a picture is taken. The concentration ranges for quantitation are 0.05–1 nmol for $KBrO_4$ and 0.01–1 nmol for $KBrO_3$.

For the image processing a computer was running the Cybertech WINCAM 2.1 image analysis software. As shown below in Figs. 1–4

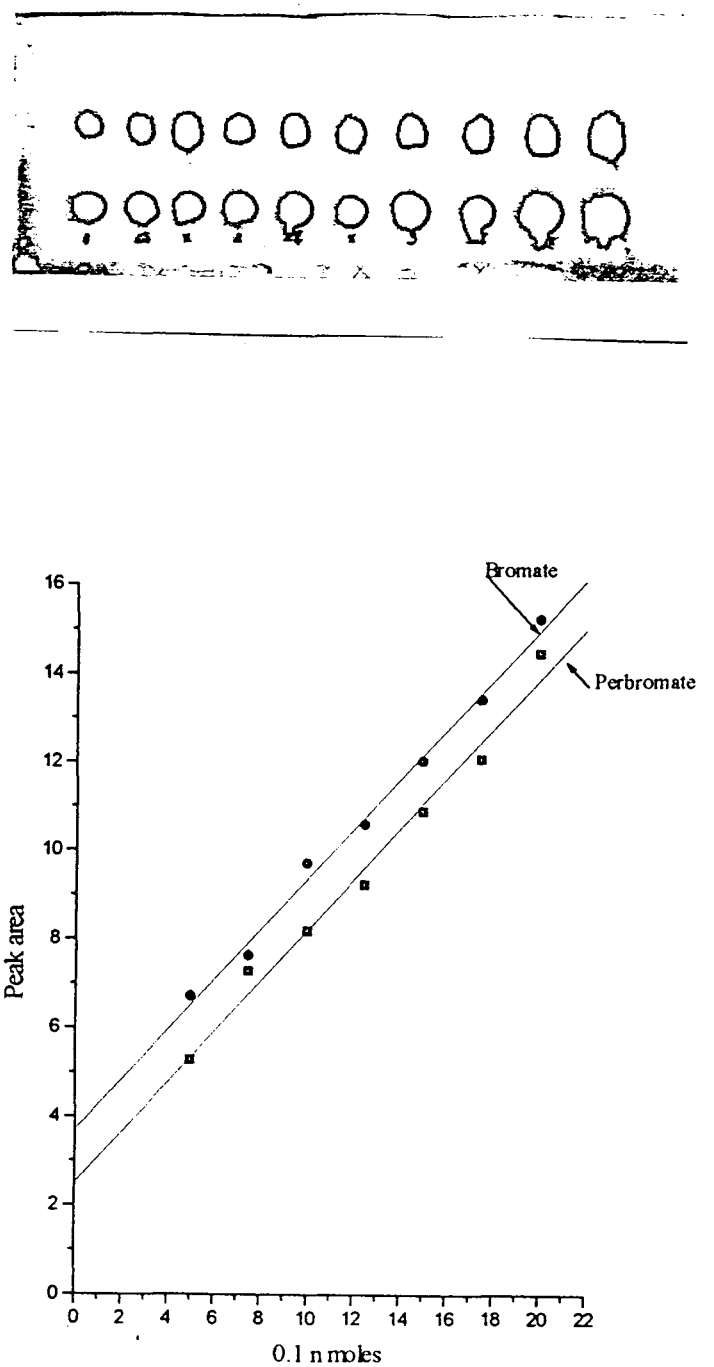


Fig. 4. Analysis of an impure sample of potassium perbromate. From top to bottom: Photo of the developed chromatogram with the CCD camera. Calibration curve. Perbromate: $y = (0.57 \pm 0.03)x + 2.51 \pm 0.45$; $r = 0.9915$. Bromate: $y = (0.56 \pm 0.02)x + 3.70 \pm 0.29$; $r = 0.9965$. Densitometer results for perbromate. Densitometer results for bromate. The sample is in positions 3, 6 and 8. The other spots are the solutions shown in the calibration curve above.

Densitometer: 1

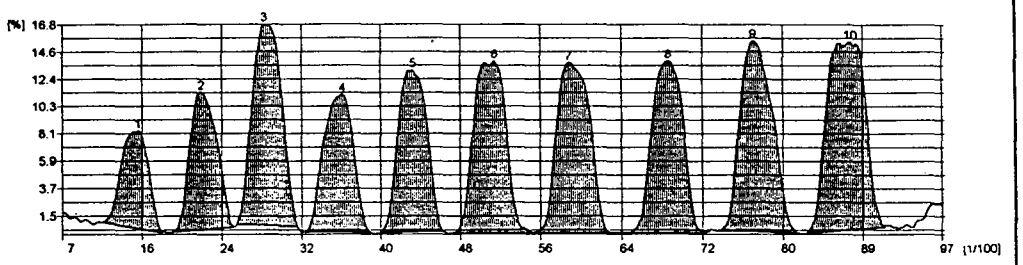


| Peak | Position (1/100) | Height (%) | Area | Area (%) |
|---|---|---|---|---|
| 1 | 15.24 | 7.80 | 0.9451 | 5.27 |
| 2 | 21.66 | 10.97 | 1.3024 | 7.26 |
| 3 | 28.07 | 16.04 | 2.0888 | 11.65 |
| 4 | 36.10 | 10.97 | 1.4631 | 8.16 |
| 5 | 43.32 | 12.90 | 1.6478 | 9.19 |
| 6 | 51.60 | 13.69 | 1.9395 | 10.81 |
| 7 | 59.09 | 13.60 | 1.9433 | 10.84 |
| 8 | 68.98 | 13.73 | 1.8600 | 10.37 |
| 9 | 77.54 | 15.28 | 2.1551 | 12.02 |
| 10 | 87.43 | 15.03 | 2.5898 | 14.44 |

Densitometer: 2

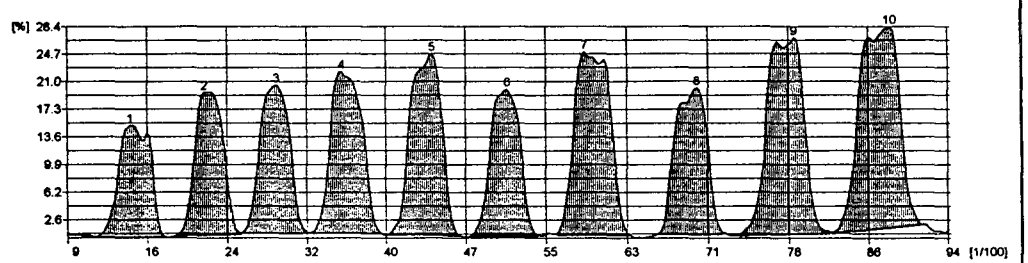


| Peak | Position (1/100) | Height (%) | Area | Area (%) |
|---|---|---|---|---|
| 1 | 14.97 | 14.95 | 2.0285 | 6.70 |
| 2 | 22.19 | 19.20 | 2.3037 | 7.61 |
| 3 | 29.14 | 19.76 | 2.4727 | 8.17 |
| 4 | 35.56 | 21.67 | 2.9304 | 9.68 |
| 5 | 44.39 | 24.26 | 3.1945 | 10.55 |
| 6 | 51.60 | 19.65 | 2.4459 | 8.08 |
| 7 | 59.09 | 24.52 | 3.6329 | 12.00 |
| 8 | 69.79 | 19.59 | 2.6067 | 8.61 |
| 9 | 79.14 | 26.34 | 4.0539 | 13.39 |
| 10 | 88.50 | 27.01 | 4.6000 | 15.20 |

Fig. 4 (*continued*).

this yields the integrated peaks, their heights and areas as well as the calibration curve including its statistical evaluation.

Fig. 1 shows the results when perbromate–bromate mixtures of a molar ratio 1:10 were prepared with 0.05 nmol of perbromate and 0.5–3.5 nmol of bromate. Both yield a linear response in this range.

Fig. 2 shows the results with a molar ratio perbromate–bromate of 20:1. Again the response is linear in the range 0.2–1.4 nmol for perbromate and 0.01–0.07 nmol for bromate.

During spotting of the sample the bromate is concentrated on the outer rim of the spots and this produces the two peaked densitometer curves.

For sample analysis 3 spots of the solution to be analysed are placed between the calibration spots. As there are several factors which influence the liberation of iodine from perbromate it is evident that the calibration solution must be run on the same layer as the samples.

Fig. 3 shows the chromatograms obtained with a solution of 18 mg of $KBrO_4$ in deionised water which had been left to stand for four years on a shelf in the laboratory with usual light and temperature variations. The chromatogram yielded a molar ratio of 0.92 nmoles perbromate and 0.11 nmoles bromate. Thus after four years only ca. 10% of the original perbromate had been reduced to bromate.

Fig. 4 is a sample from an improved synthesis made about a year ago. It was an attempt to use the synthesis described by Appelman [4], i.e. oxidation of an alkaline solution of perbromate with gaseous fluorine, and to reduce the number of purification steps of this synthesis. Preliminary qualitative chromatograms had shown that the product contained considerable amounts of bromate. The bromate content was here found to be $37.8 \pm 2.3\%$. In paper and thin-layer chromatography visual examination gives an estimate with an accuracy of $\pm 20\%$. This it is always possible to make a rough check of the results by visual inspection.

## References

[1] E.H. Appelman, J. Am. Chem. Soc., 90 (1968) 1900.
[2] M. Lederer and M. Sinibaldi, J. Chromatogr., 60 (1971) 275.
[3] L.A. Lazarou, P.A. Siskos, M.A. Koupparis, T.P. Hadjiioannou and E.H. Appelman, Anal. Chim. Acta, 94 (1977) 475.
[4] E.H. Appelman, Inorg. Synth., 13 (1972) 1.

# Author Index Vol. 712

## PUBLICATION SCHEDULE FOR THE 1995 SUBSCRIPTION

*Journal of Chromatography A* and *Journal of Chromatography B: Biomedical Applications*

| MONTH | J–J | A | S | O | N | D |
|---|---|---|---|---|---|---|
| Journal of Chromatography A | 689–708/1 | 708/2<br>709/1<br>709/2<br>710/1 | 710/2<br>711/1<br>711/2 | 712/1<br>712/2<br>715/1 | 715/2<br>716/1 + 2<br>717/1 + 2 | 718/1<br>718/2<br>701/1 + 2 |
| Bibliography Section | 713 | | 714/1 | | | 714/2 |
| Journal of Chromatography B: Biomedical Applications | 663–669 | 670/1<br>670/2 | 671/1 + 2 | 672/1<br>672/2 | 673/1<br>673/2 | 674/1<br>674/2 |

## INFORMATION FOR AUTHORS

(Detailed *Instructions to Authors* were published in *J. Chromatogr. A*, Vol. 657, pp. 463–469. A free reprint can be obtained by application to the publisher, Elsevier Science B.V., P.O. Box 330, 1000 AH Amsterdam, Netherlands.)

**Types of Contributions.** The following types of papers are published: Regular research papers (full-length papers), Review articles, Short Communications and Discussions. Short Communications are usually descriptions of short investigations, or they can report minor technical improvements of previously published procedures; they reflect the same quality of research as full-length papers, but should preferably not exceed five printed pages. Discussions (one or two pages) should explain, amplify, correct or otherwise comment substantively upon an article recently published in the journal. For Review articles, see inside front cover under Submission of Papers.

**Submission.** Every paper must be accompanied by a letter from the senior author, stating that he/she is submitting the paper for publication in the *Journal of Chromatography A* or *B*.

**Manuscripts.** Manuscripts should be typed in **double spacing** on consecutively numbered pages of uniform size. The manuscript should be preceded by a sheet of manuscript paper carrying the title of the paper and the name and full postal address of the person to whom the proofs are to be sent. As a rule, papers should be divided into sections, headed by a caption (*e.g.*, Abstract, Introduction, Experimental, Results, Discussion, etc.). All illustrations, photographs, tables, etc., should be on separate sheets.

**Abstract.** All articles should have an abstract of 50–100 words which clearly and briefly indicates what is new, different and significant. No references should be given.

**Introduction.** Every paper must have a concise introduction mentioning what has been done before on the topic described, and stating clearly what is new in the paper now submitted.

**Experimental conditions** should preferably be given on a *separate* sheet, headed "Conditions". These conditions will, if appropriate, be printed in a block, directly following the heading "Experimental".

**Illustrations.** The figures should be submitted in a form suitable for reproduction, drawn in Indian ink on drawing or tracing paper. Each illustration should have a caption, all the *captions* being typed (with double spacing) together on a *separate sheet*. If structures are given in the text, the original drawings should be provided. Coloured illustrations are reproduced at the author's expense, the cost being determined by the number of pages and by the number of colours needed. The written permission of the author and publisher must be obtained for the use of any figure already published. Its source must be indicated in the legend.

**References.** References should be numbered in the order in which they are cited in the text, and listed in numerical sequence on a separate sheet at the end of the article. Please check a recent issue for the layout of the reference list. Abbreviations for the titles of journals should follow the system used by *Chemical Abstracts*. Articles not yet published should be given as "in press" (journal should be specified), "submitted for publication" (journal should be specified), "in preparation" or "personal communication".

Vols. 1–651 of the *Journal of Chromatography*; *Journal of Chromatography, Biomedical Applications* and *Journal of Chromatography, Symposium Volumes* should be cited as *J. Chromatogr.* From Vol. 652 on, *Journal of Chromatography A* (incl. Symposium Volumes) should be cited as *J. Chromatogr. A* and *Journal of Chromatography B: Biomedical Applications* as *J. Chromatogr. B*.

**Dispatch. Before sending the manuscript to the Editor please check that the envelope contains four copies of the paper complete with references, captions and figures. One of the sets of figures must be the originals suitable for direct reproduction. Please also ensure that permission to publish has been obtained from your institute.**

**Proofs.** One set of proofs will be sent to the author to be carefully checked for printer's errors. Corrections must be restricted to instances in which the proof is at variance with the manuscript.

**Reprints.** Fifty reprints will be supplied free of charge. Additional reprints can be ordered by the authors. An order form containing price quotations will be sent to the authors together with the proofs of their article.

0021-9673(19951013)712:2;1-9